The first school on Quantum Sensors for Fundamental Physics
@ Durham University

January 9, 2020

Laser Interferometric Search for Non-Standard Physics

Yuta Michimura

Department of Physics, University of Tokyo

michimura@granite.phys.s.u-tokyo.ac.jp

Self Introduction

- Yuta Michimura (道村唯太)
  Department of Physics, University of Tokyo
- Laser interferometric
  gravitational wave detectors
  - KAGRA
  - DECIGO
- Fundamental physics with laser interferometry
  - Lorentz invariance test
  - Macroscopic quantum mechanics
  - Axion search

  etc…

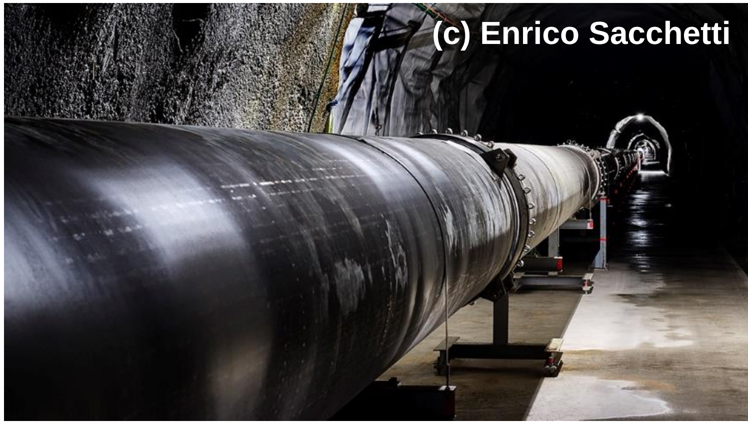

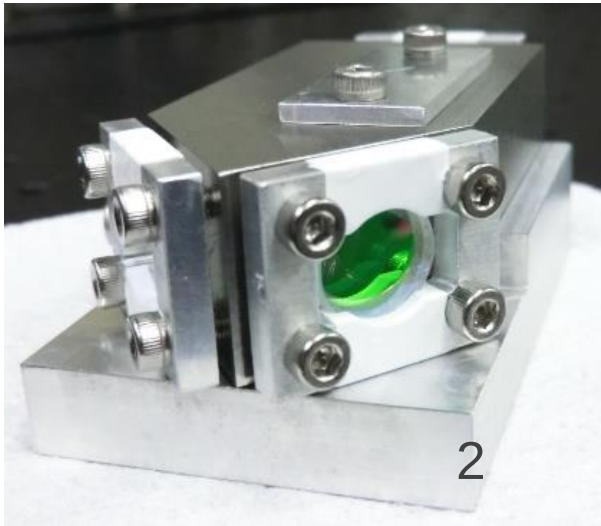

Laser Interferometry

- Detects length change as interference fringe
- Excellent sensor for
  - displacement of mechanical oscillators
  - force acting on mechanical oscillators
  - deviations of the speed of light
  - laser frequency change

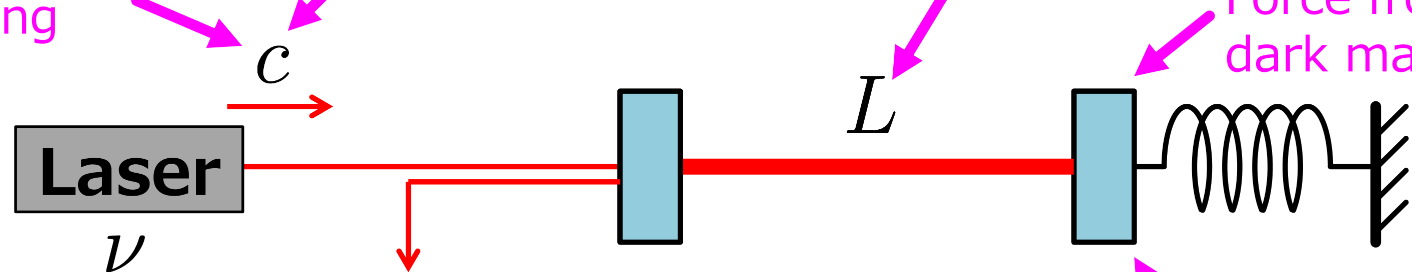

$$\frac{\delta\phi}{\phi} = \frac{\delta L}{L} = \frac{\delta\nu}{\nu} = \frac{\delta c}{c}$$

… even if it is not quantum-limited

Plan of the Talk

- **Basics of Laser Interferometry** (60 min)
  - Michelson interferometer
  - Fabry-Perot cavity
  - Quantum noise and other classical noises
- **Test of Lorentz Invariance** (30 min)
- **Search for Axion Dark Matter** (30 min)
- **Macroscopic Quantum Mechanics** (40 min)
- **KAGRA Gravitational Wave Telescope** (20 min)

- Slides available at https://tinyurl.com/YM20200109

Plan of the Talk

- **Basics of Laser Interferometry** (60 min)
  - Michelson interferometer
  - Fabry-Perot cavity
  - Quantum noise and other classical noises
- **Test of Lorentz Invariance** (30 min)
- **Search for Axion Dark Matter** (30 min)
- **Macroscopic Quantum Mechanics** (40 min)
- **KAGRA Gravitational Wave Telescope** (20 min)

- Slides available at https://tinyurl.com/YM20200109

Michelson Interferometer

- measures differential arm length change

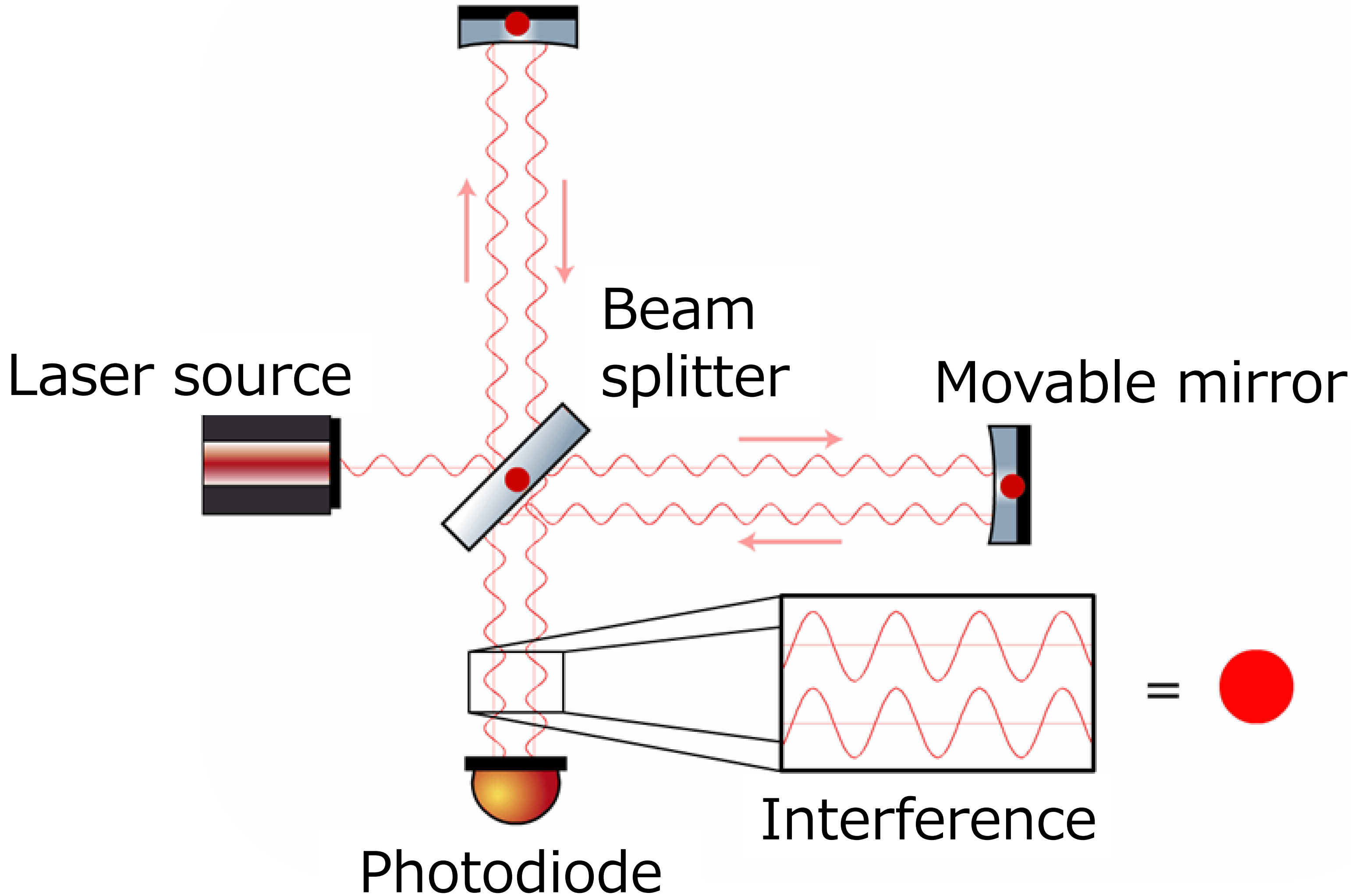

Michelson Interferometer

- measures differential arm length change

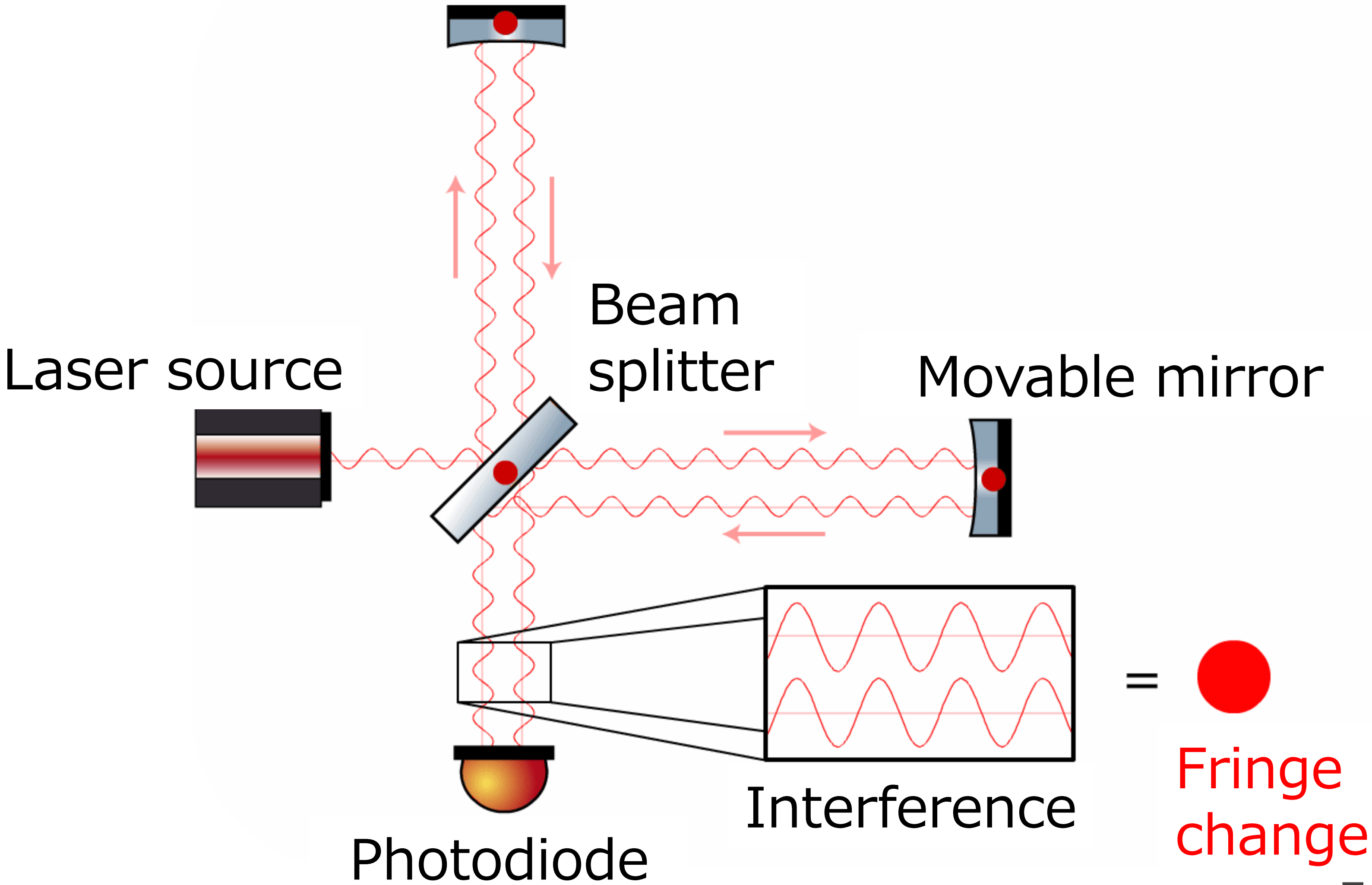

Michelson Interferometer

- Let's look into how Michelson interferometer works

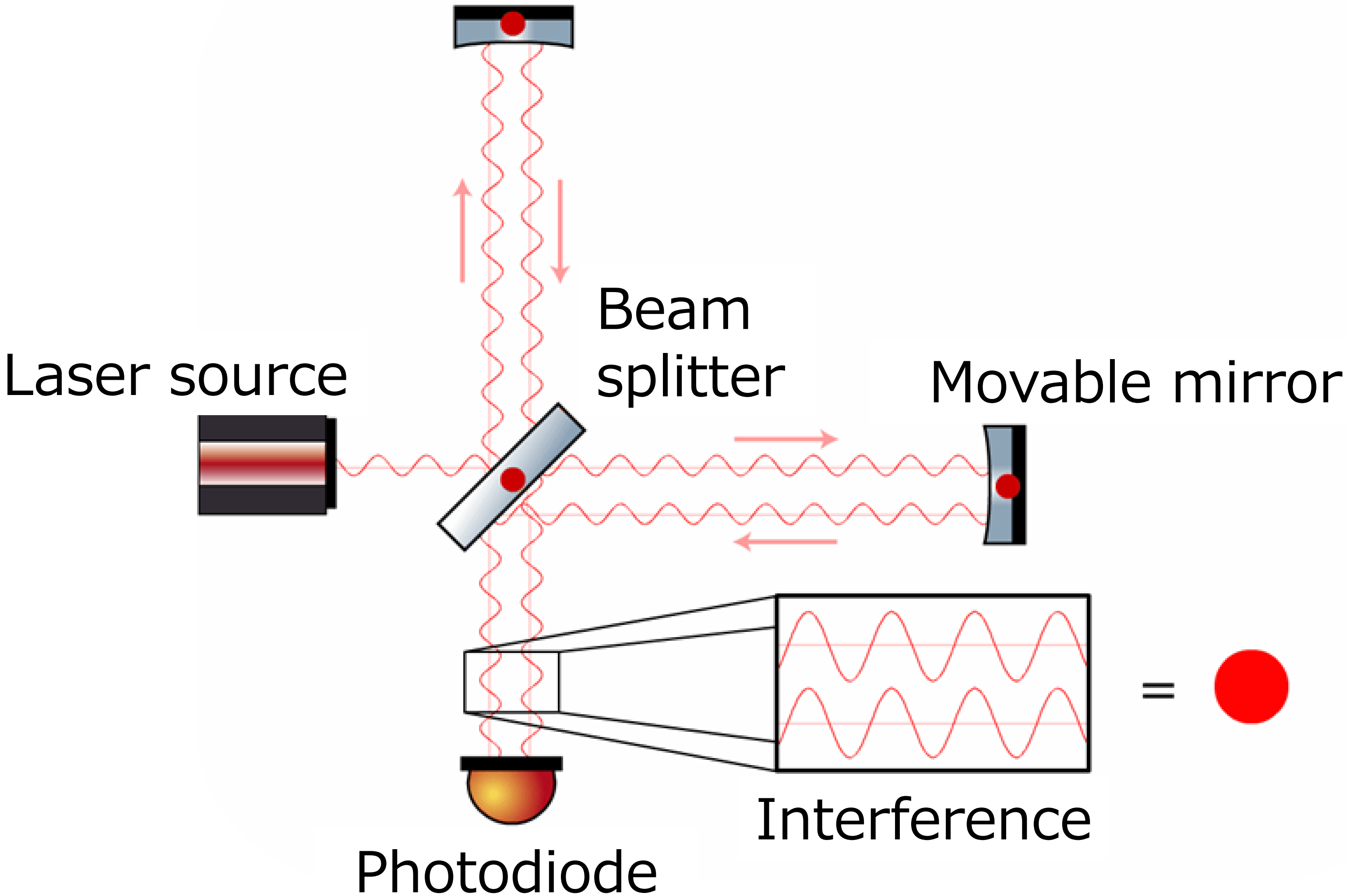

Laser Beam

- Electro-magnetic waves

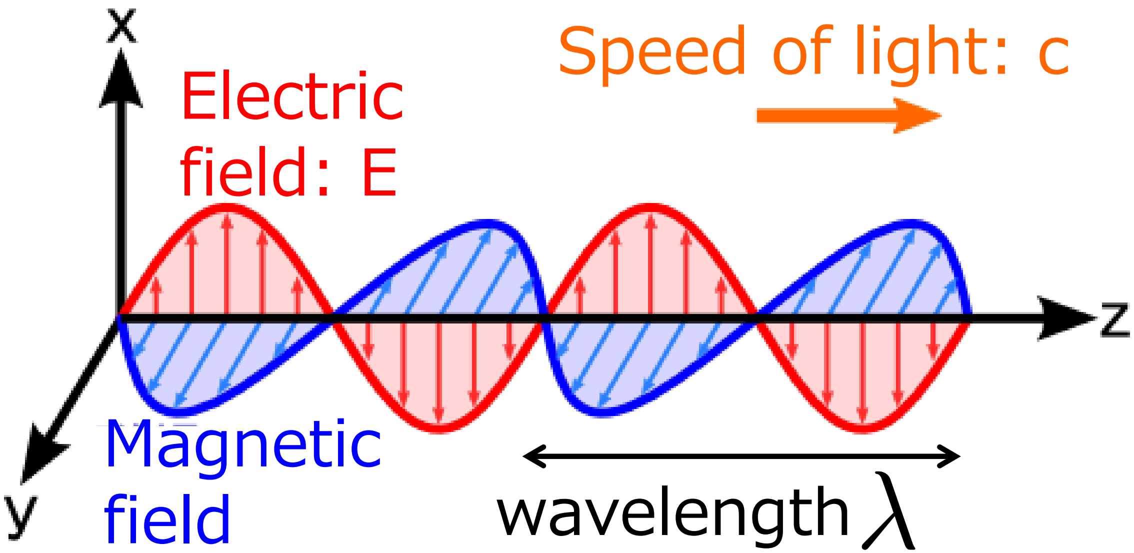

- Electric field can be written as

$$E = E_0 e^{i(\omega t - \phi)}$$

amplitude

angular frequency of laser

phase

$$\omega = \frac{2\pi c}{\lambda}$$

$$\phi = \frac{2\pi L}{\lambda}$$ phase at distance L

Photodiodes

- Photodiodes (PDs)
  Convert photons into electrons
  Detects light power (square of amplitude)

$$P \propto |E|^2 = E_0^2$$

We can only detect power change
Phase change cannot be detected directly

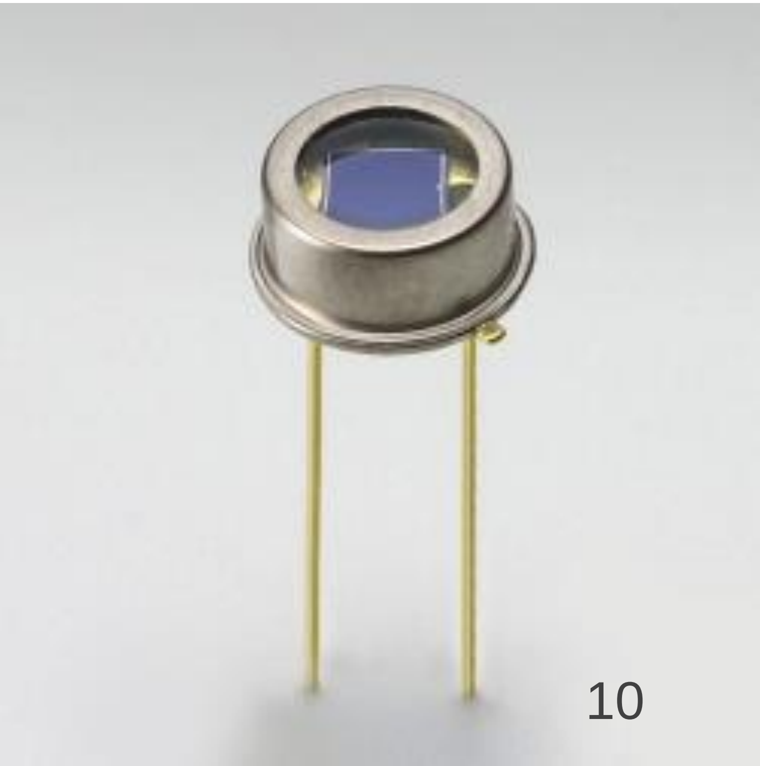

Beam Splitter

- Split beam in two
- Half in power, 1/√2 in amplitude
- Sign flip in back reflection

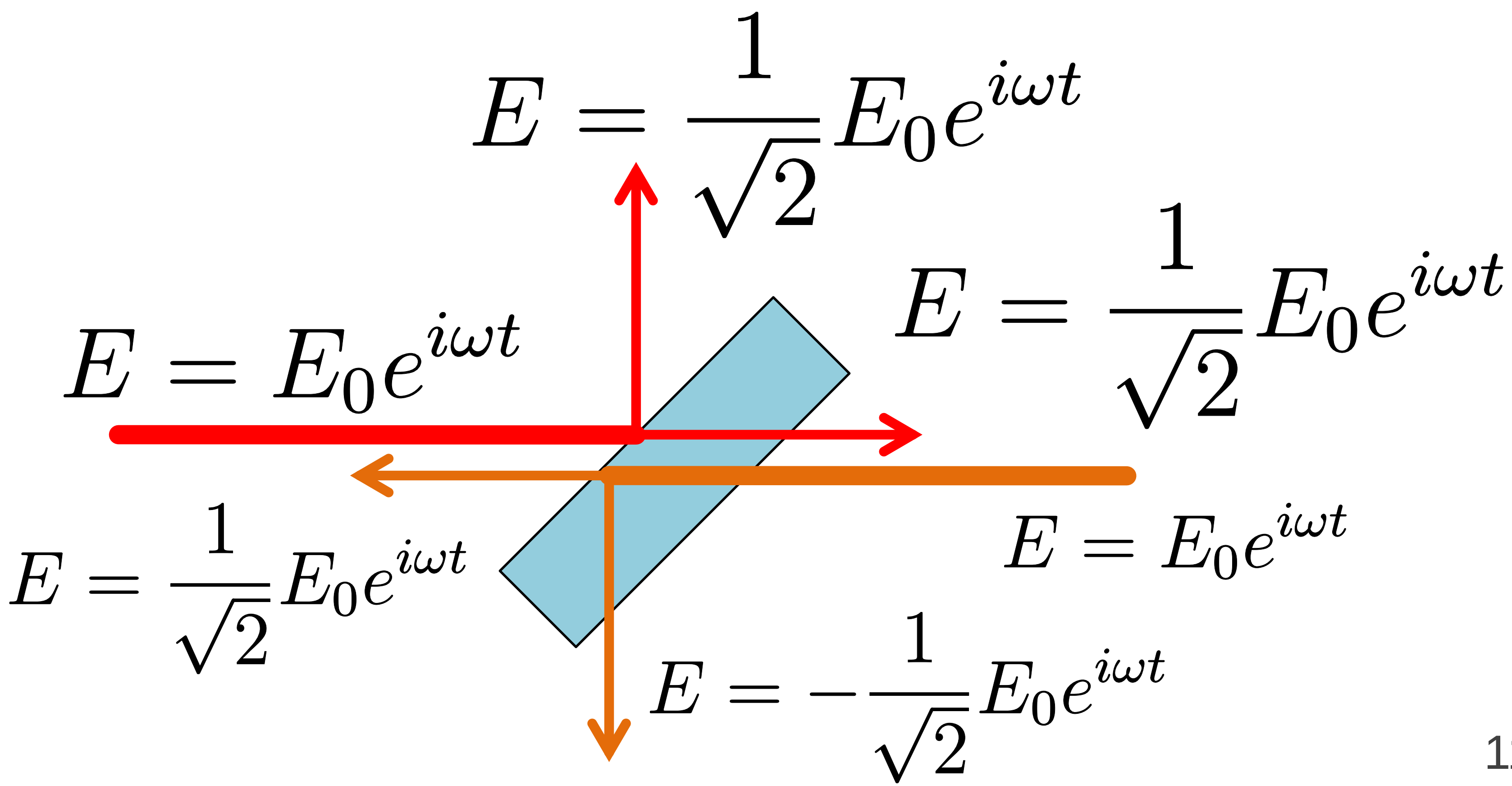

Output of Michelson Interferometer

- What is the power detected at the photodiode?

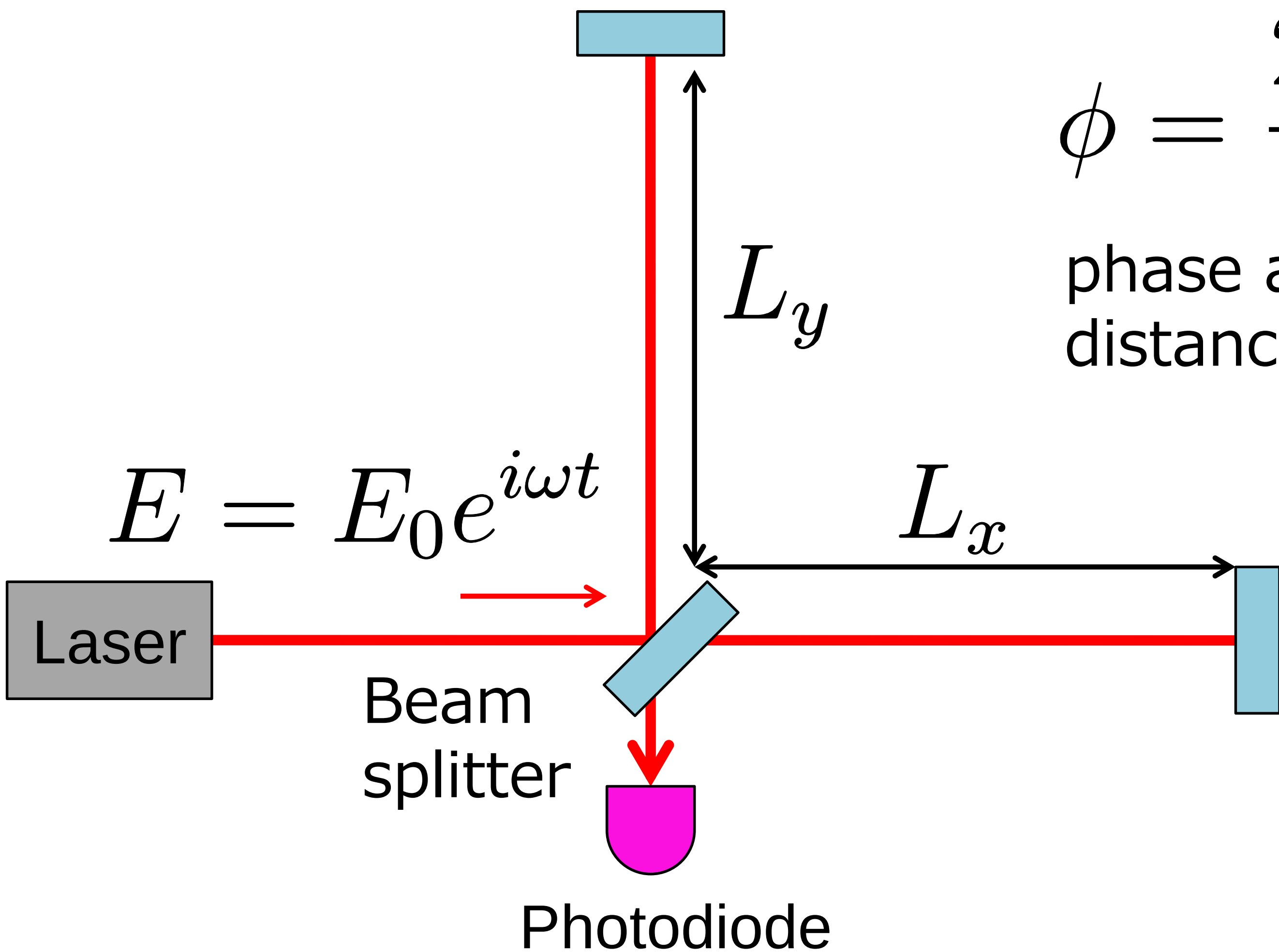

$$\phi = \frac{2\pi L}{\lambda}$$

phase at distance L

Output of Michelson Interferometer

- What is the power detected at the photodiode?

From Y-am From X-arm

$$P_{\mathrm{PD}} = \left| \frac{1}{2} E_0 e^{i(\omega t - \frac{4\pi L_y}{\lambda})} - \frac{1}{2} E_0 e^{i(\omega t - \frac{4\pi L_x}{\lambda})} \right|^2$$

$$= \frac{1}{4} |E_0|^2 \left| e^{-i\frac{4\pi L_y}{\lambda}} - e^{-i\frac{4\pi L_x}{\lambda}} \right|^2$$

$$= \frac{1}{2} P_0 \left(1 - \cos \frac{4\pi L_-}{\lambda} \right)$$

Input power

$$L_- = L_y - L_x$$

Differential arm length

Output of Michelson Interferometer

- Power changes with differential arm length change (interference)

$$P_{\mathrm{PD}} = \frac{1}{2} P_0 \left(1 - \cos \frac{4\pi L_-}{\lambda} \right)$$

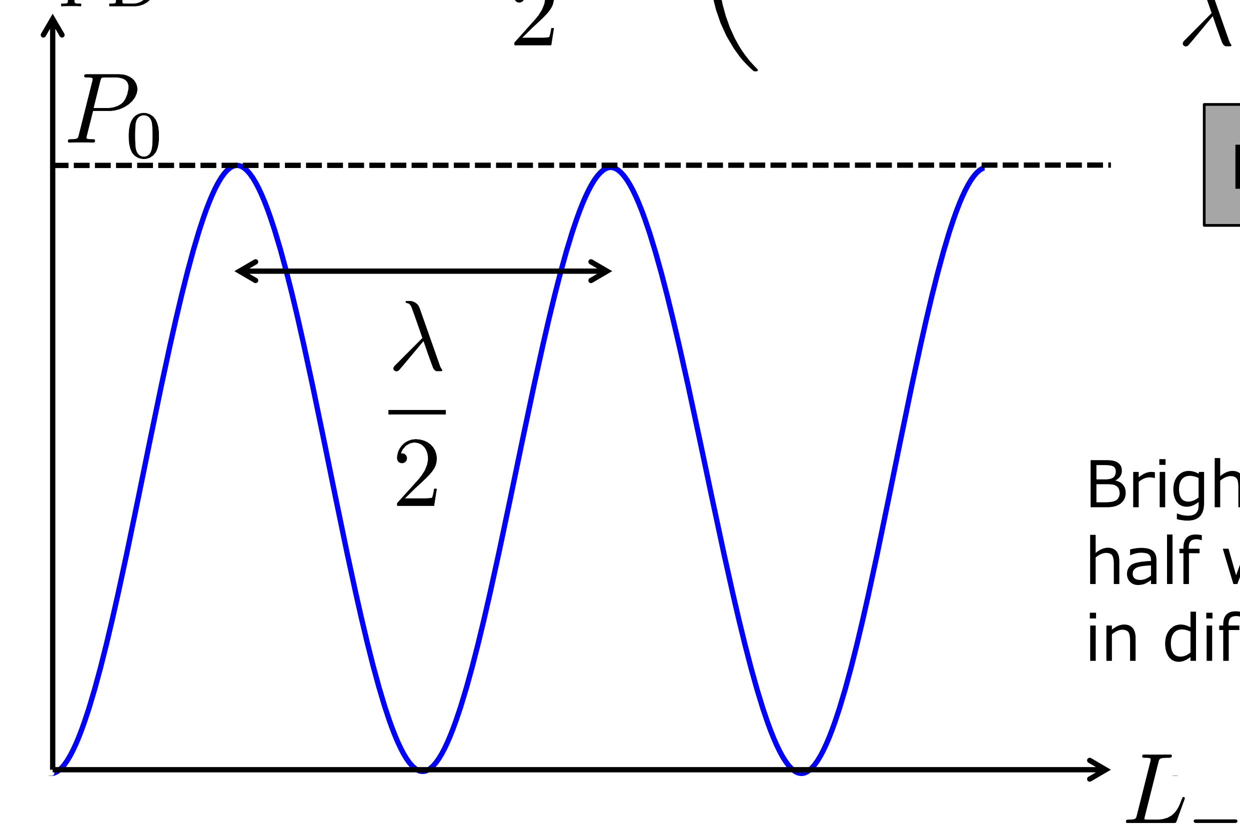

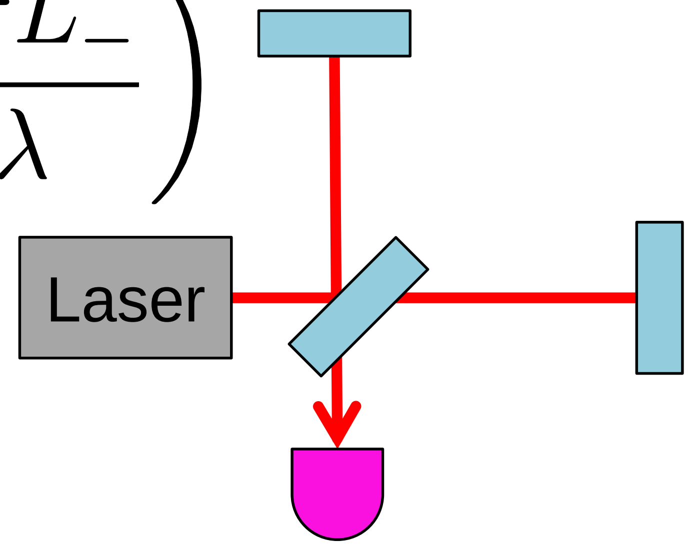

Bright fringe in every half wavelength change in differential arm length

Output of Michelson Interferometer

- Ratio between power change and length change

$$\frac{\partial P_{\mathrm{PD}}}{\partial L_-} = \frac{2\pi P_0}{\lambda} \sin \frac{4\pi L_-}{\lambda}$$

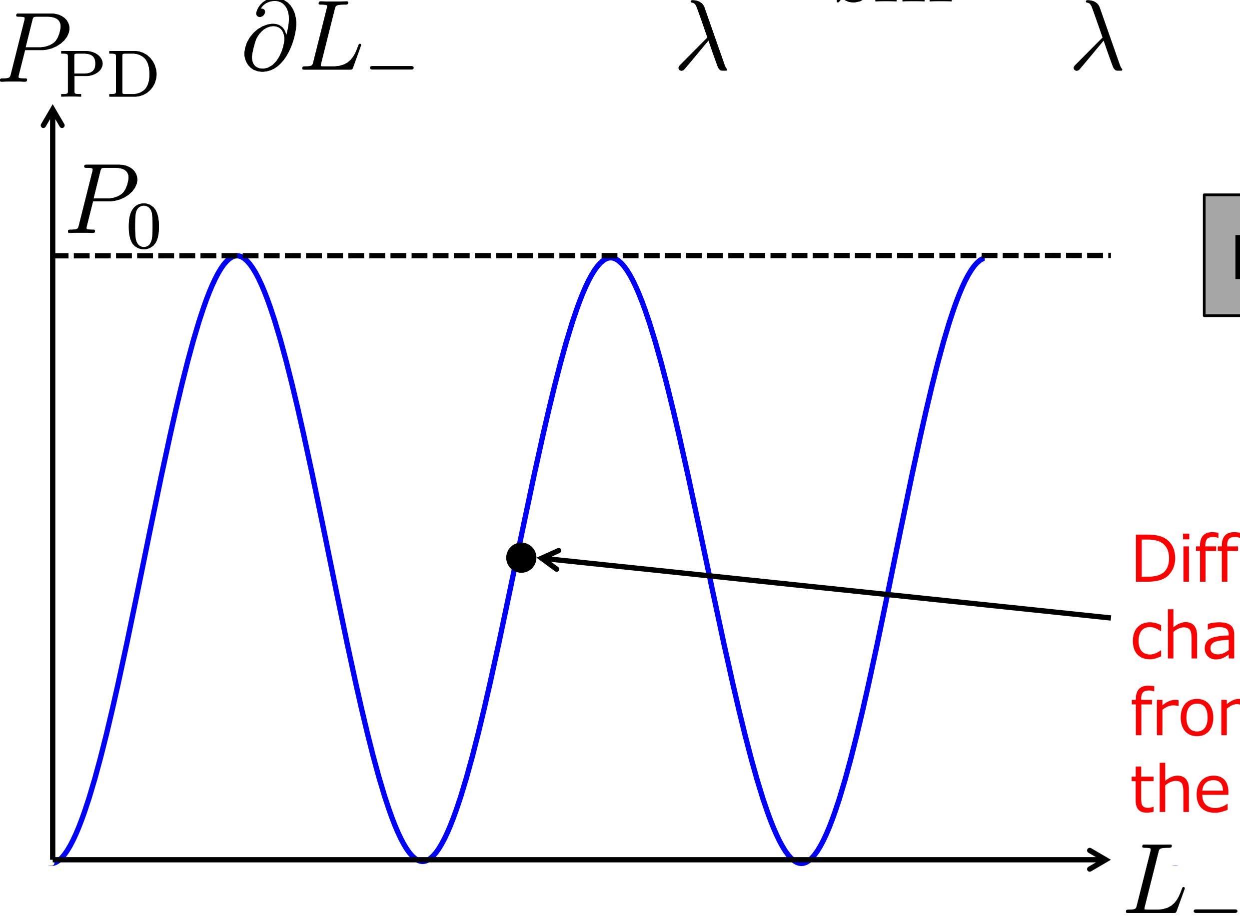

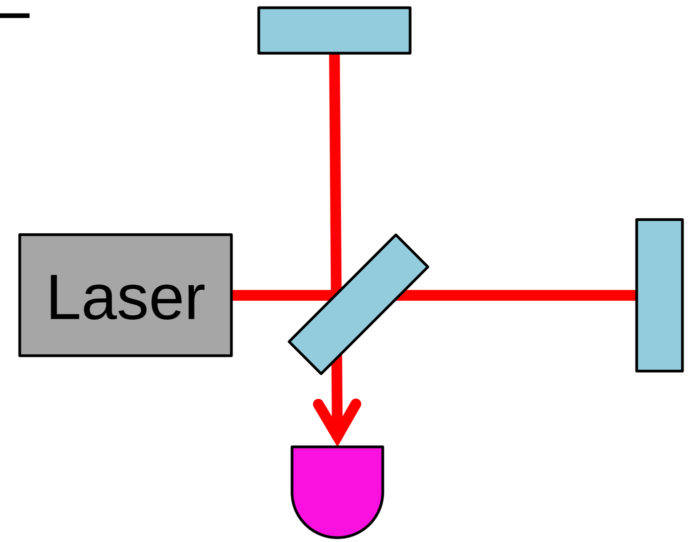

Differential arm length change can be detected from power change at the photodiode

Enhancing the Signal

- Use of Fabry-Pérot cavity to sense mirror displacement multiple times
- Sensing noise is reduced (displacement noise stays the same)

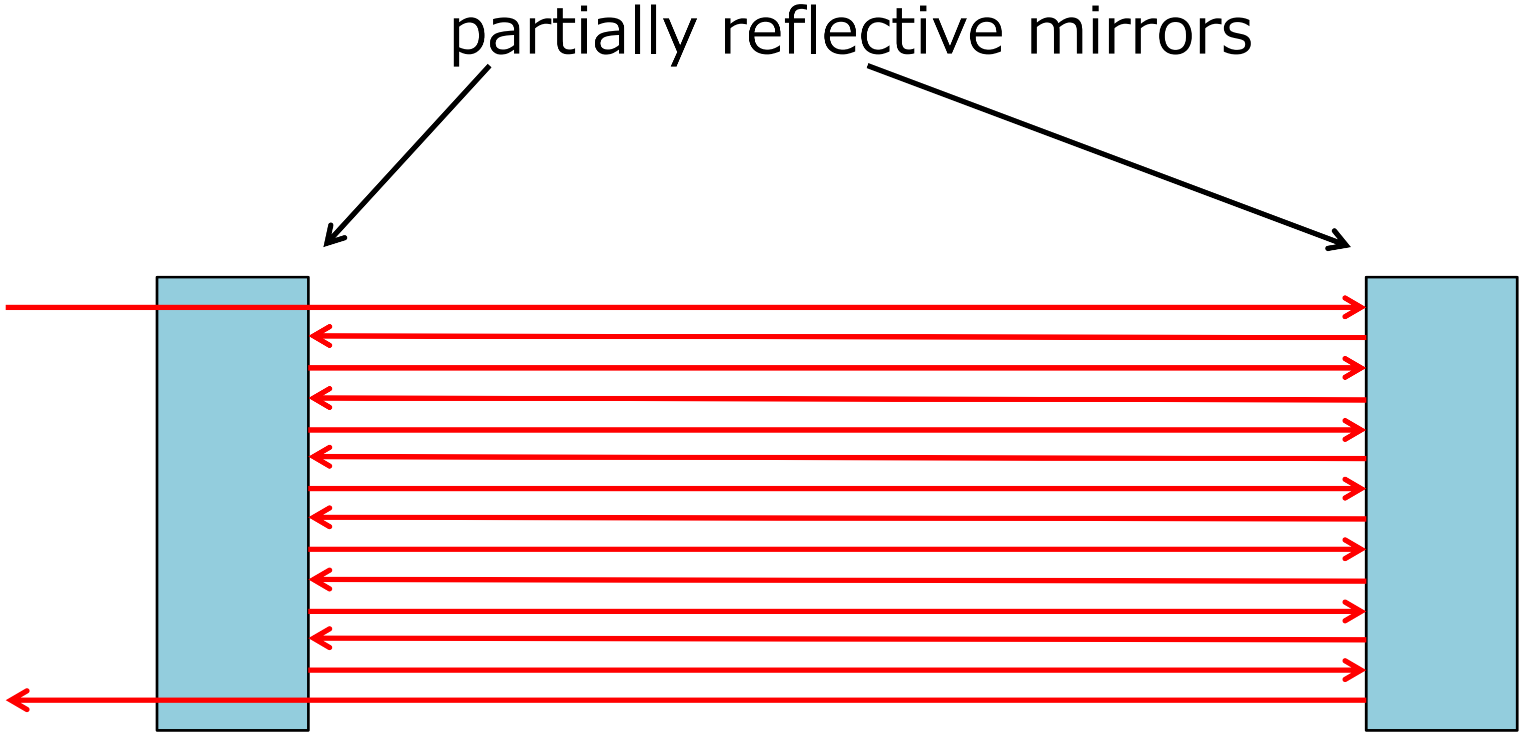

Fabry-Pérot Cavity

- Made from two parallel mirrors

amplitude
reflectivity, transmittance

$r_1,\ t_1$
input mirror

$r_2,\ t_2$
end mirror

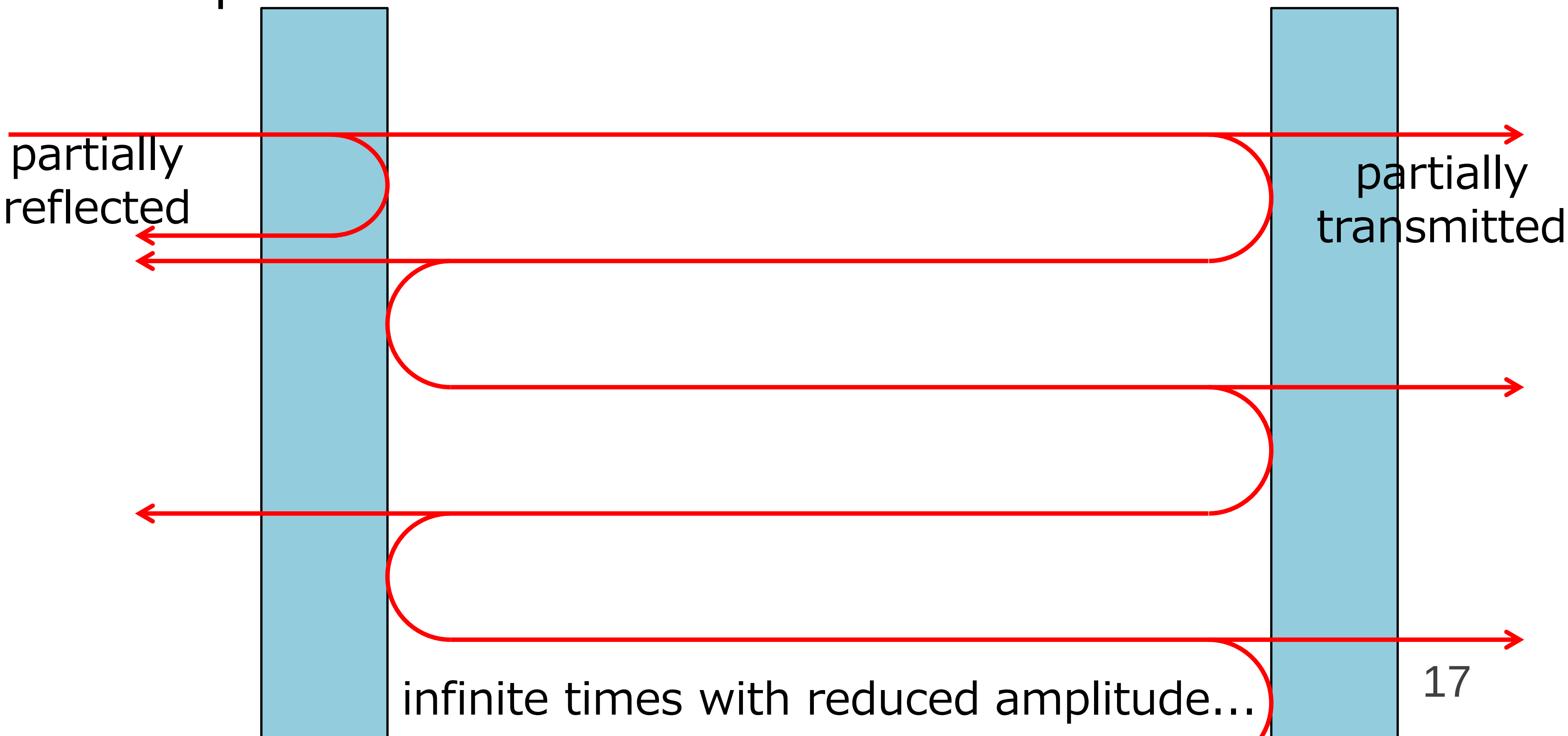

Fabry-Pérot Cavity

- Let's calculate electric field inside the cavity

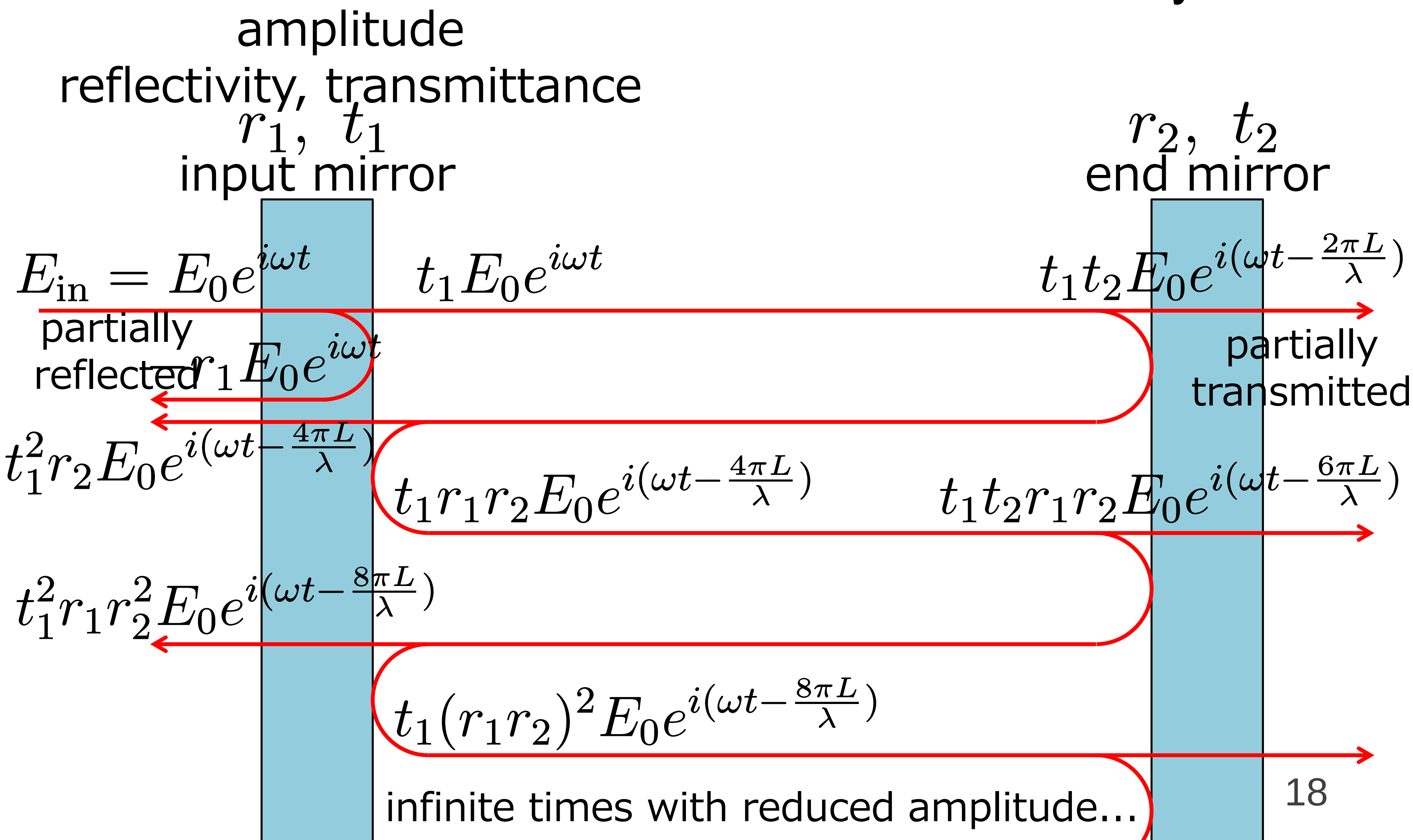

Intra-Cavity Field

- Intra-cavity field can be expressed as

$$
\begin{aligned}
E_{\text{circ}} &= t_1 E_0 e^{i\omega t} + t_1 r_1 r_2 E_0 e^{i(\omega t - \frac{4\pi L}{\lambda})} + t_1 (r_1 r_2)^2 E_0 e^{i(\omega t - \frac{4\pi L}{\lambda})} + \ldots \\
&= \underbrace{(t_1 + t_1 r_1 r_2 2 e^{i\frac{4\pi L}{\lambda}} + t_1 (r_1 r_2)^2 2 e^{i\frac{8\pi L}{\lambda}} + \ldots}_{\text{infinite geometric series with a common ratio of } r_1 r_2 e^{i\frac{4\pi L}{\lambda}}}) \underbrace{E_0 e^{i\omega t}}_{\text{input field}} \\
&= \frac{t_1}{1 - r_1 r_2 e^{i\frac{4\pi L}{\lambda}}} E_{\text{in}}
\end{aligned}
$$

Reflected Field

- Reflected field can be expressed as

$$E_{\mathrm{refl}} = -r_1 E_0 e^{i\omega t} + t_1^2 r_2 E_0 e^{i(\omega t - \frac{4\pi L}{\lambda})} + t_1^2 r_1 r_2^2 E_0 e^{i(\omega t - \frac{4\pi L}{\lambda})} + \dots$$

$$= (-r_1 + \underbrace{t_1^2 r_2 e^{i\frac{4\pi L}{\lambda}} + t_1^2 r_1 r_2^2 2 e^{i\frac{8\pi L}{\lambda}} + \dots}_{\text{infinite geometric series with a common ratio of } r_1 r_2 e^{i\frac{4\pi L}{\lambda}}}) E_0 e^{i\omega t}$$

$$= \left(-r_1 + \frac{t_1^2 r_2 e^{i\frac{4\pi L}{\lambda}}}{1 - r_1 r_2 e^{i\frac{4\pi L}{\lambda}}} \right) E_{\mathrm{in}}$$

Intra-Cavity Power

- Power inside the cavity

$$|E_{\mathrm{circ}}|^2 = \left| \frac{t_1}{1 - r_1 r_2 e^{i\frac{4\pi L}{\lambda}}} \right|^2 P_{\mathrm{in}}$$

resonance

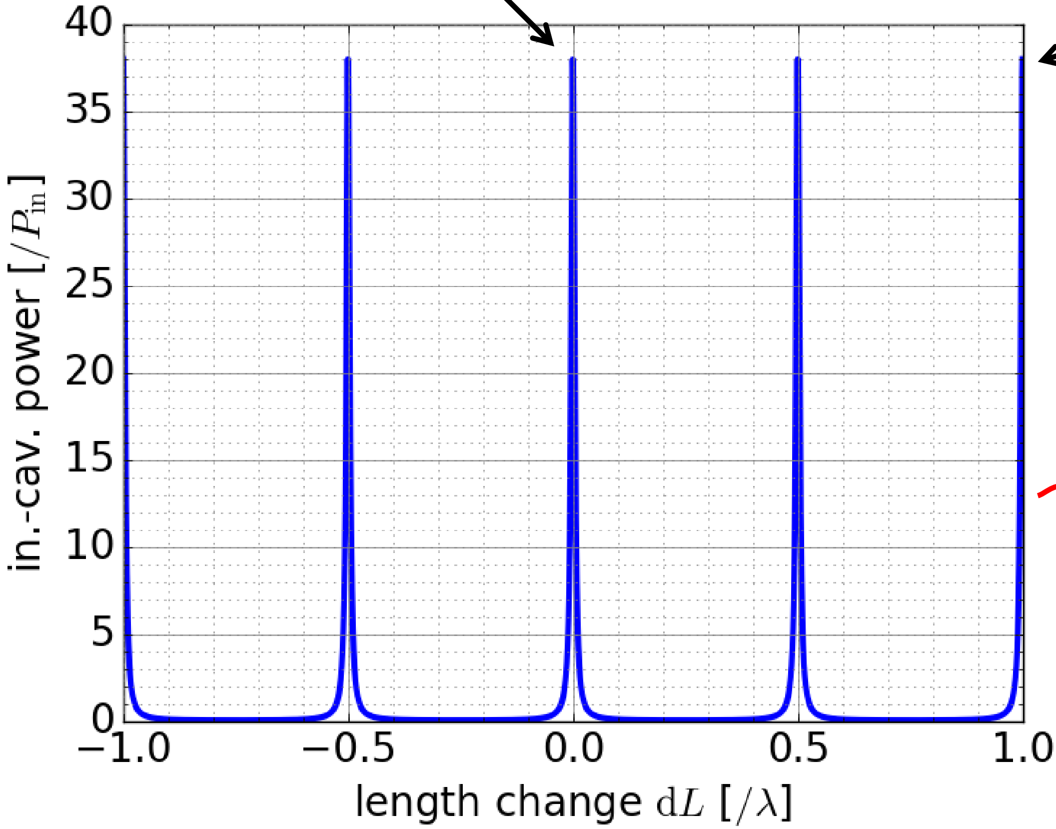

Intra-cavity power can be much higher than input power on resonance

constructive interference

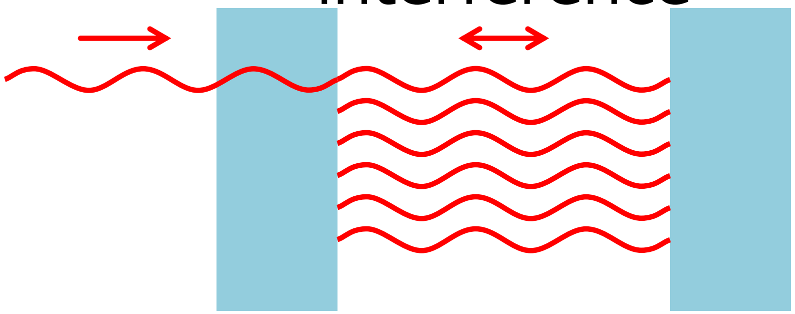

Intra-Cavity Power

- Power inside the cavity

$$|E_{\mathrm{circ}}|^2 = \left| \frac{t_1}{1 - r_1 r_2 e^{i\frac{4\pi L}{\lambda}}} \right|^2 P_{\mathrm{in}}$$

anti-resonance

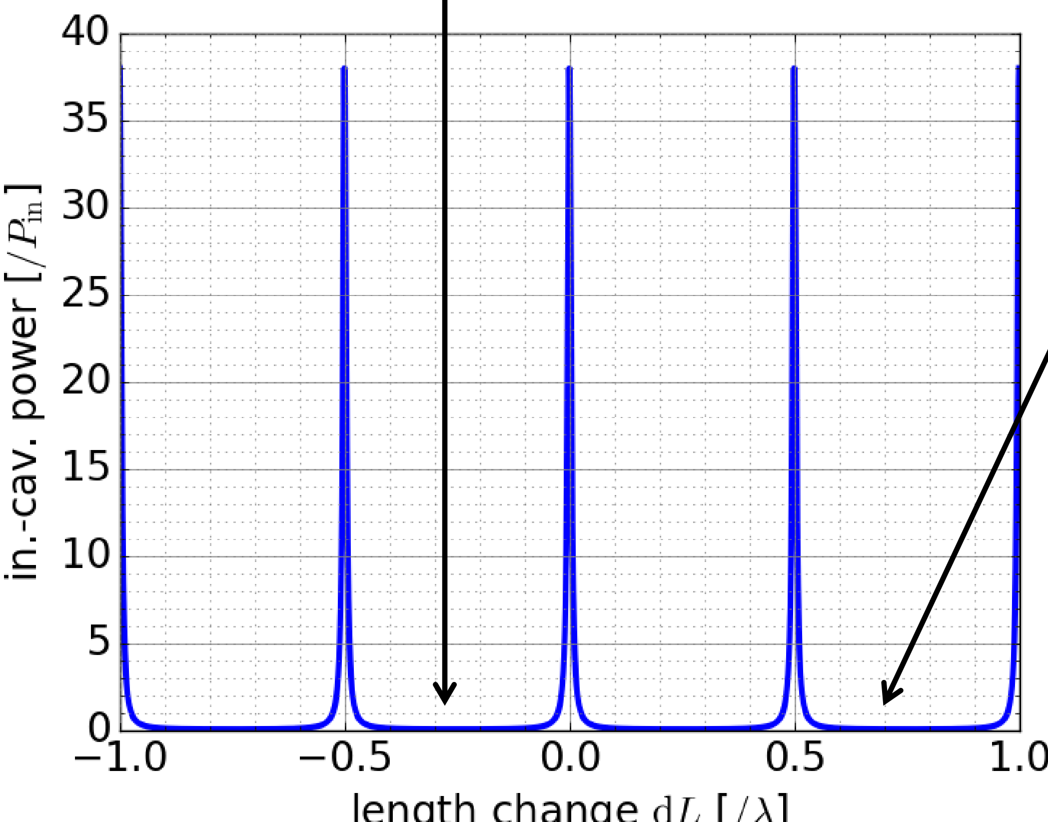

Almost no intra-cavity power at anti-resonance

destructive interference

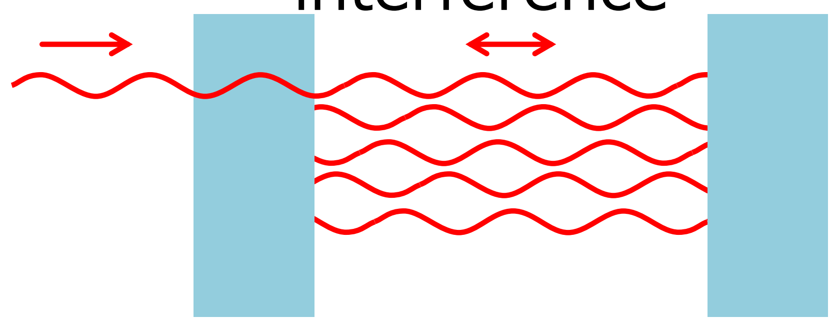

Resonant Frequency

- Cavity will be resonant when cavity round-trip length is integer multiples of laser wavelength

$$2L = N\lambda$$

- In other words, cavity will be resonant when laser frequency is integer multiples of free spectral range

$$\omega_{\mathrm{cav}} = N\omega_{\mathrm{FSR}} = N\frac{\pi c}{L}$$

- Resonant frequency shifts with mirror displacement

$$\delta\omega_{\mathrm{cav}} = \frac{\omega_{\mathrm{cav}}}{L}\delta L$$

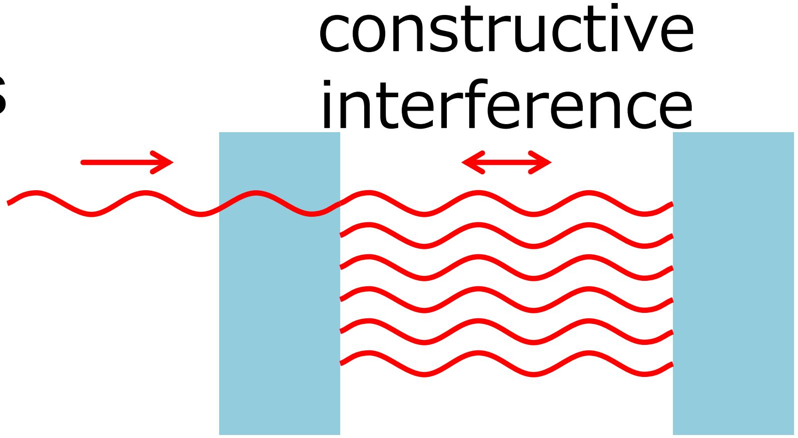

Finesse

- Power inside the cavity

$$|E_{\mathrm{circ}}|^2 = \left| \frac{t_1}{1 - r_1 r_2 e^{i\frac{4\pi L}{\lambda}}} \right|^2 P_{\mathrm{in}}$$

Resonance

Spacing $\frac{\lambda}{2}$

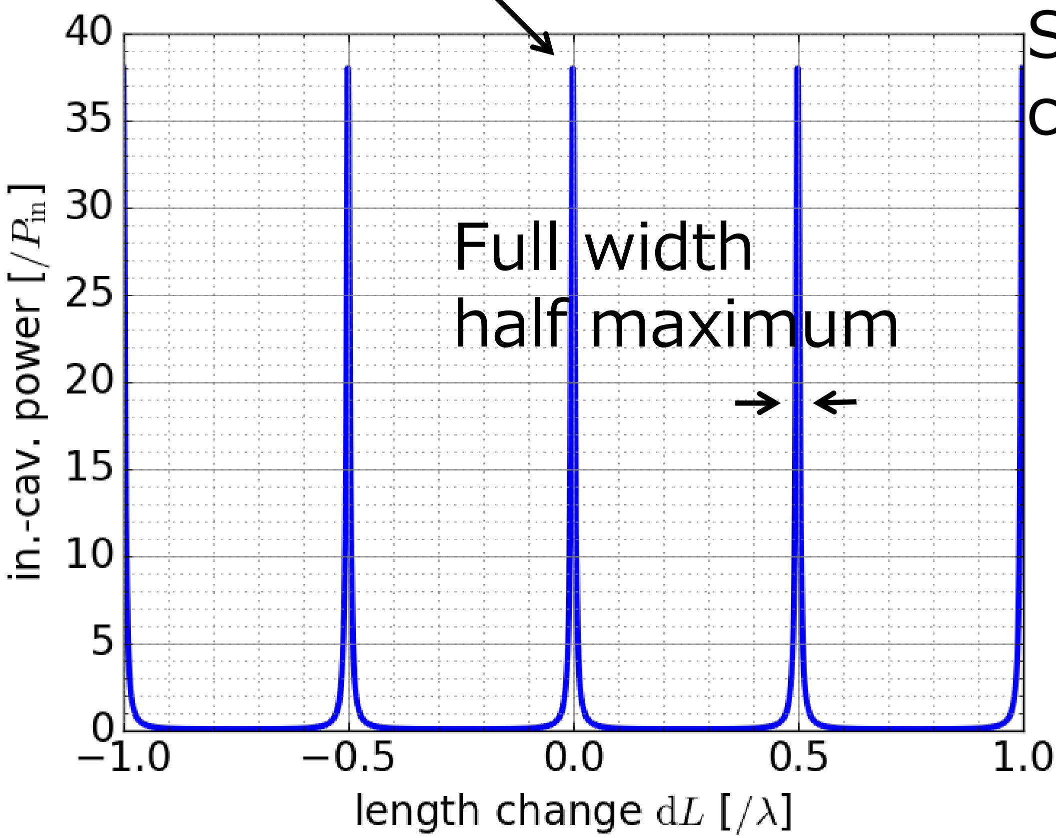

Sharpness of the resonance can be evaluated with

$$\frac{\text{Spacing}}{\text{FWHM}}$$

$$= \frac{\pi\sqrt{r_1 r_2}}{1 - r_1 r_2} \equiv \mathcal{F}$$

Finesse

Higher finesse for higher reflectivity

Cavity Build-up

- Power inside the cavity

$$|E_{\mathrm{circ}}|^2 = \left| \frac{t_1}{1 - r_1 r_2 e^{i\frac{4\pi L}{\lambda}}} \right|^2 P_{\mathrm{in}}$$

Resonance

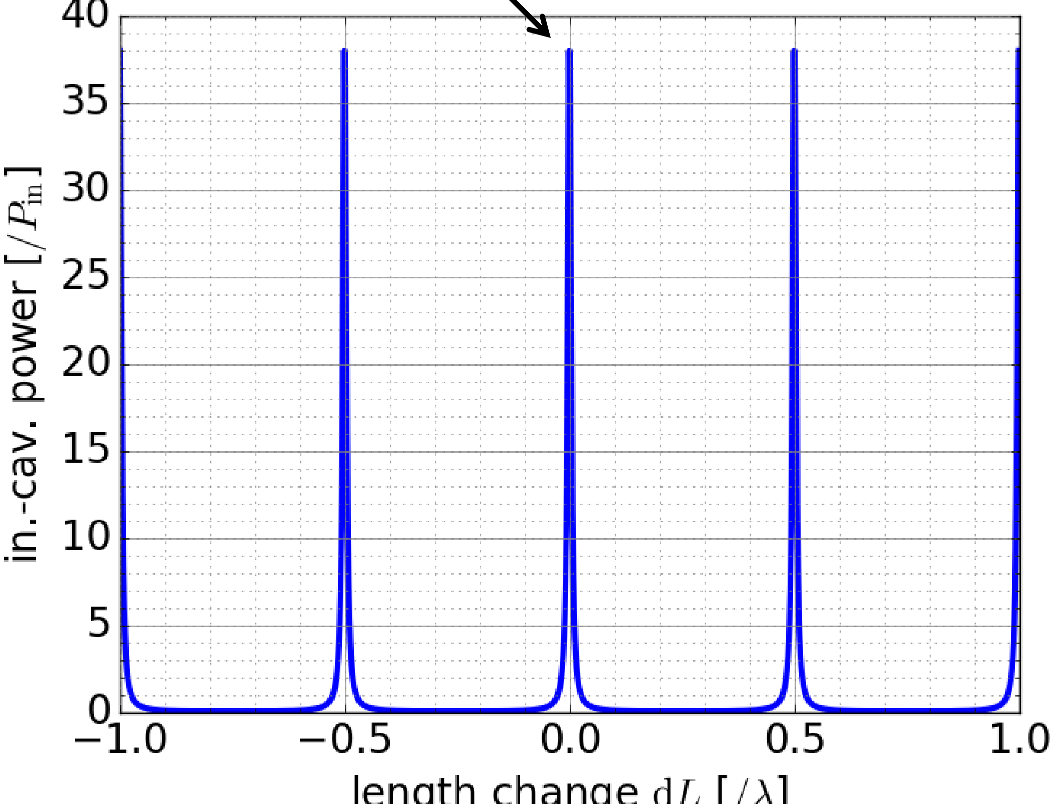

Intra-cavity power at resonance

$$|E_{\mathrm{circ}}|^2_{\mathrm{max}} = \left| \frac{t_1}{1 - r_1 r_2} \right|^2 P_{\mathrm{in}}$$

$$\simeq \boxed{\frac{2\mathcal{F}}{\pi}} P_{\mathrm{in}}$$

with
$r_1 \sim 1$, $r_2 = 1$

Cavity build-up

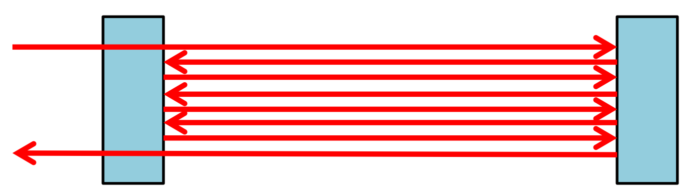

Phase of Reflected light

- Reflected field

$$E_{\mathrm{refl}} = \left(-r_1 + \frac{t_1^2 r_2 e^{i\frac{4\pi L}{\lambda}}}{1 - r_1 r_2 e^{i\frac{4\pi L}{\lambda}}} \right) E_{\mathrm{in}}$$

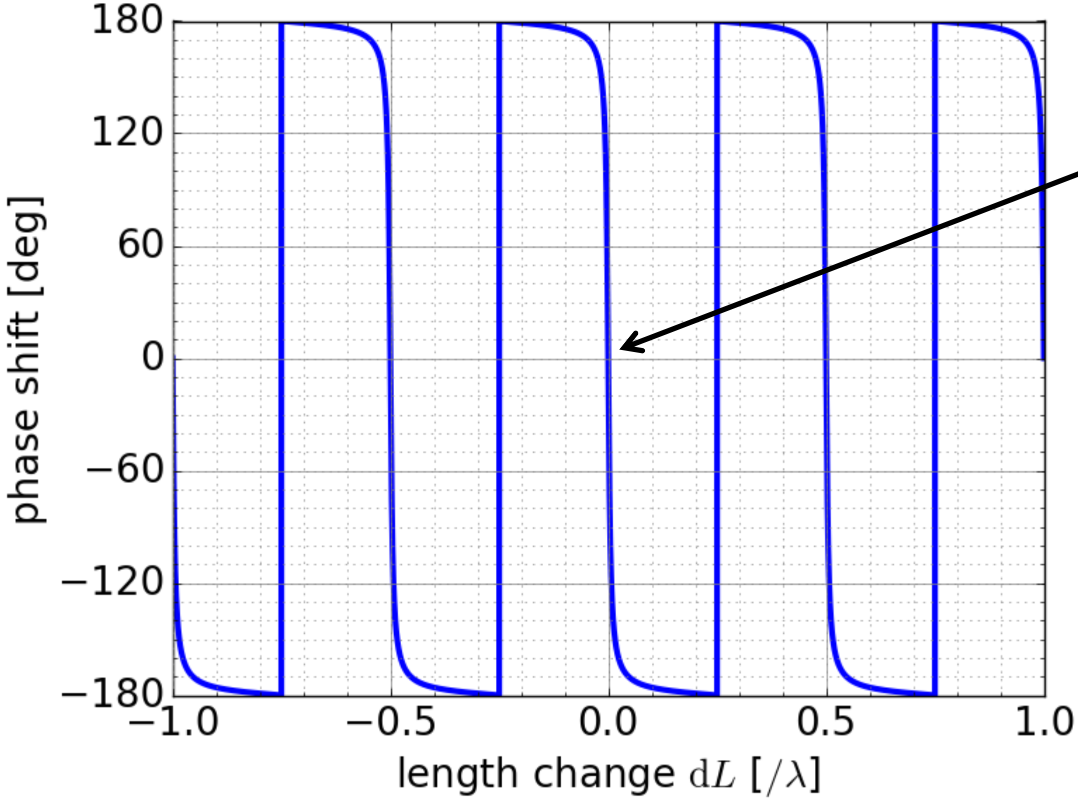

Phase of the reflected beam changes drastically at the resonance

$$\frac{\delta\phi}{\delta L} \simeq \boxed{\frac{2\mathcal{F}}{\pi}} \frac{4\pi}{\lambda}$$

Cavity build-up

Michelson and Fabry-Pérot

- The phase of the reflected light is different by $\frac{2\mathcal{F}}{\pi}$

$\rightarrow$ FP is more sensitive to mirror displacement

by $\frac{2\mathcal{F}}{\pi}$ (~ finesse)

but linear range is smaller

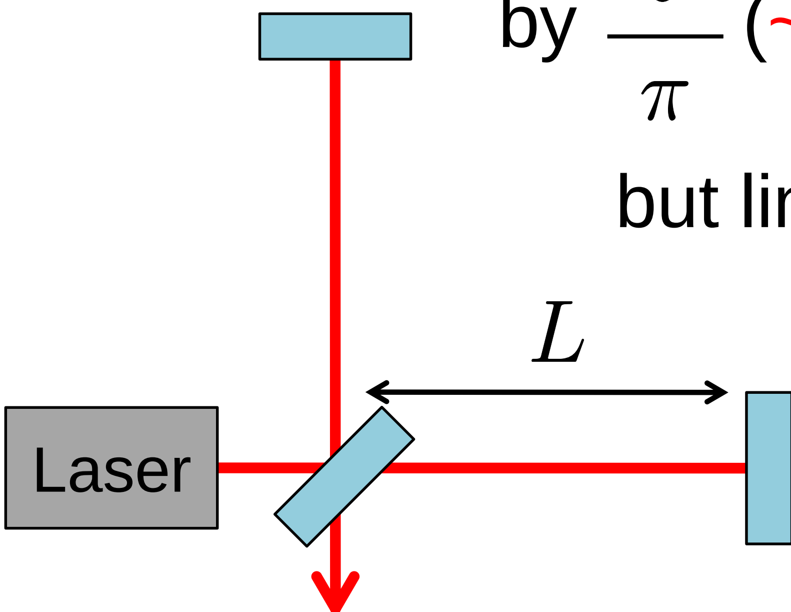

$$\phi = \frac{4\pi L}{\lambda}$$

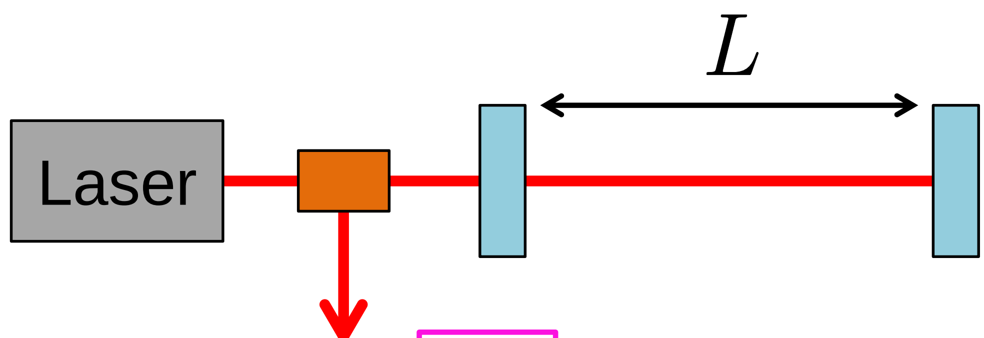

$$\frac{\delta\phi}{\delta L} \simeq \boxed{\frac{2\mathcal{F}}{\pi}}\frac{4\pi}{\lambda}$$

High-Frequency Response

- The effect of mirror displacement cancel at high frequencies

$$f_c = \frac{1}{2\pi}\Bigg(\underbrace{\frac{2\mathcal{F}}{\pi}\frac{L}{c}}_{\tau}\Bigg)^{-1} = \frac{c}{4L\mathcal{F}}$$

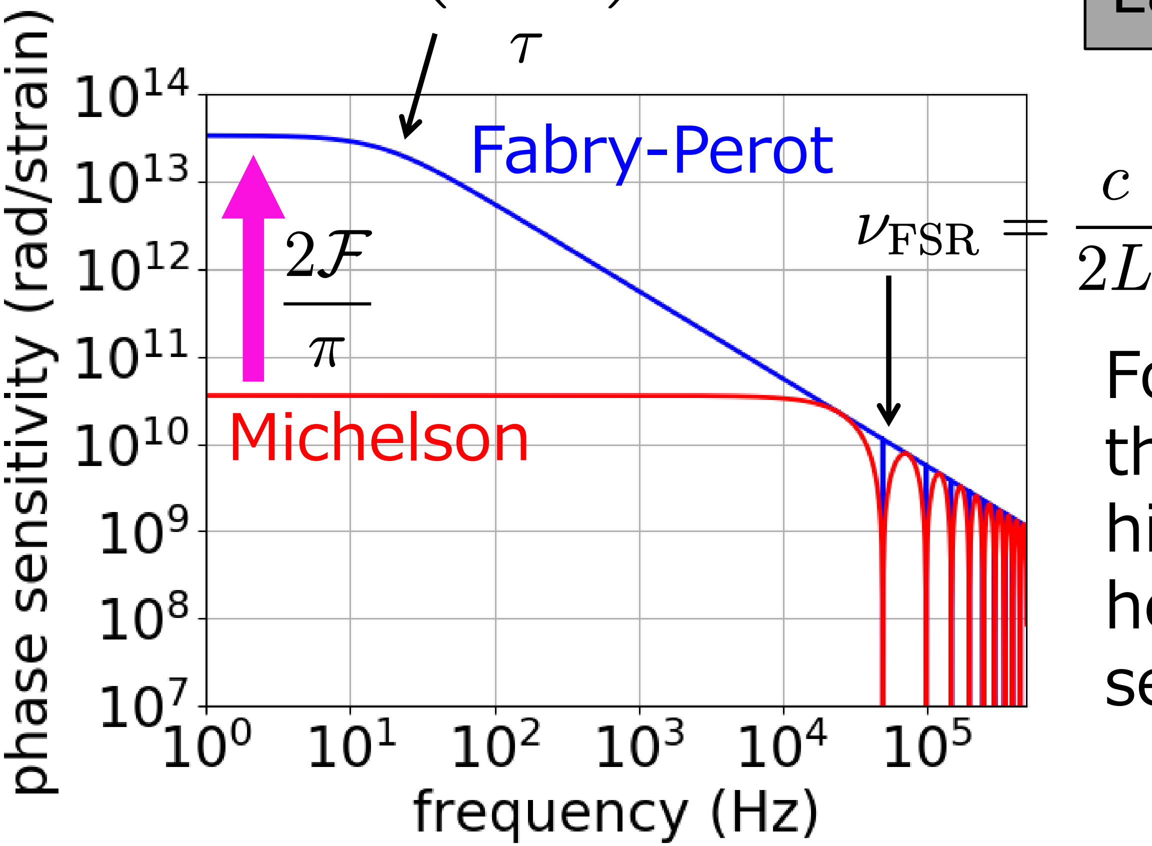

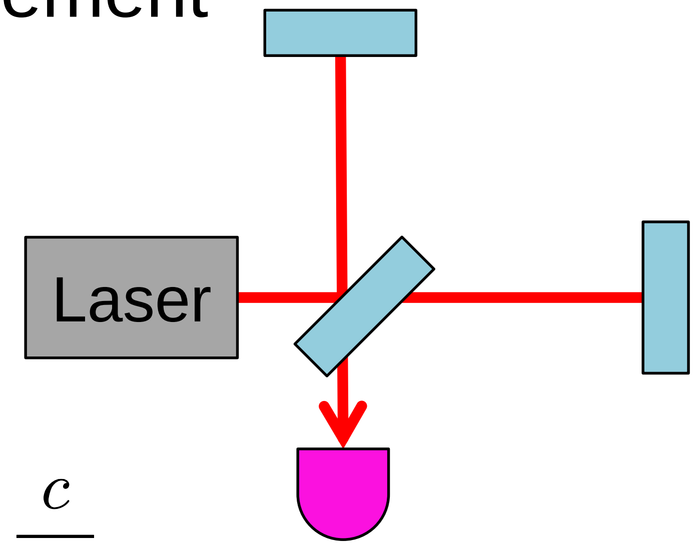

For a given frequency, there is a limit where higher finesse won't help increasing the sensitivity

Sensitivity

- Sensitivity of laser interferometers is fundamentally limited by
  - Seismic noise
  - Thermal noise
  - Quantum noise (shot noise and radiation pressure noise)

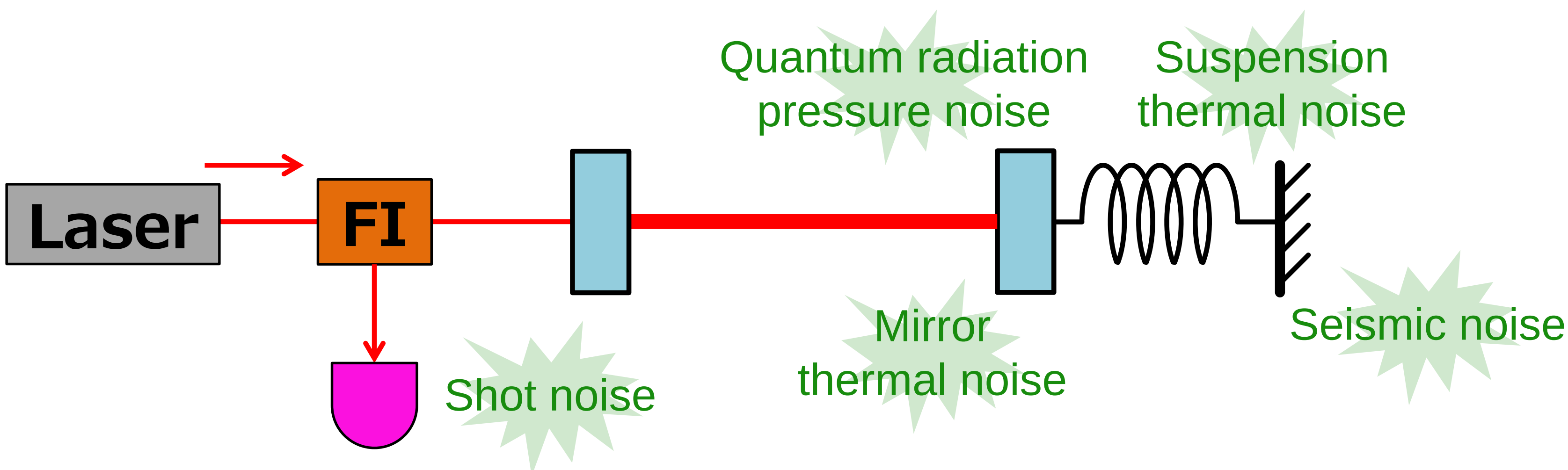

Thermal Noise

- Comes from Fluctuation-Dissipation Theorem

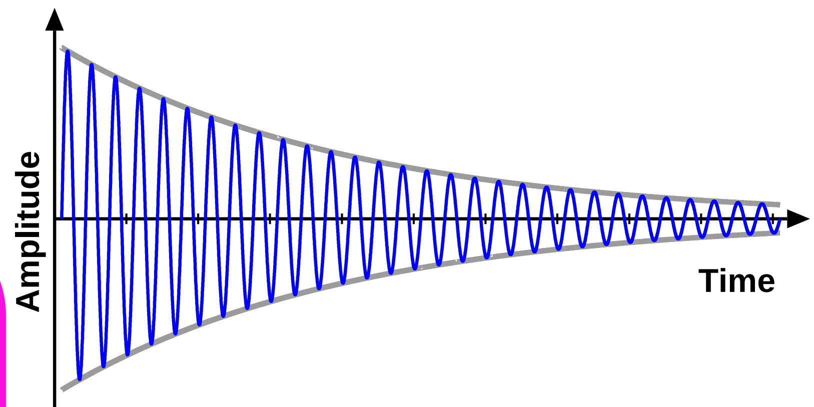

Damped harmonic oscillator

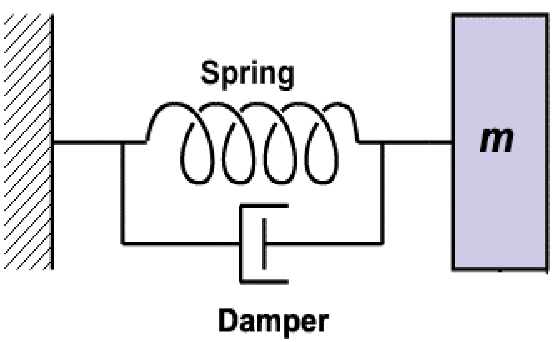

Energy dissipation

Thermal fluctuating force

Thermal bath

T_{th}

Thermal Noise Spectrum

- Thermal fluctuating force is

$$\sqrt{S^F_{\mathrm{th}}(\omega)} = \sqrt{4k_{\mathrm{B}}T_{\mathrm{th}}m\gamma_{\mathrm{m}}}$$

when equation of motion is given by

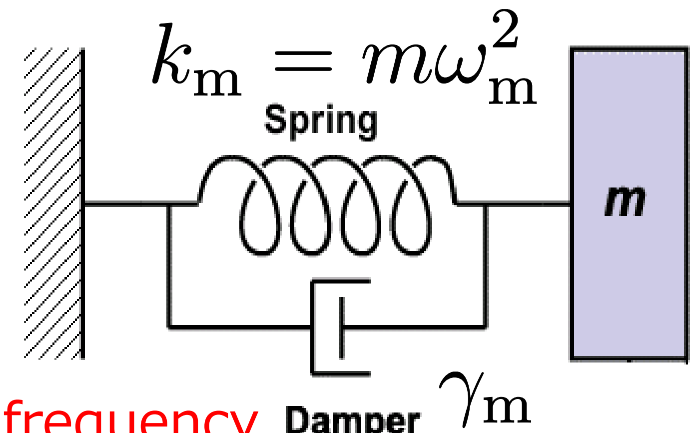

Mechanical resonant frequency

$$m[\ddot{x}(t) + \gamma_{\mathrm{m}}\dot{x}(t) + \omega_{\mathrm{m}}^2 x(t)] = F(t)$$

Energy damping rate

$$\gamma_{\mathrm{m}} = \frac{\omega_{\mathrm{m}}}{Q_{\mathrm{m}}}$$ viscous damping

$$\gamma_{\mathrm{m}}(\omega) = \frac{\omega_{\mathrm{m}}^2}{\omega Q_{\mathrm{m}}}$$ structural damping

- Force to displacement is given by mechanical susceptibility

$$\chi_{\mathrm{m}}(\omega) = \frac{x(\omega)}{F(\omega)} = \frac{1}{m(\omega_{\mathrm{m}}^2 - \omega^2 + i\gamma_{\mathrm{m}}\omega)}$$

Quantum Noise

- Radiation pressure noise
  Number of photons impinging on the mirror fluctuates with $\sqrt{P}$
- Shot noise
  Number of photons impinging on the photodiode fluctuates with $\sqrt{P}$
  Signal scales with P
  In total, shot noise scales with $1/\sqrt{P}$

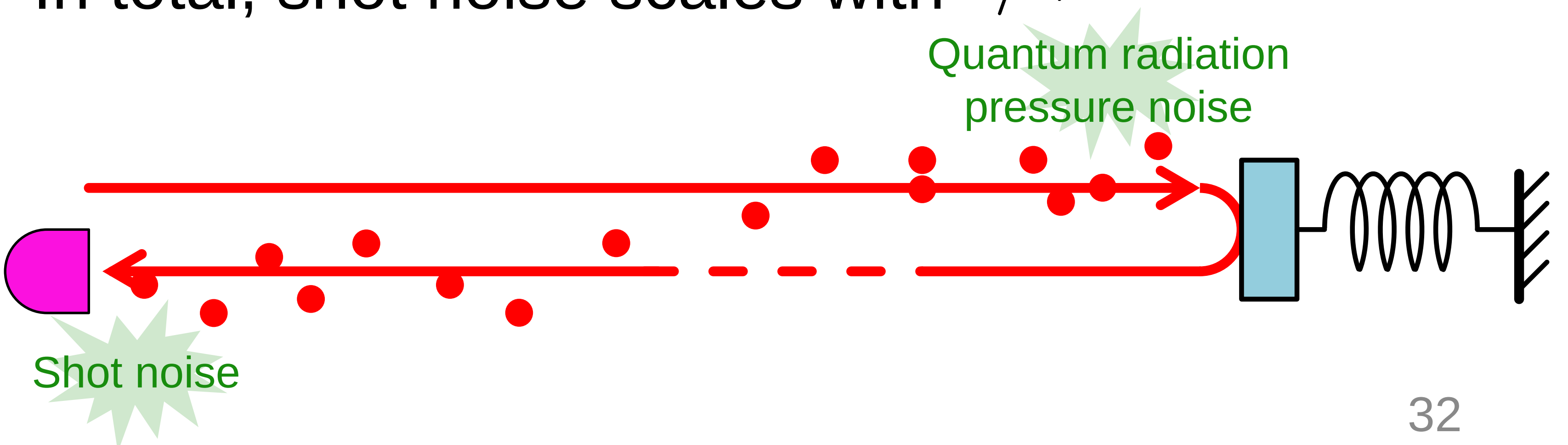

Quantum Noise Spectrum

- Given by

$$\sqrt{S_{\mathrm{qn}}^{x}(f)} = \sqrt{\frac{x_{\mathrm{SQL}}^{2}}{2}\left(\frac{1}{\mathcal{K}} + \mathcal{K}\right)}$$

Shot

Radiation pressure

laser frequency

mechanical susceptibility

$$\mathcal{K} = \frac{8\omega_{\mathrm{L}} P_{\mathrm{circ}} |\chi_{\mathrm{m}}(\omega)|}{L c \omega_{\mathrm{cp}}} \frac{1}{1 + (\omega/\omega_{\mathrm{cp}})^2}$$

cavity pole

- Standard quantum limit

$$x_{\mathrm{SQL}} = \sqrt{2\hbar |\chi_{\mathrm{m}}(\omega)|}$$

Standard Quantum Limit

- There’s a limit to sensitivity which cannot be surpassed by simply changing the laser power

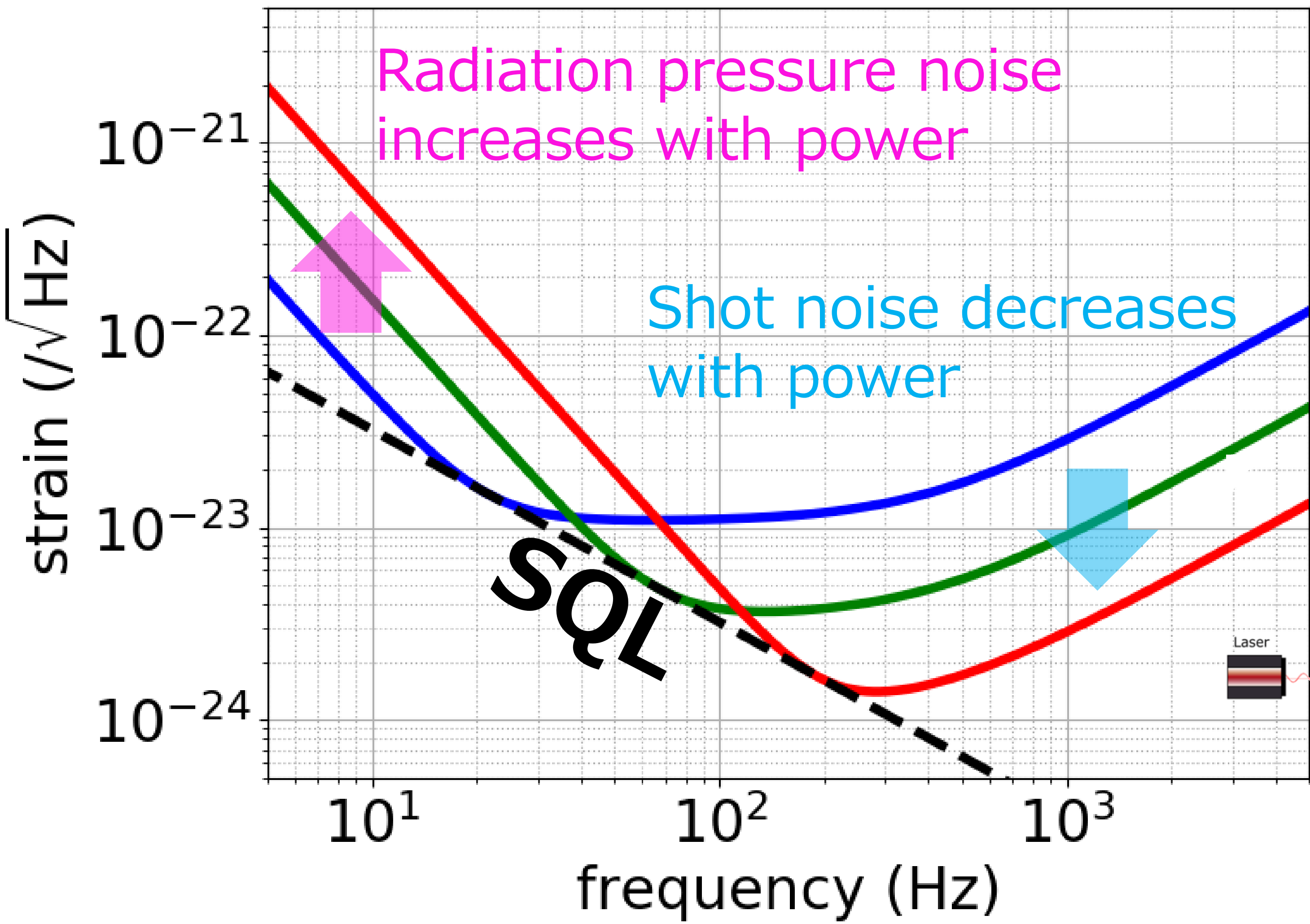

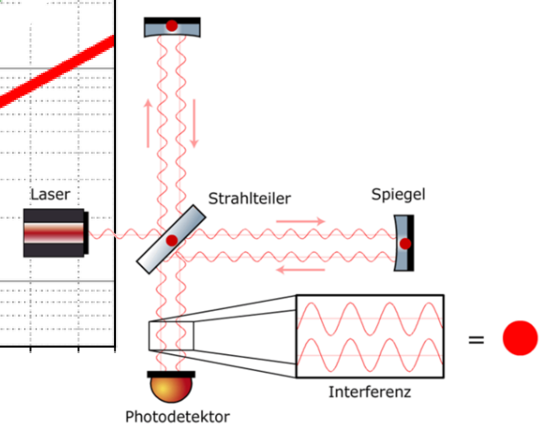

Example Sensitivity Curve

- ~1e-18 m/rtHz displacement sensitivity and ~1e-15 N/rtHz force sensitivity possible with realistic parameters
- 1 mg, 10 cm cavity, Finesse 1e3, 100 W circulating, Qm=1e9, Tth=300 K

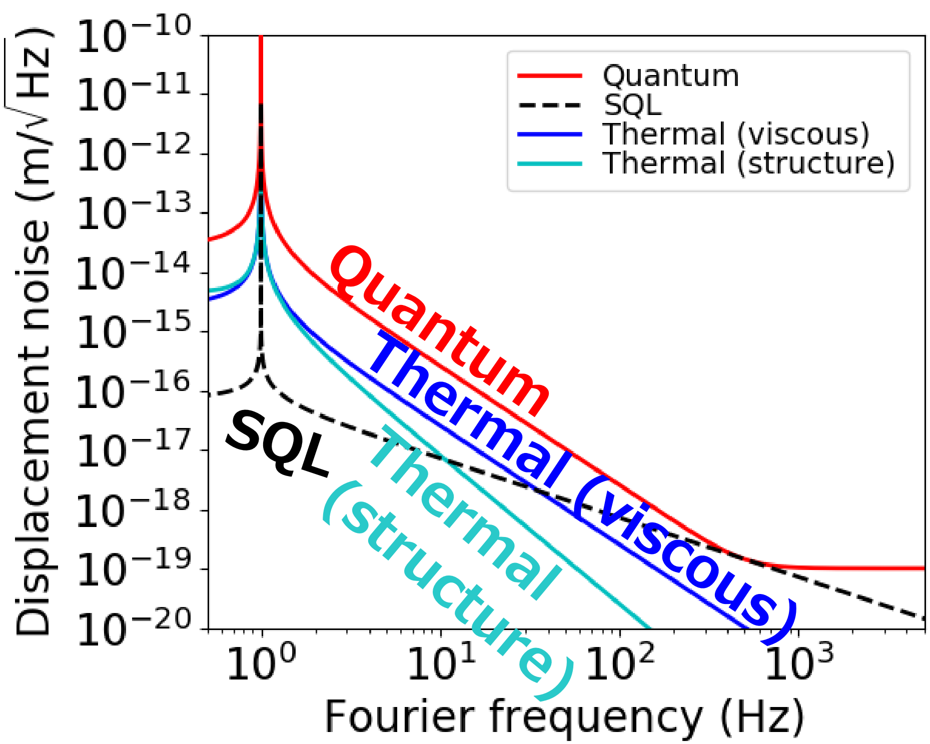

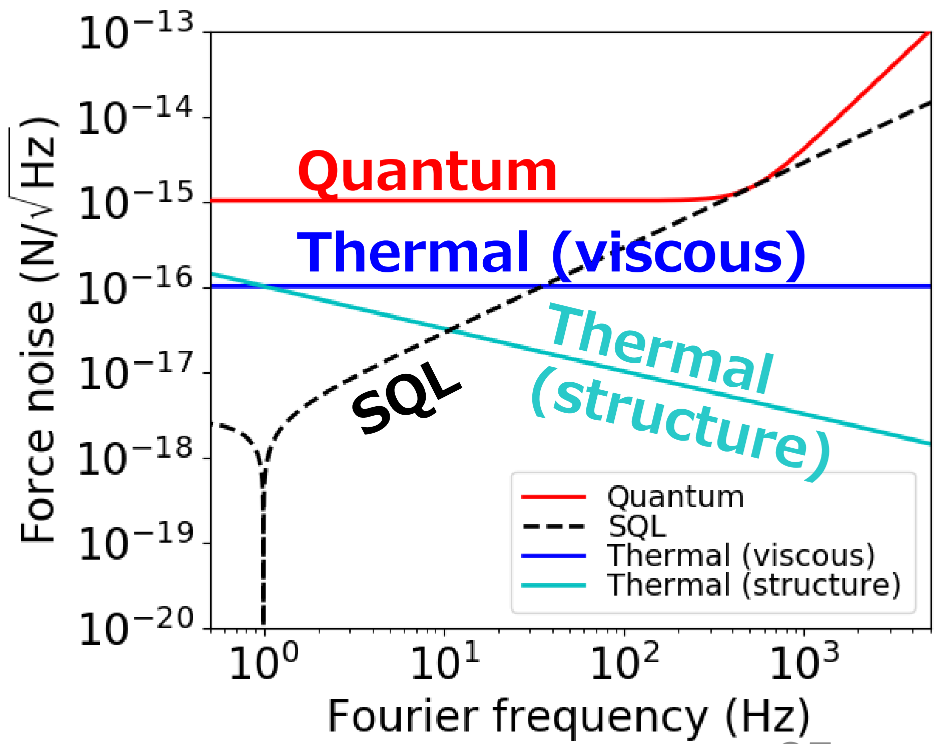

Summary of the Basics

- Optical cavities are sensitive to mirror displacement
- Resonant frequency changes with

$$\frac{\delta\nu}{\nu} = \frac{\delta L}{L} = \frac{\delta c}{c}$$

- Quantum noise and thermal noise are fundamental noise sources limiting the sensitivity of laser interferometers
- Shot noise scales with $1/\sqrt{P_{\mathrm{circ}}}$
- Radiation pressure noise scales with $\sqrt{P_{\mathrm{circ}}}/m$
- Thermal noise scales with $\sqrt{T_{\mathrm{th}}/Q_{\mathrm{m}}}$

Plan of the Talk

- **Basics of Laser Interferometry** (60 min)
  - Michelson interferometer
  - Fabry-Perot cavity
  - Quantum noise and other classical noises
- **Test of Lorentz Invariance** (30 min)
- **Search for Axion Dark Matter** (30 min)
- **Macroscopic Quantum Mechanics** (40 min)
- **KAGRA Gravitational Wave Telescope** (20 min)

- Slides available at https://tinyurl.com/YM20200109

Lorentz Invariance

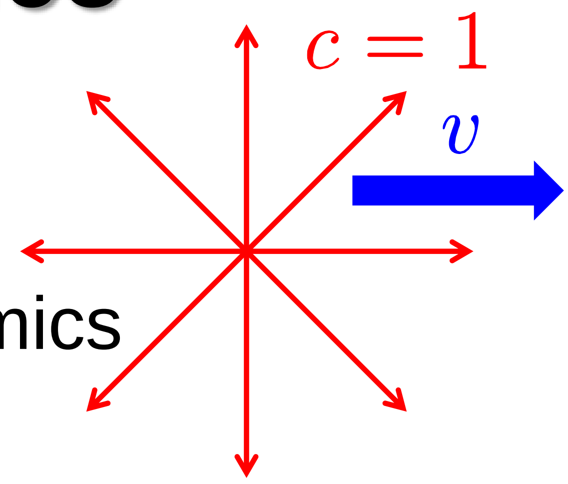

- Special Relativity (1905)
  speed of light is constant
- Lorentz invariance in electrodynamics
- no one could find any violation
- but…
  - quantum gravity suggests
    violation at some level
    e.g. $\delta c/c \sim 10^{-17}$

    D. Colladay and V. Alan Kostelecký:PRD 58 (1998) 116002

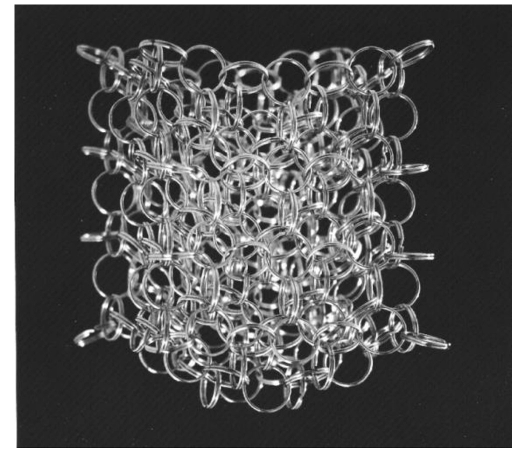

http://www.cpt.univ-mrs.fr/~rovelli/loop_quantum_gravity.jpg

  - anisotropy in CMB
    possible preferred frame?

$\longrightarrow$ motivation for testing SR

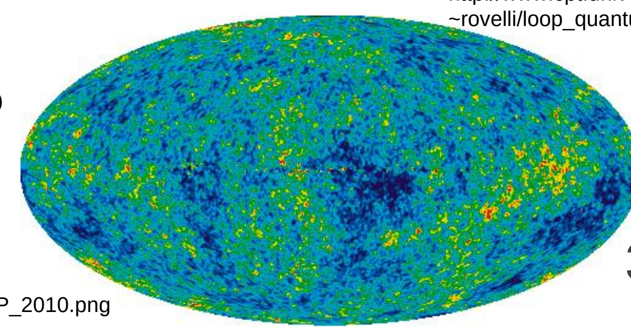

http://en.wikipedia.org/wiki/File:WMAP_2010.png

Test of Lorentz Invariance

- We focus especially on the isotropy of the speed of light (Lorentz invariance in photons)
- two types of test: even-parity and odd-parity

odd-parity test
(Ives-Stilwell type test)

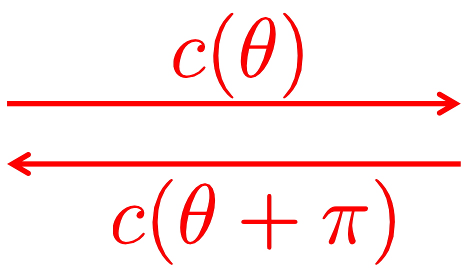

even-parity test
(Michelson-Morley type test)

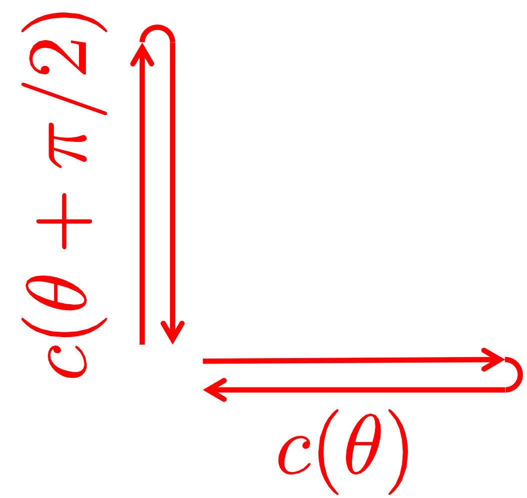

Previous Even-Parity Experiments

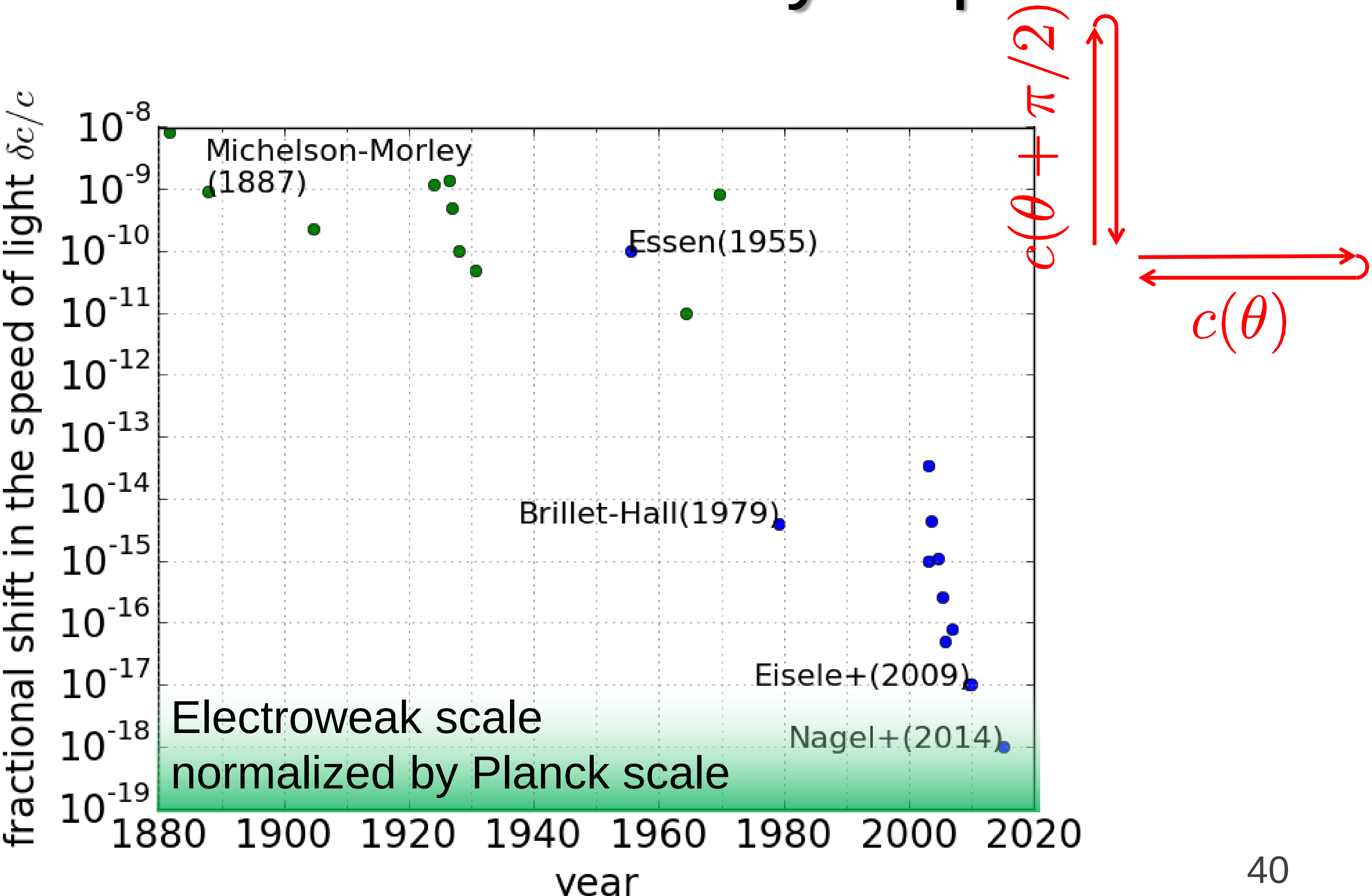

Previous Even-Parity Experiments

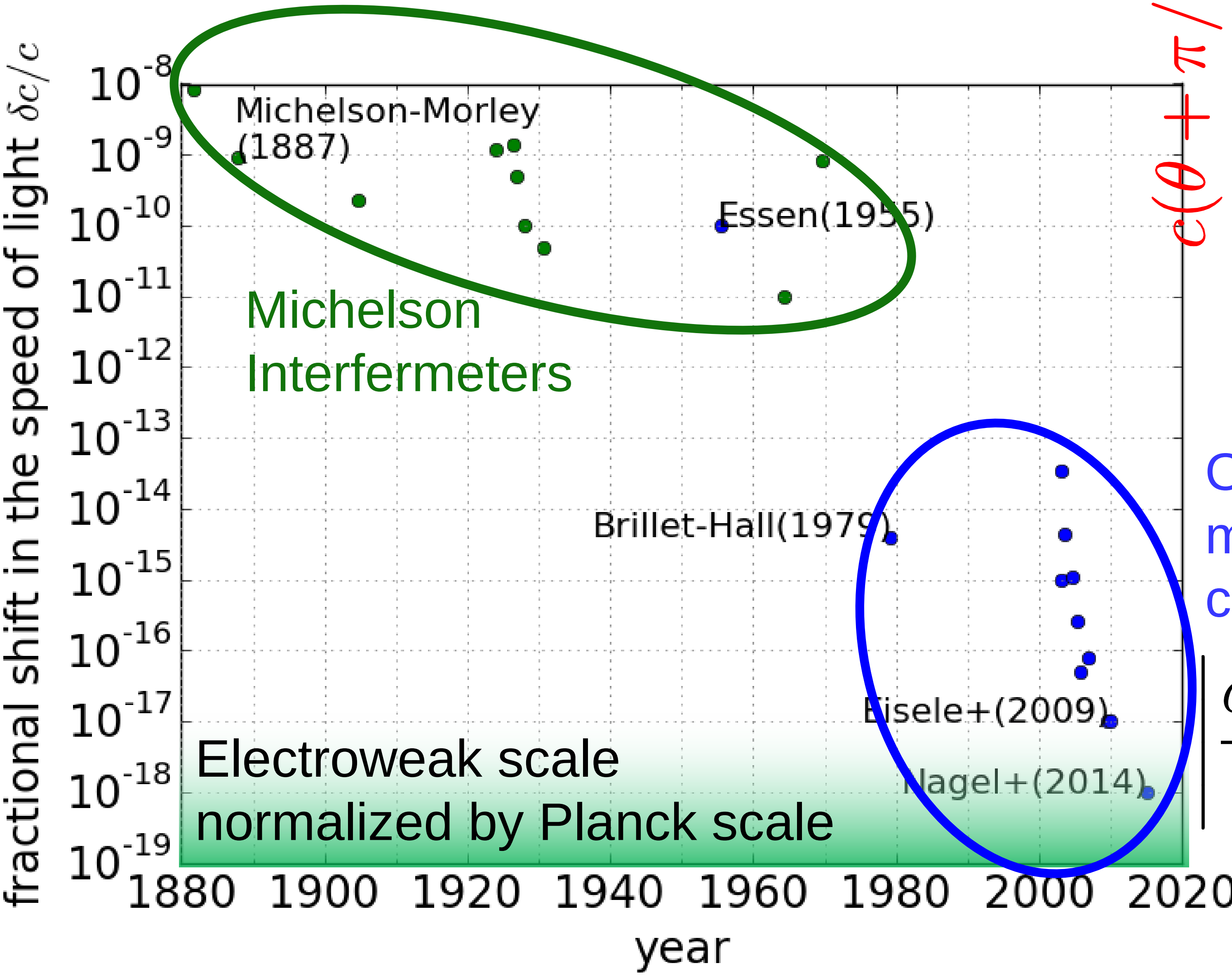

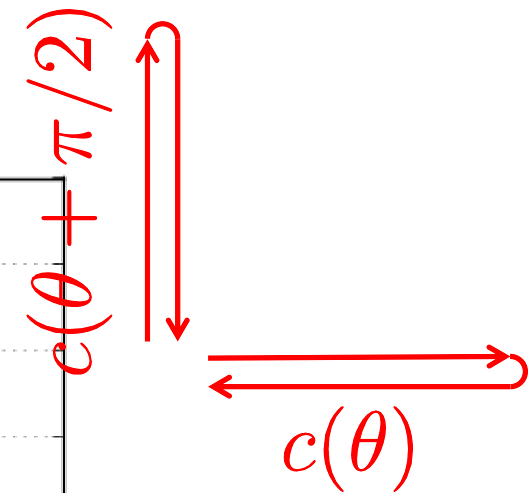

Optical and microwave cavities

$$\left|\frac{\delta c}{c}\right| \gtrsim 10^{-18}$$

Previous Odd-Parity Experiments

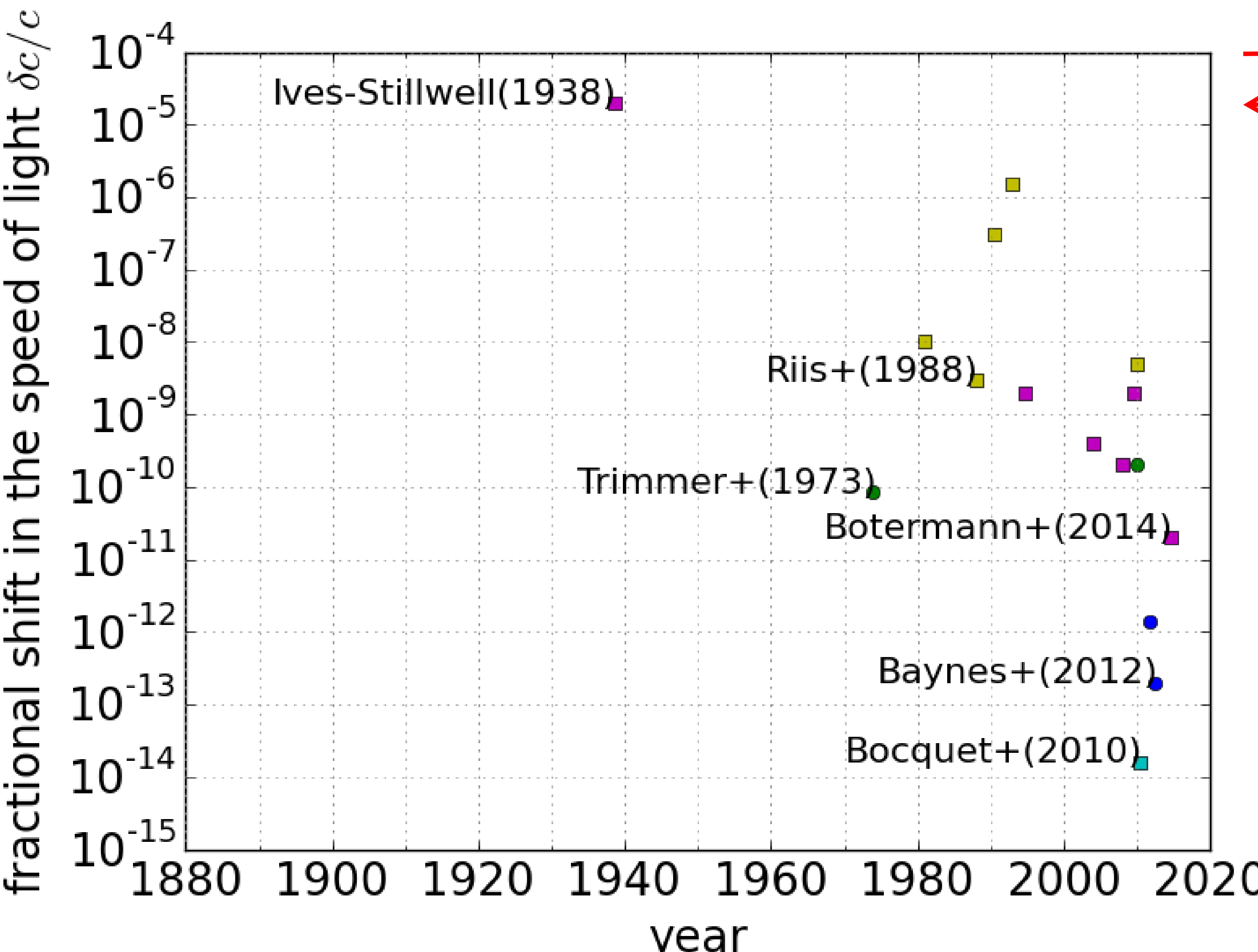

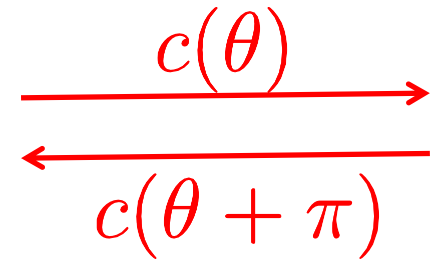

Previous Odd-Parity Experiments

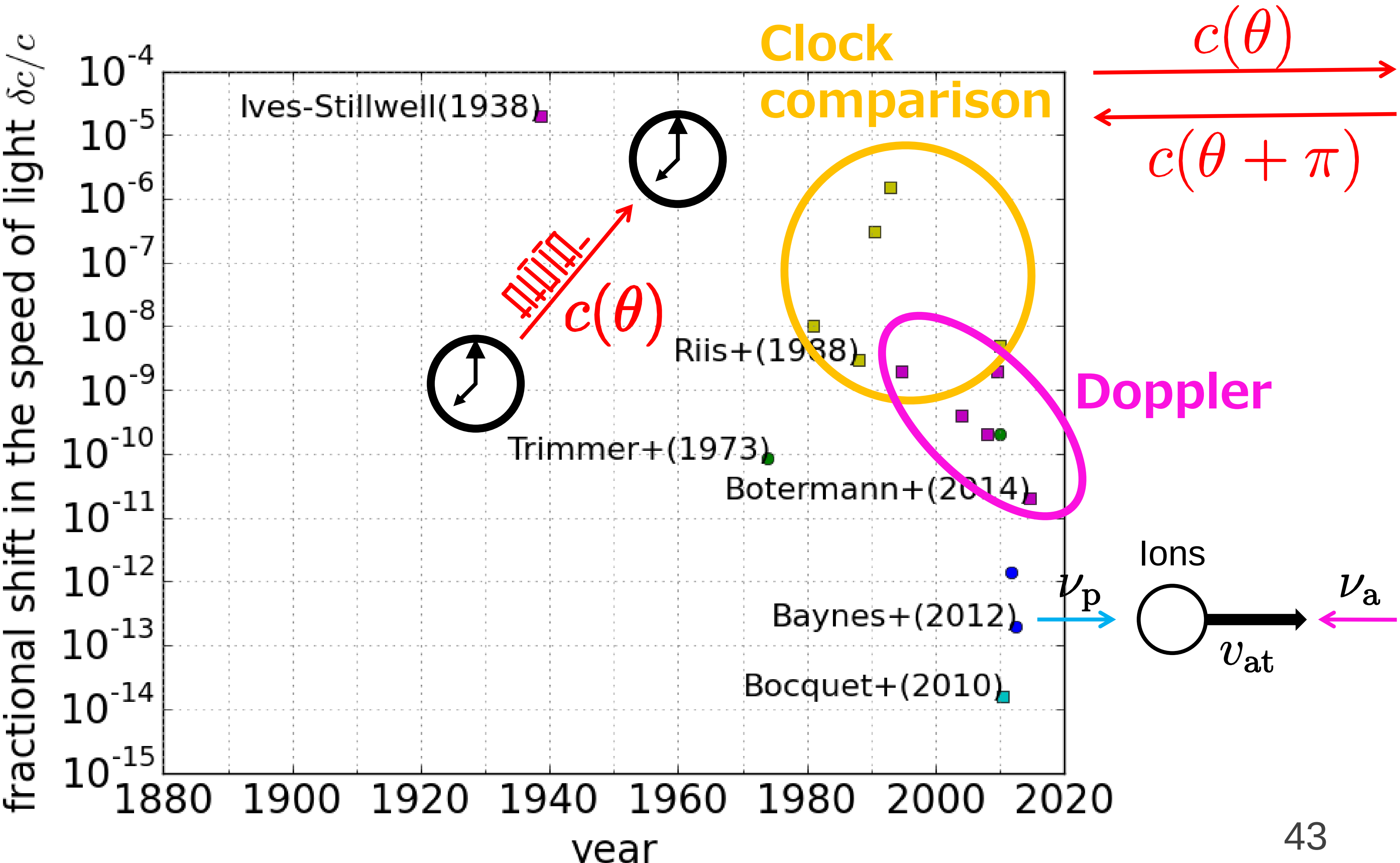

Odd-Parity with Interferometers?

- Not easy with ordinary interferometers or cavities since they are parity symmetric

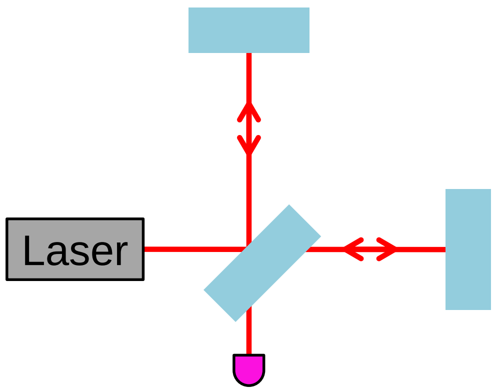

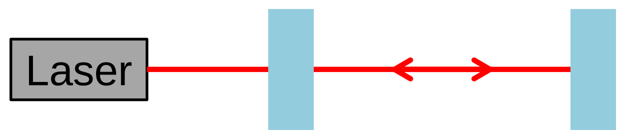

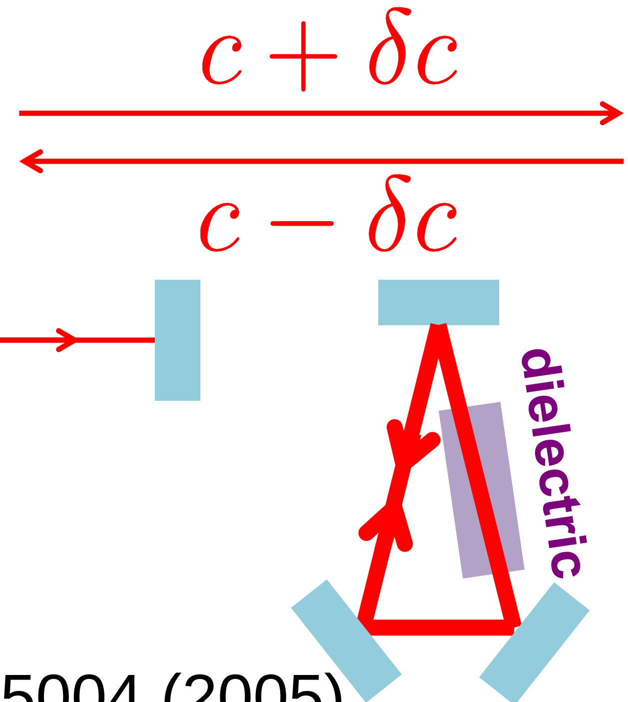

- Asymmetric optical cavity

  Proposal: M. E. Tobar+, PRD **71**, 025004 (2005)

  Demonstration: F. Baynes+, PRL **108**, 260801 (2012)

$$\left|\frac{\delta c}{c}\right| \lesssim 10^{-13}$$

$\rightarrow$ We have improved the sensitivity in this kind of experiments

Previous Odd-Parity Experiments

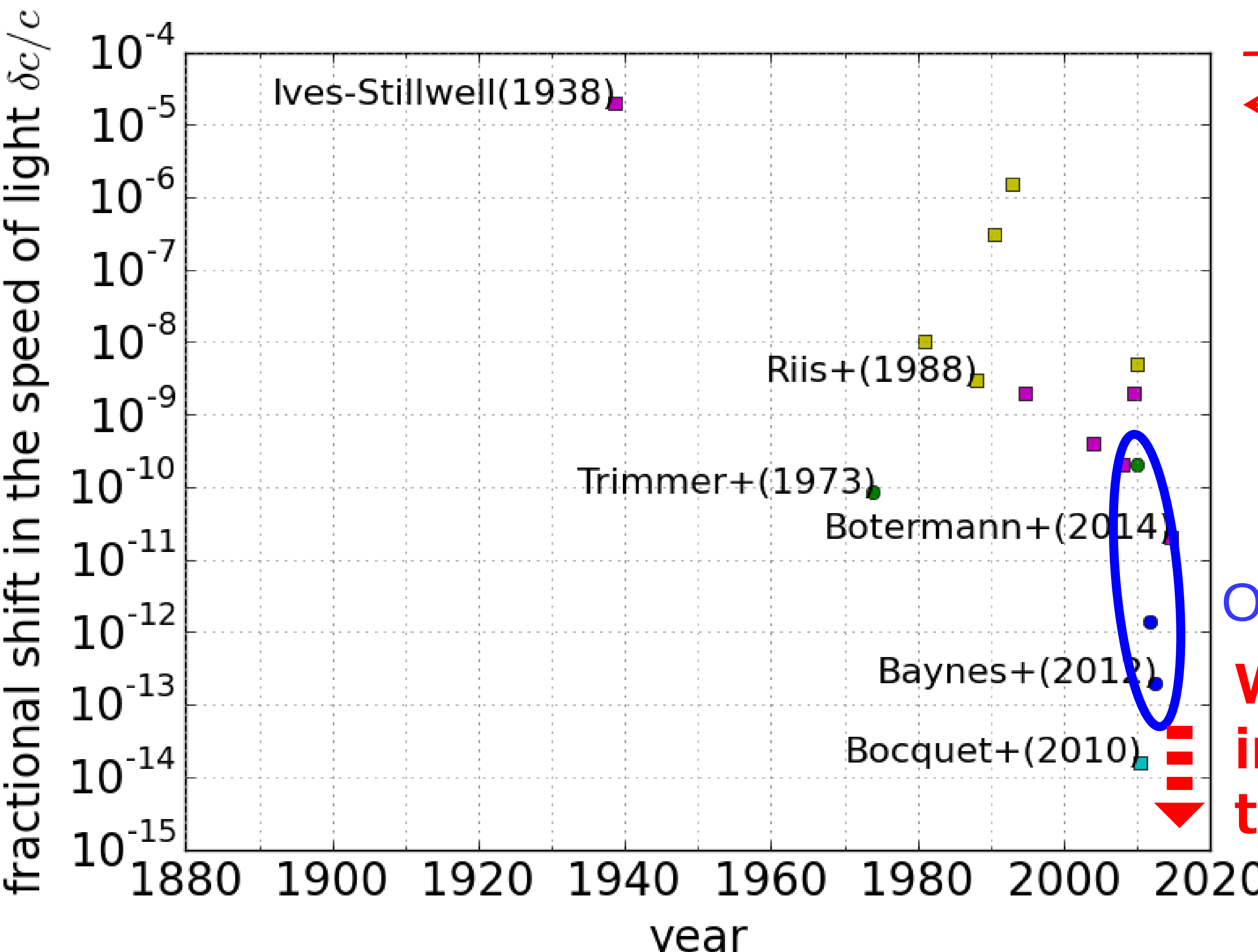

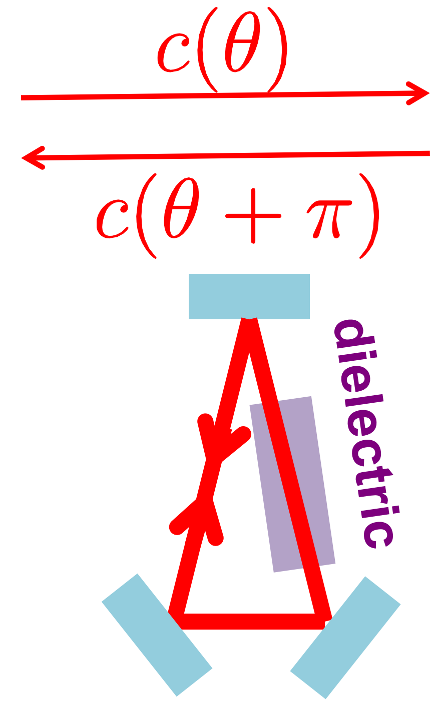

Optical cavity

We improved the limit

Higher Order Anisotropy

- multipole anisotropy comes from higher order Lorentz violation (standard model extension)

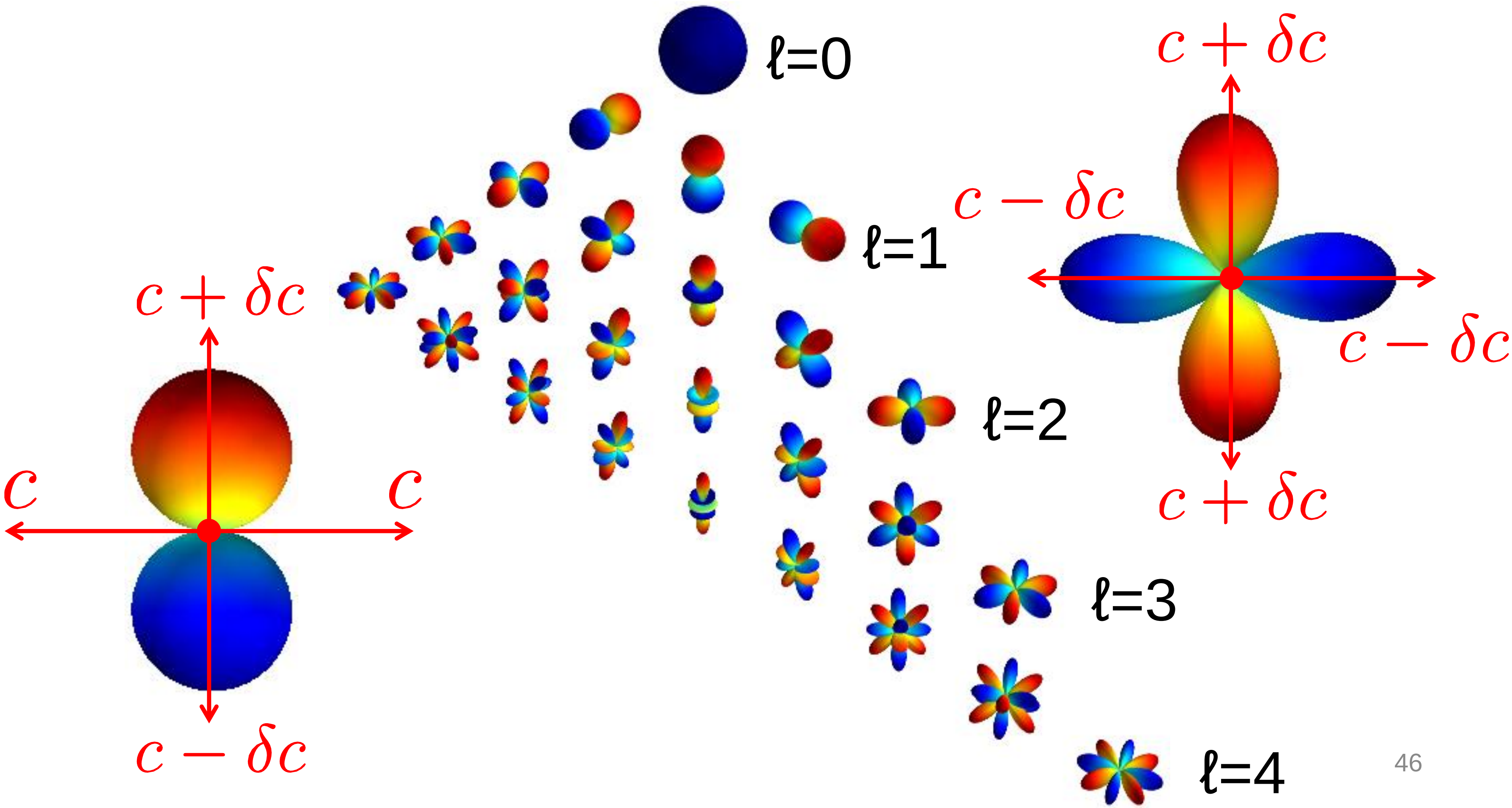

Previous Limits

- $l = \text{even}$ limits with even-parity experiments
- $l = \text{odd}$ limits with odd-parity experiments

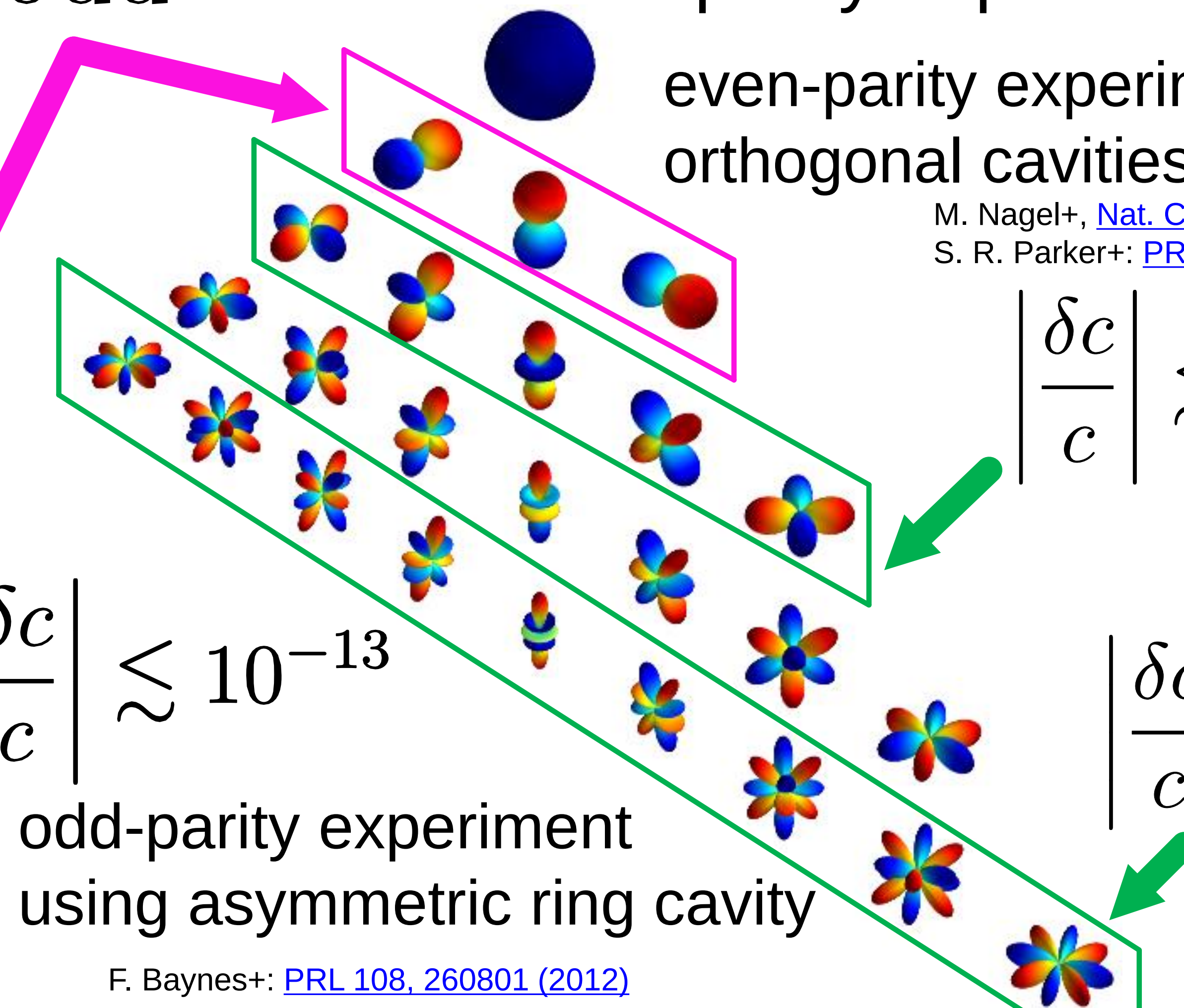

even-parity experiments using orthogonal cavities

M. Nagel+, [Nat. Commun. 6, 8174 (2015)]
S. R. Parker+: [PRL 106, 180401 (2011)]

$$\left|\frac{\delta c}{c}\right| \lesssim 10^{-18}$$

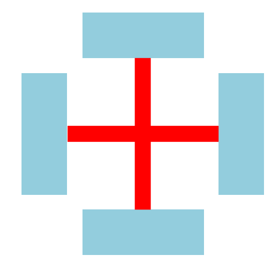

$$\left|\frac{\delta c}{c}\right| \lesssim 10^{-17}$$

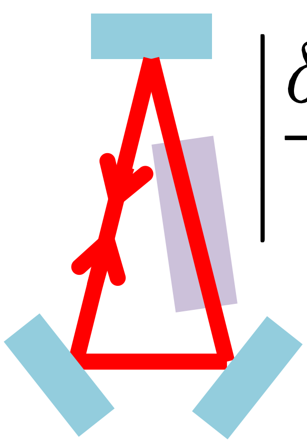

$$\left|\frac{\delta c}{c}\right| \lesssim 10^{-13}$$

odd-parity experiment using asymmetric ring cavity

F. Baynes+: [PRL 108, 260801 (2012)]

Our Limits

- improved limits on $l = 1$ (dipole) anisotropy
- new limits on $l = 3$ (hexapole) anisotropy

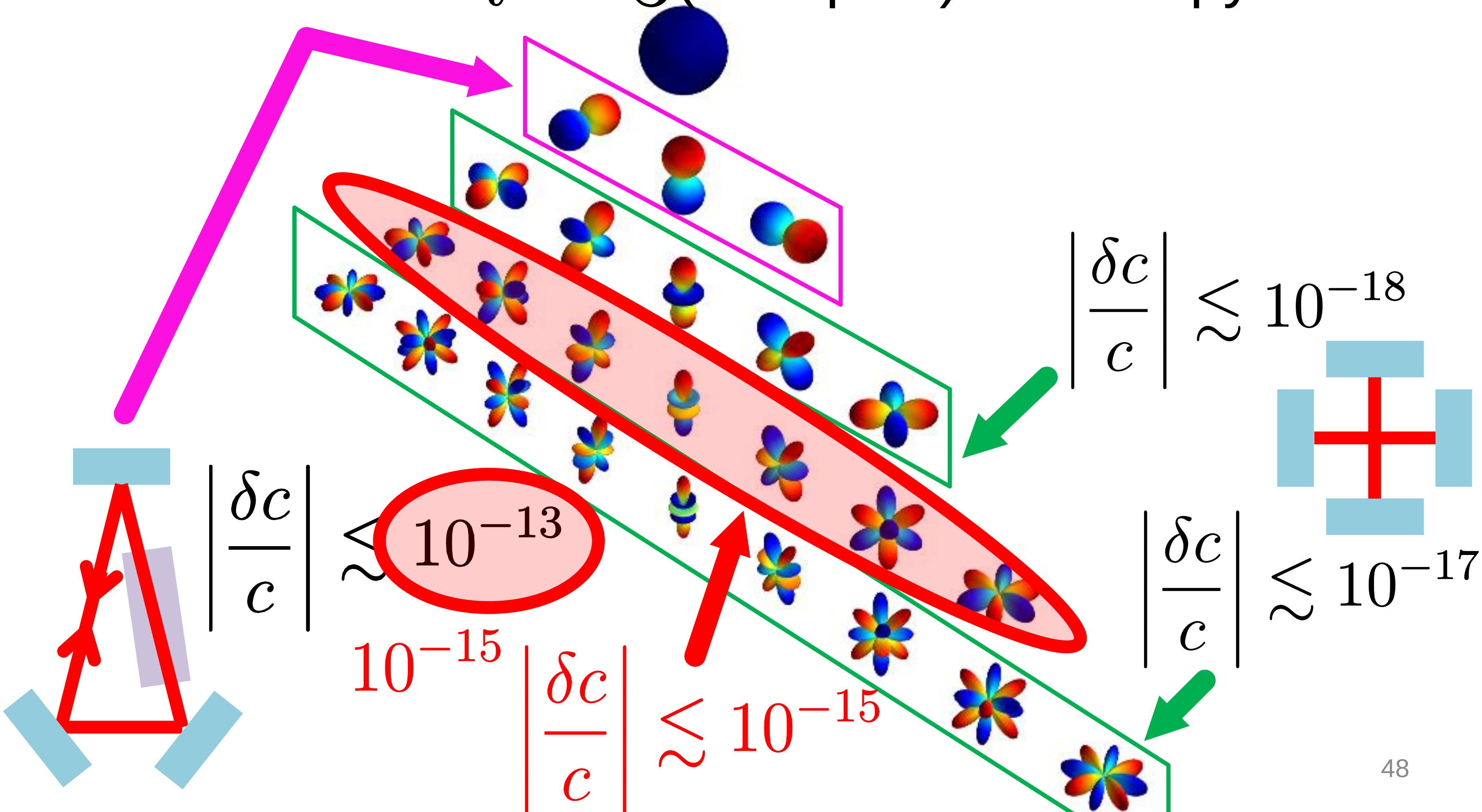

Optical Ring Cavity

- sensitive to LV when a dielectric is contained

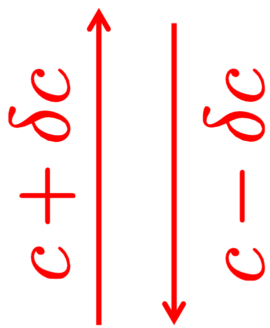

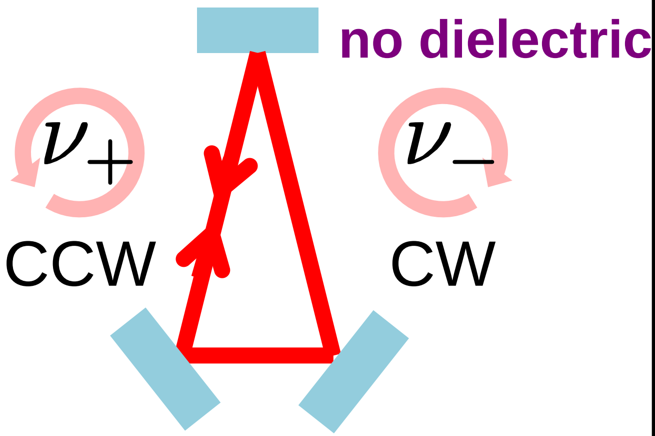

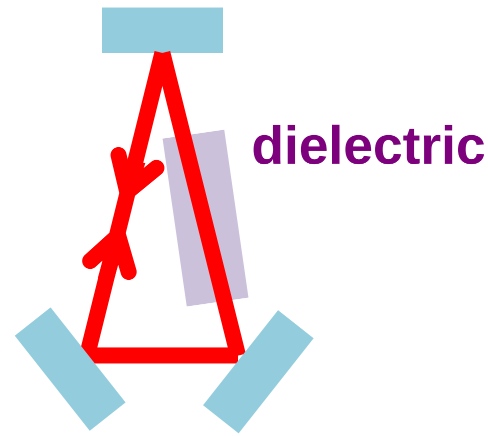

	no dielectric	dielectric
no LV	$\nu_+ = \nu_0$ $\nu_- = \nu_0$	$\nu_+ = \nu$ $\nu_- = \nu$
LV	$\nu_+ = \nu_0$ $\nu_- = \nu_0$	$\nu_+ = \nu - \delta\nu$ $\nu_- = \nu + \delta\nu$

freq. shift $\propto$ LV

- $\nu_+ - \nu_-$ gives LV signal (null measurement)

Differential Measurement

- Cavity length change gives common resonant frequency change, and can be rejected by differential measurement
- Highly insensitive to environmental disturbances
- Differential measuremend done by double-pass configuration

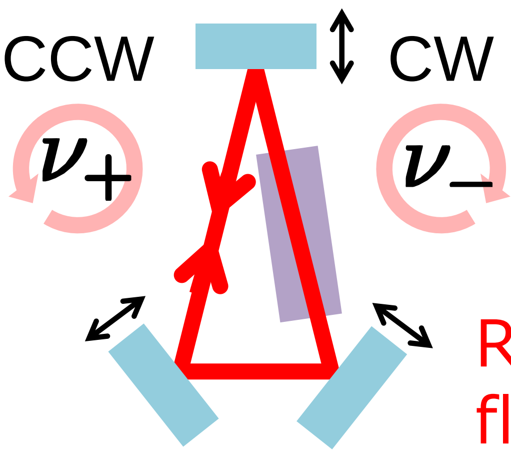

$$\nu_+ = \nu + \delta\nu_{\mathrm{noise}} - \delta\nu_{\mathrm{LV}}$$
$$\nu_- = \nu + \delta\nu_{\mathrm{noise}} + \delta\nu_{\mathrm{LV}}$$

Resonant frequency fluctuation from cavity length change is common

Resonant frequency shift from LV is differential

Double-Pass Configuration 1/4

- inject laser beam in CCW

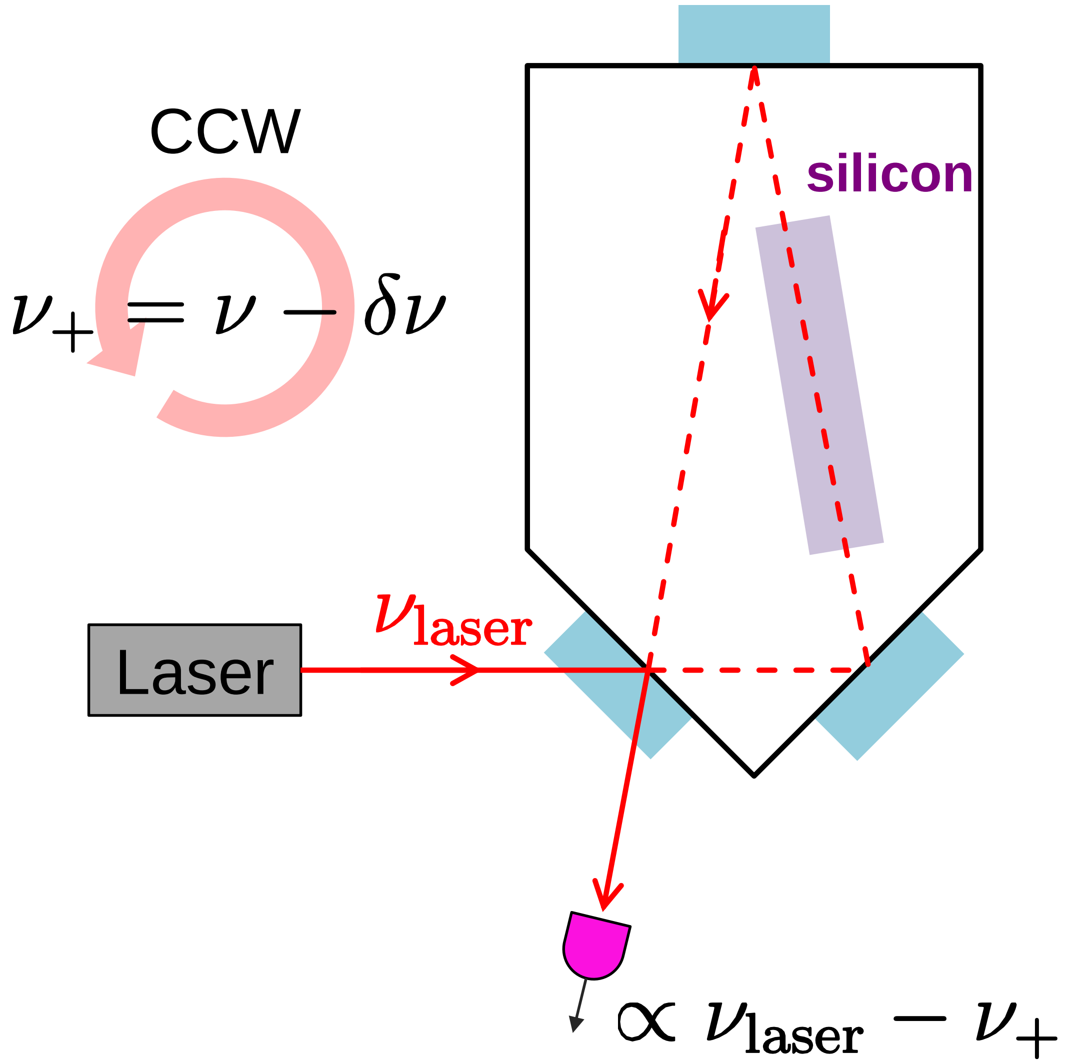

Double-Pass Configuration 2/4

- lock laser frequency to CCW resonance (ν_+)

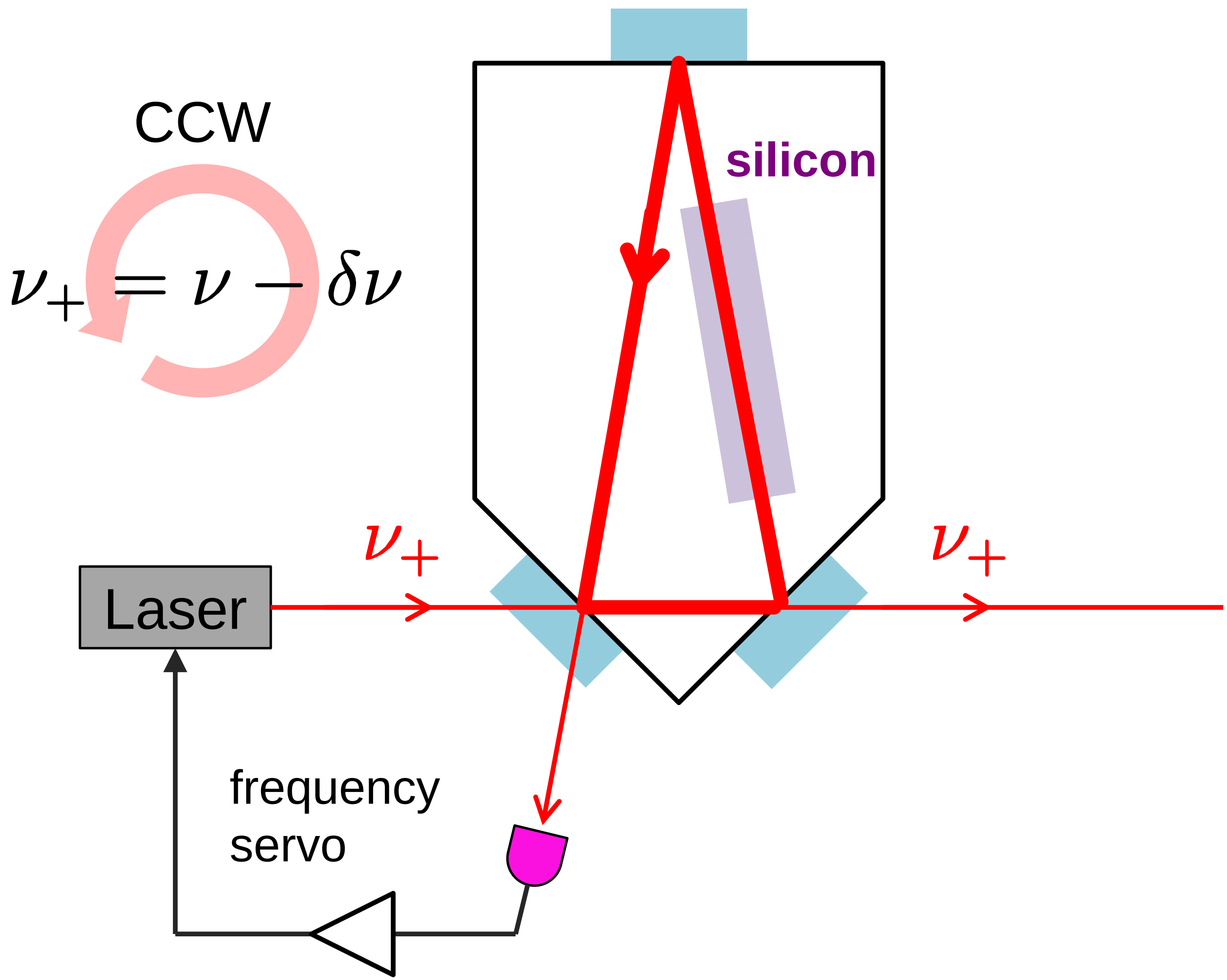

Double-Pass Configuration 3/4

- reflect the beam back into the cavity in CW

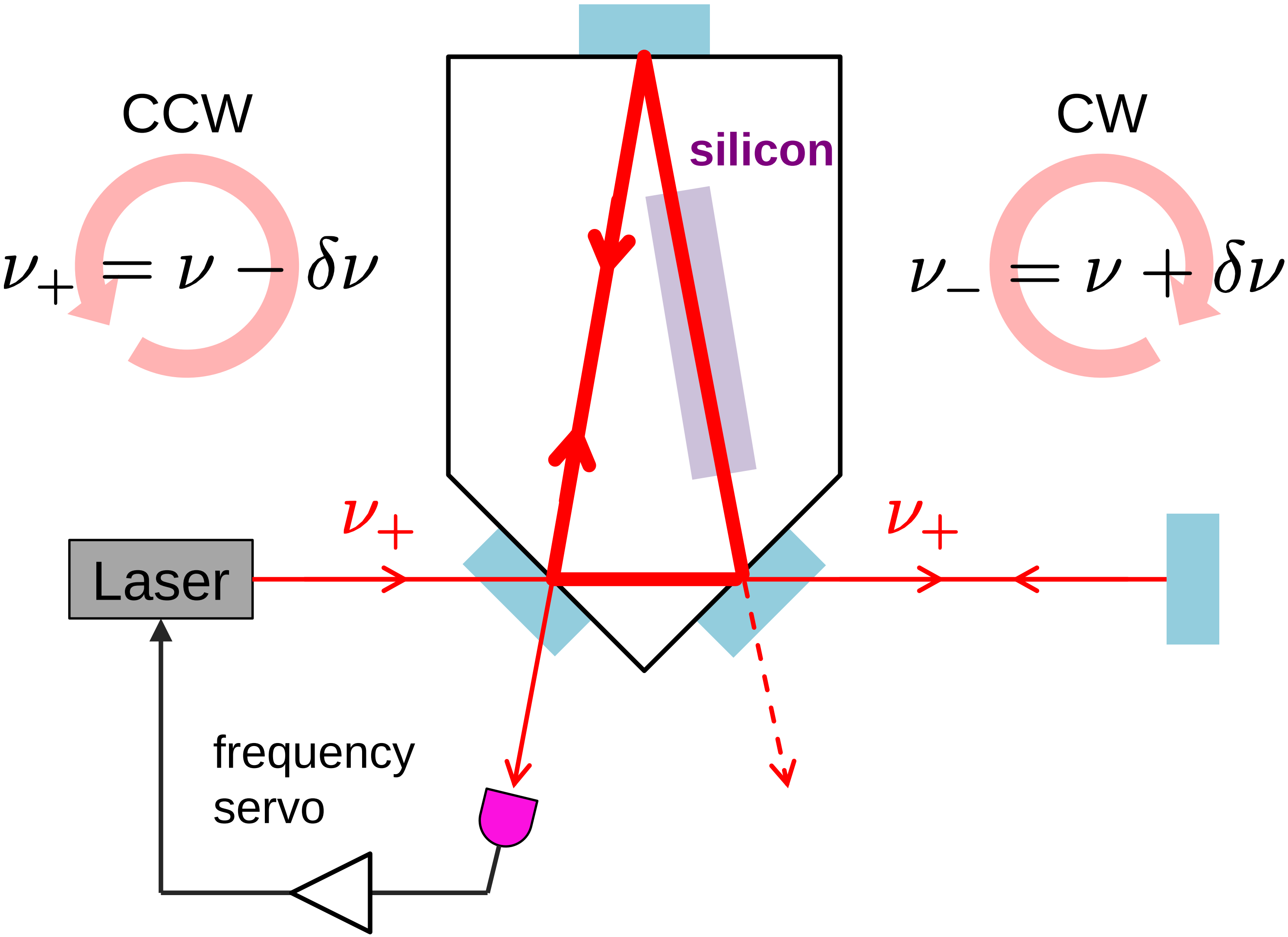

Double-Pass Configuration 4/4

- LV signal obtained from cavity reflection (null measurement)

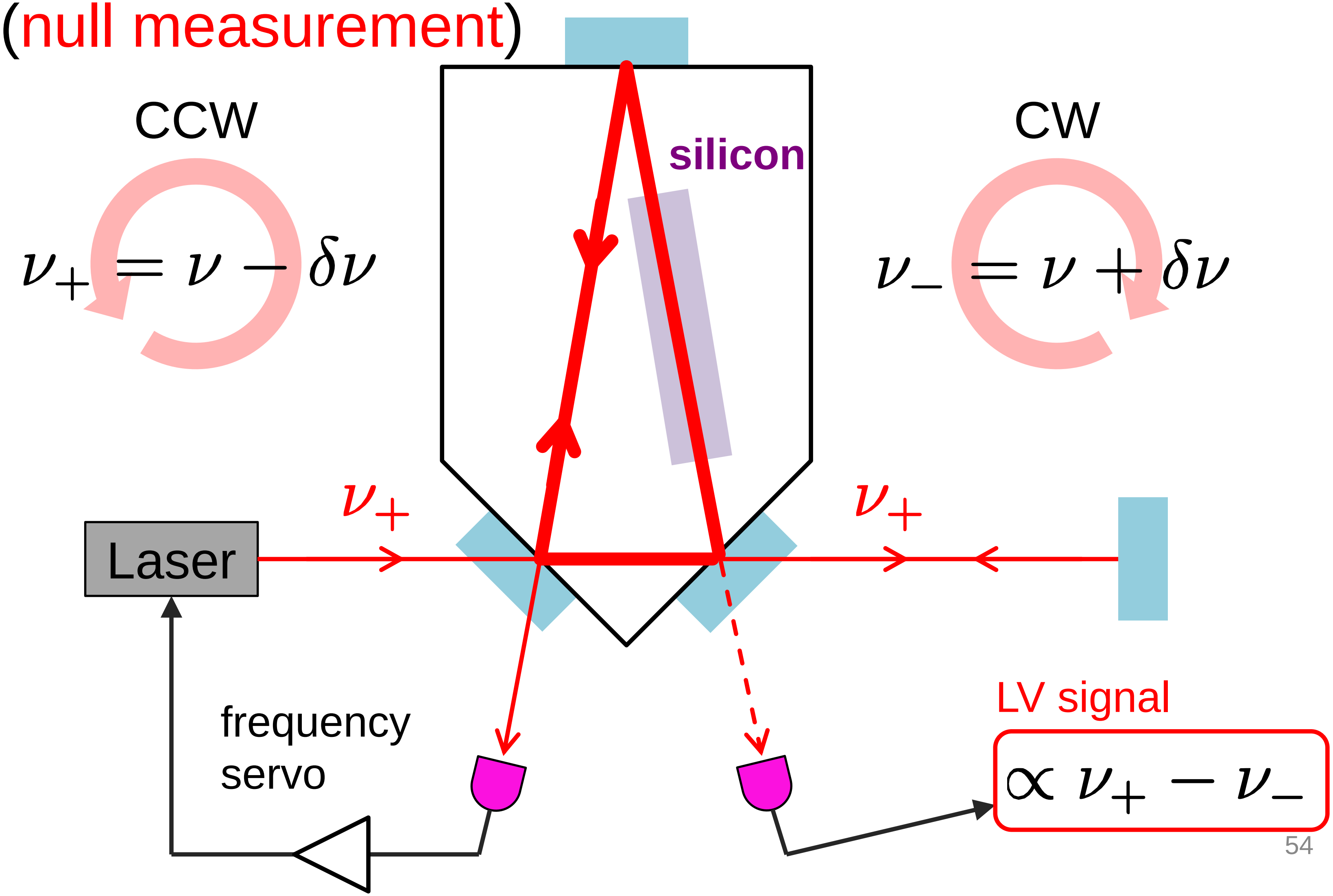

Experimental Setup

- frequency comparison using double-pass setup
- rotate and modulate LV signal

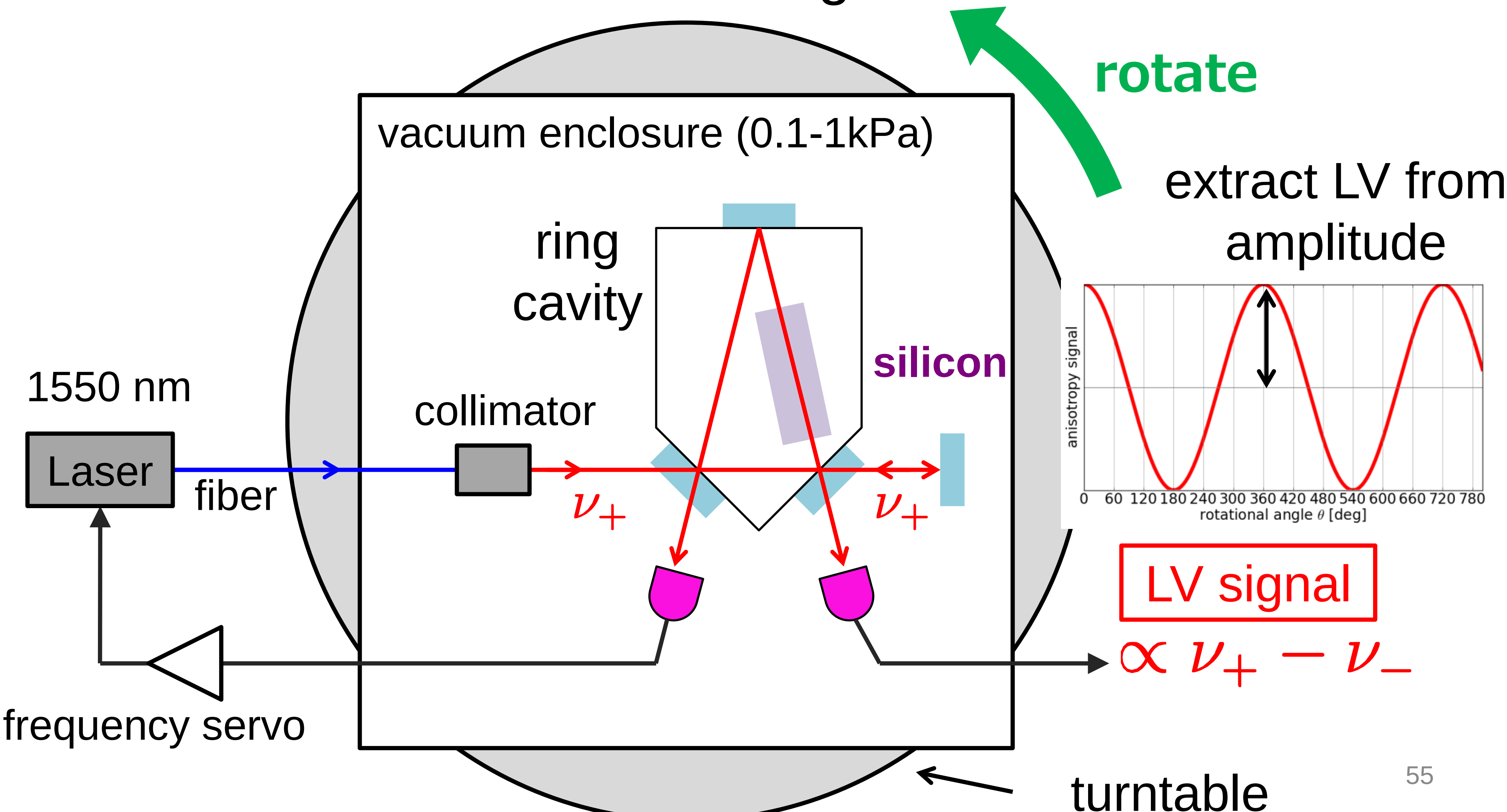

Photo of the Ring Cavity

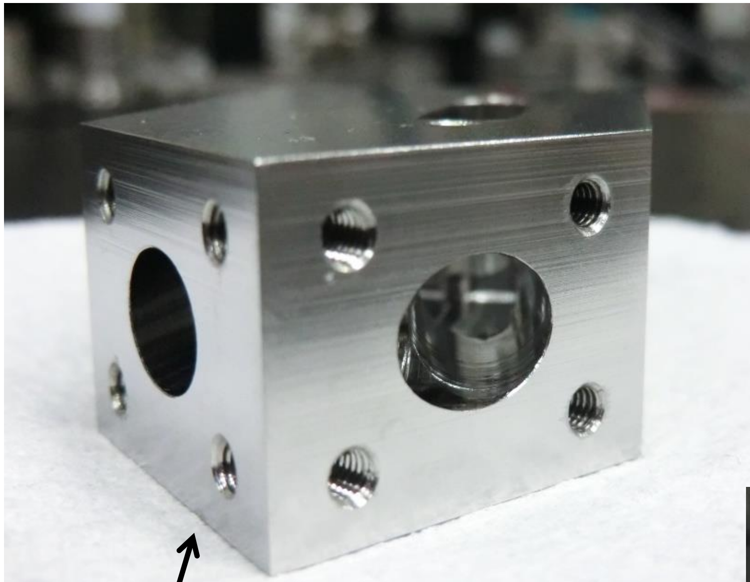

Spacer made of Super Invar (low thermal expansion 10^{-7}/K)

With mirrors

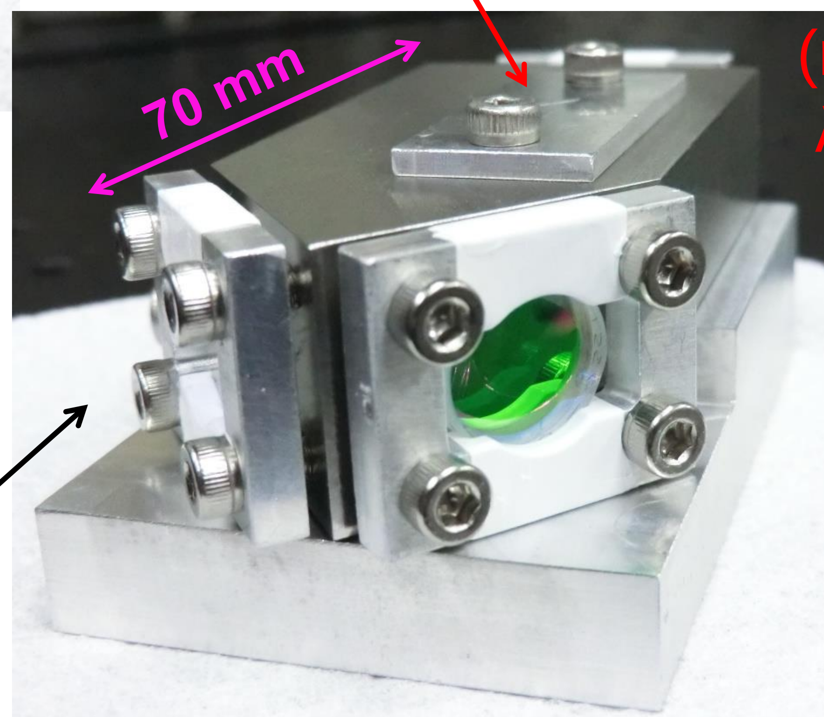

Silicon piece inside

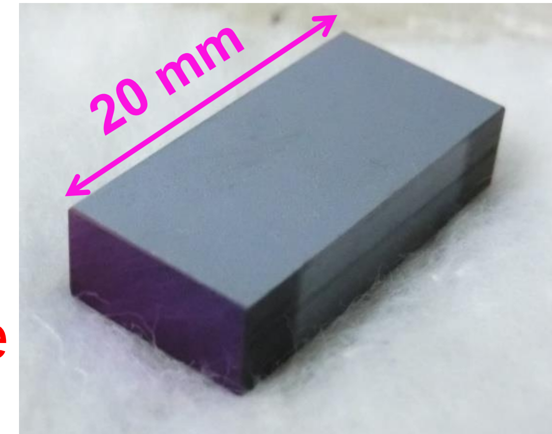

Silicon piece (n=3.69 at λ=1550 nm)

Photo of the Optics

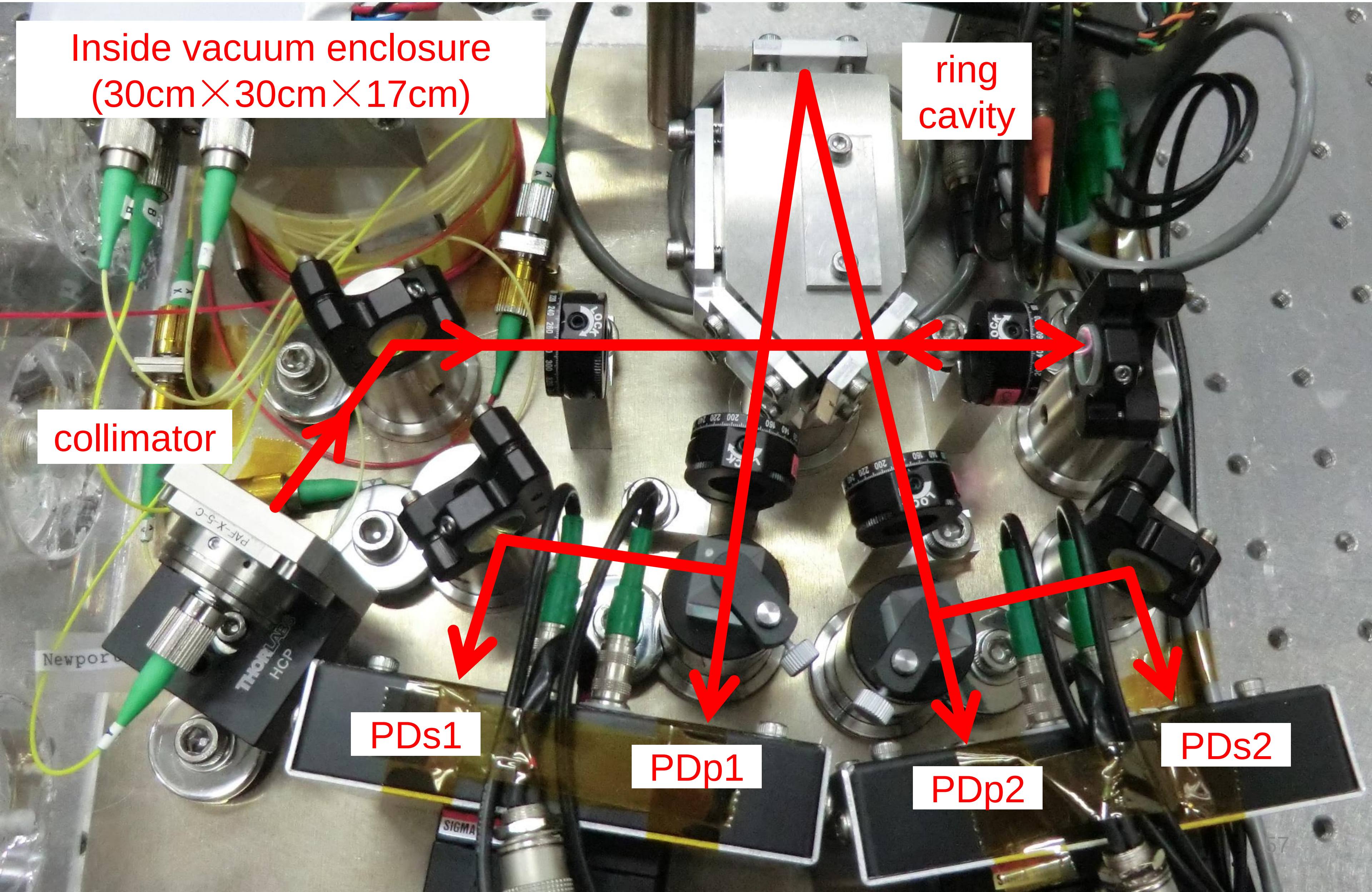

Photo of the Whole Setup

electrical cables

laser source

vacuum enclosure
+ shielding
(optics inside)

turntable

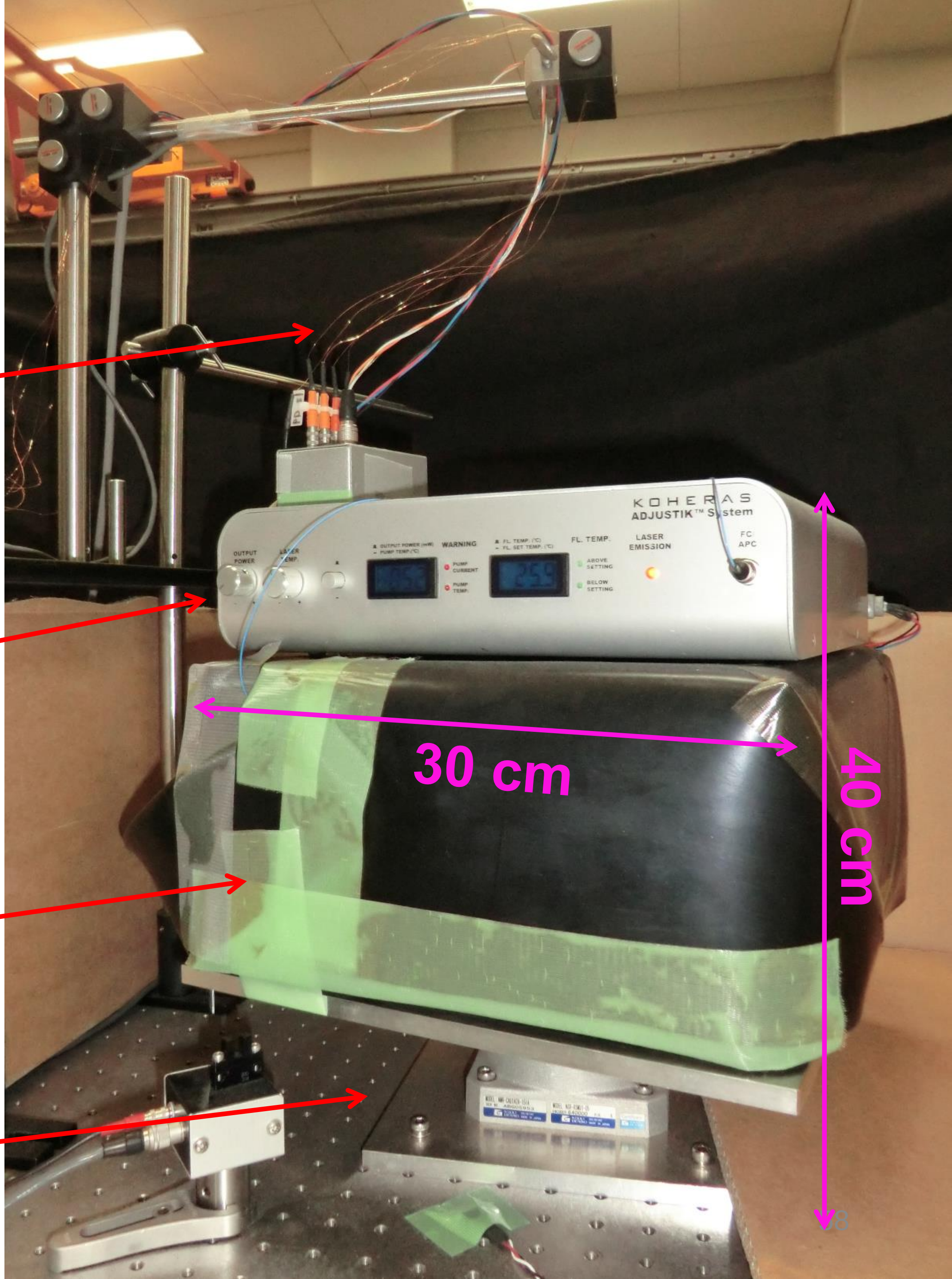

Rotation

- 12 sec / rotation, alternately

Observation Data

- from July 2012 to October 2013 at Tokyo
- 393 days, 1.67 million rotations
- duty cycle: 53% (64% after Oct 2012)

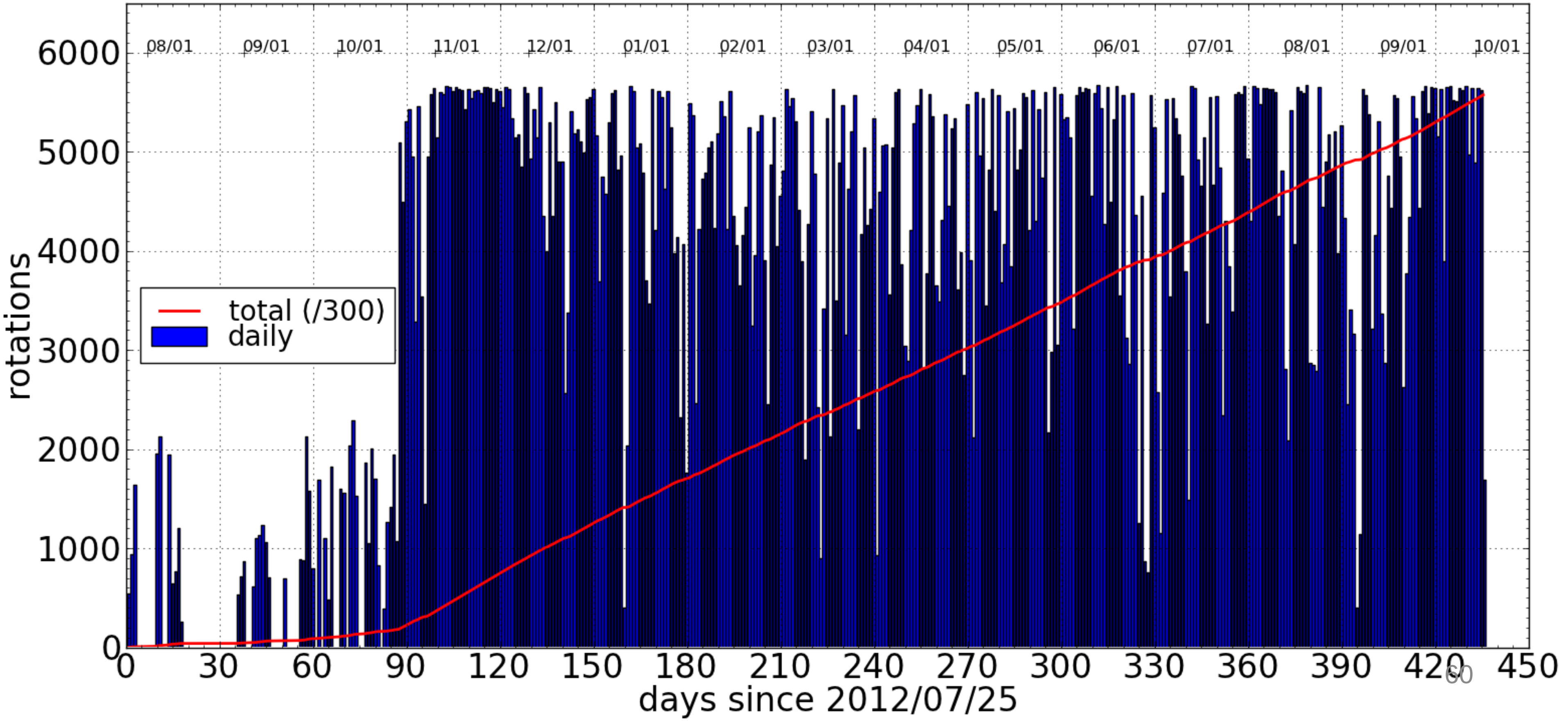

Data Analysis 1/3

- demodulate each 1 rotation data with ω_{rot}

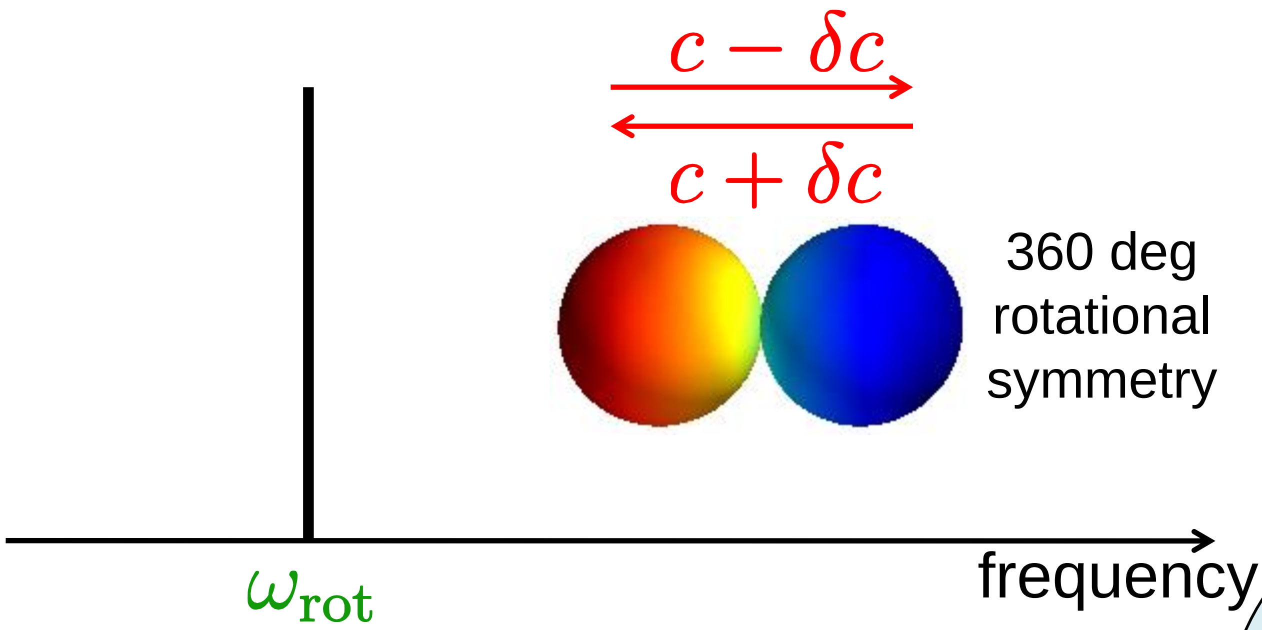

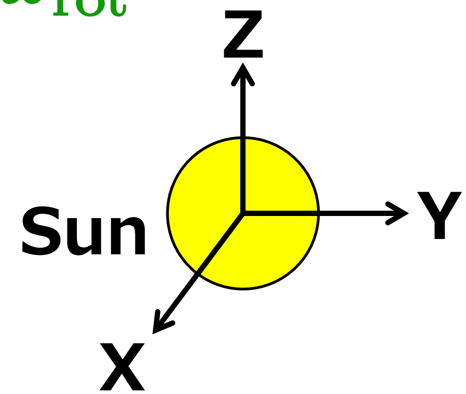

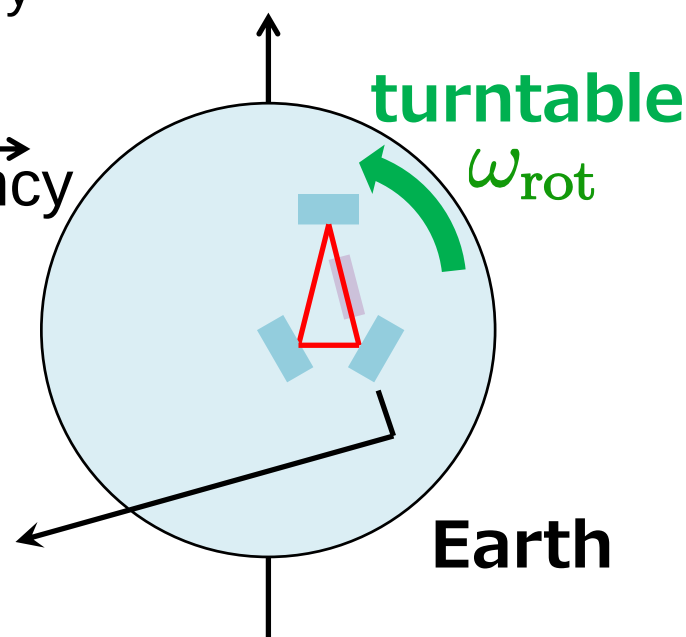

acquired LV signal

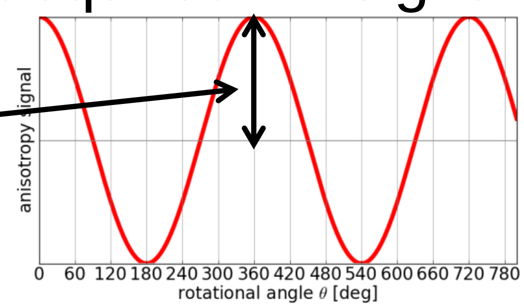

demodulation amplitudes are proportional to LV

Data Analysis 2/3

- next, demodulate 1 day data with $\omega_\oplus$

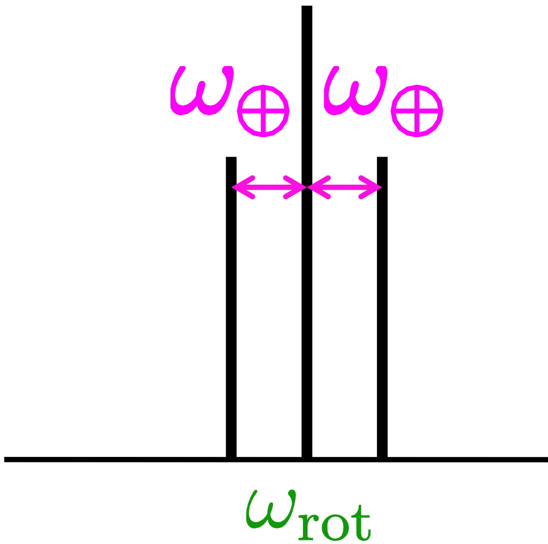

frequency

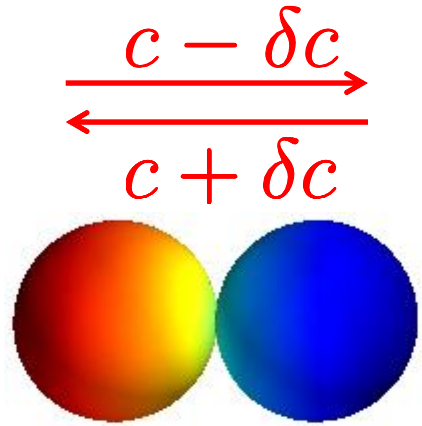

360 deg rotational symmetry

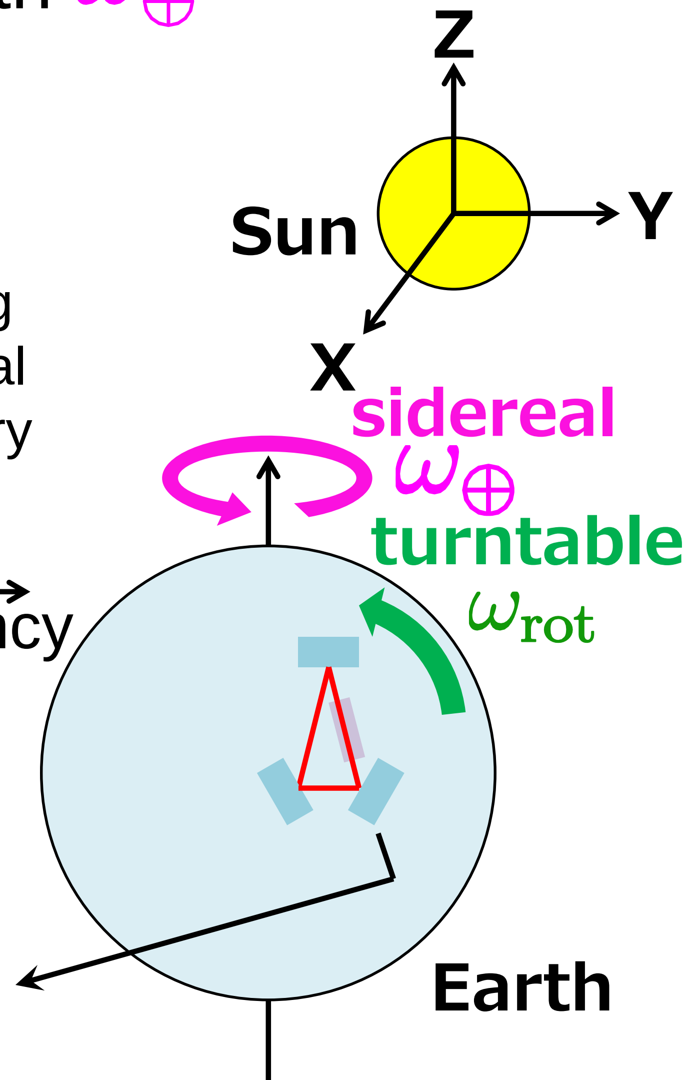

acquired LV signal

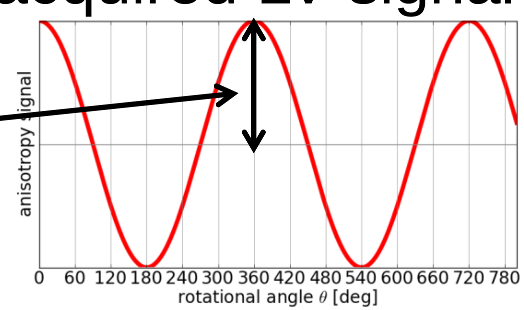

demodulation amplitudes are modulated by sidereal frequency

Data Analysis 3/3

- higher order LV appear at higher harmonics

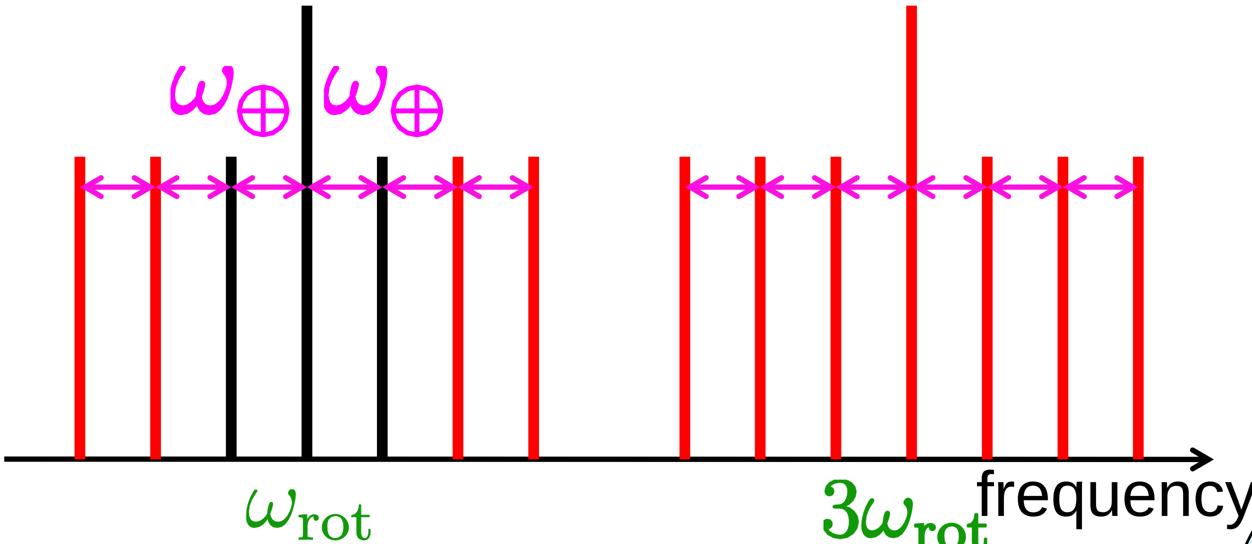

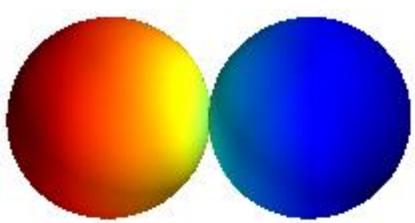

360 deg
rotational symmetry

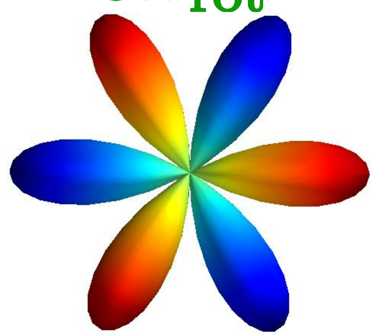

120 deg
rotational symmetry

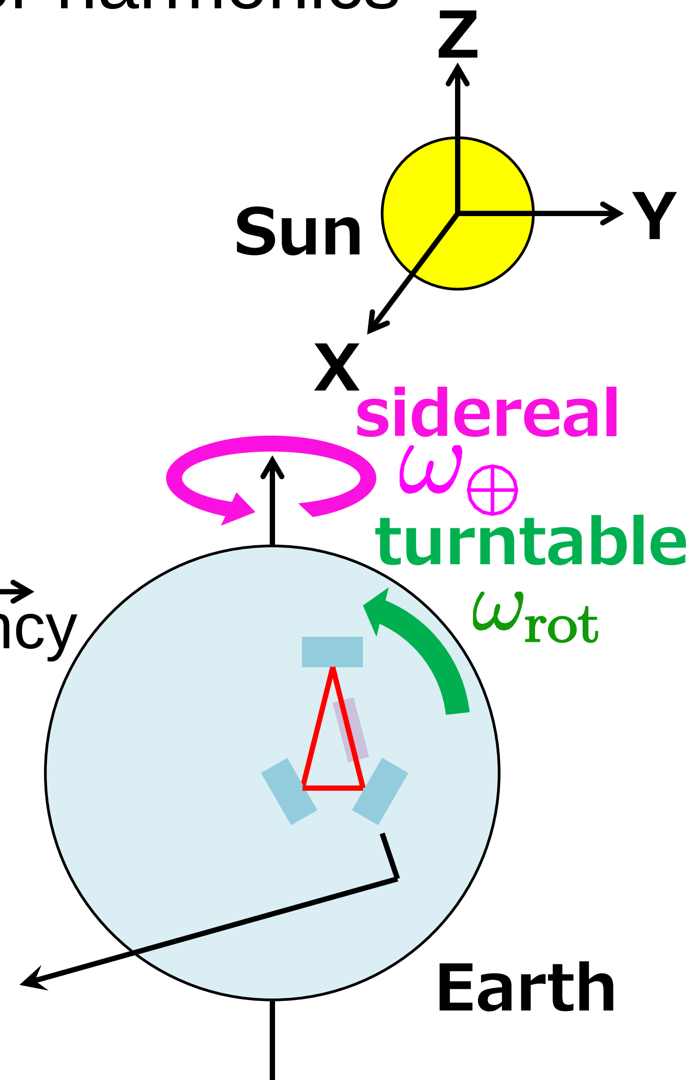

Demodulation Amps(ω_{rot})

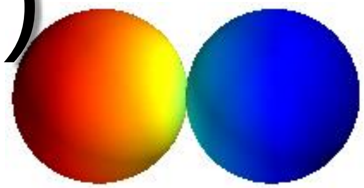

- zero consistent at 2σ
  $\longrightarrow$ no significant LV can be claimed

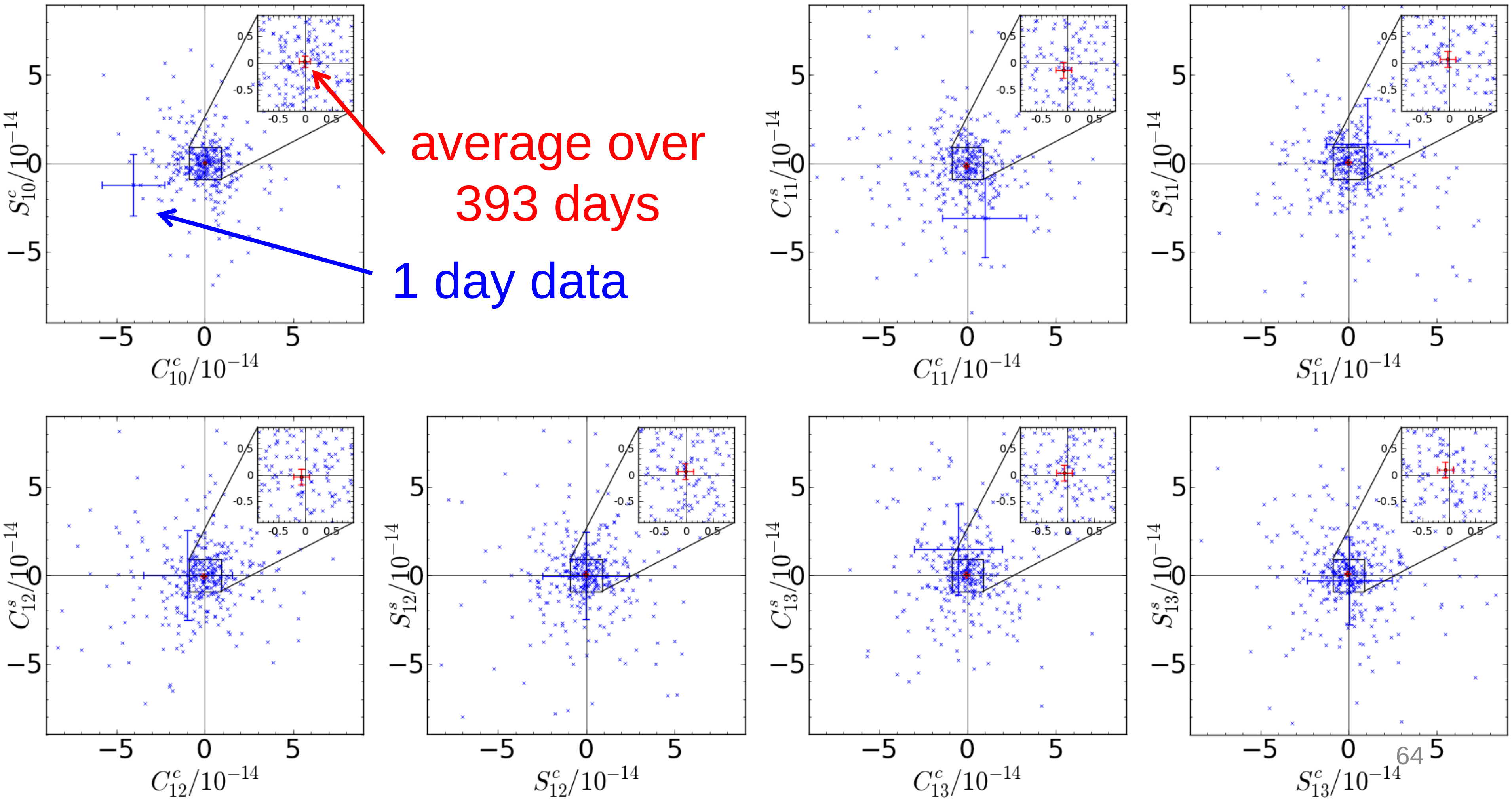

Demodulation Amps($3\omega_{\mathrm{rot}}$)

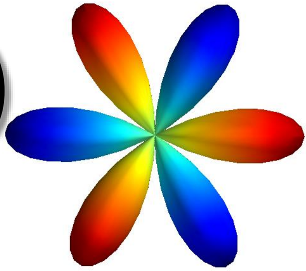

- zero consistent at 2σ

  $\longrightarrow$ no significant LV can be claimed

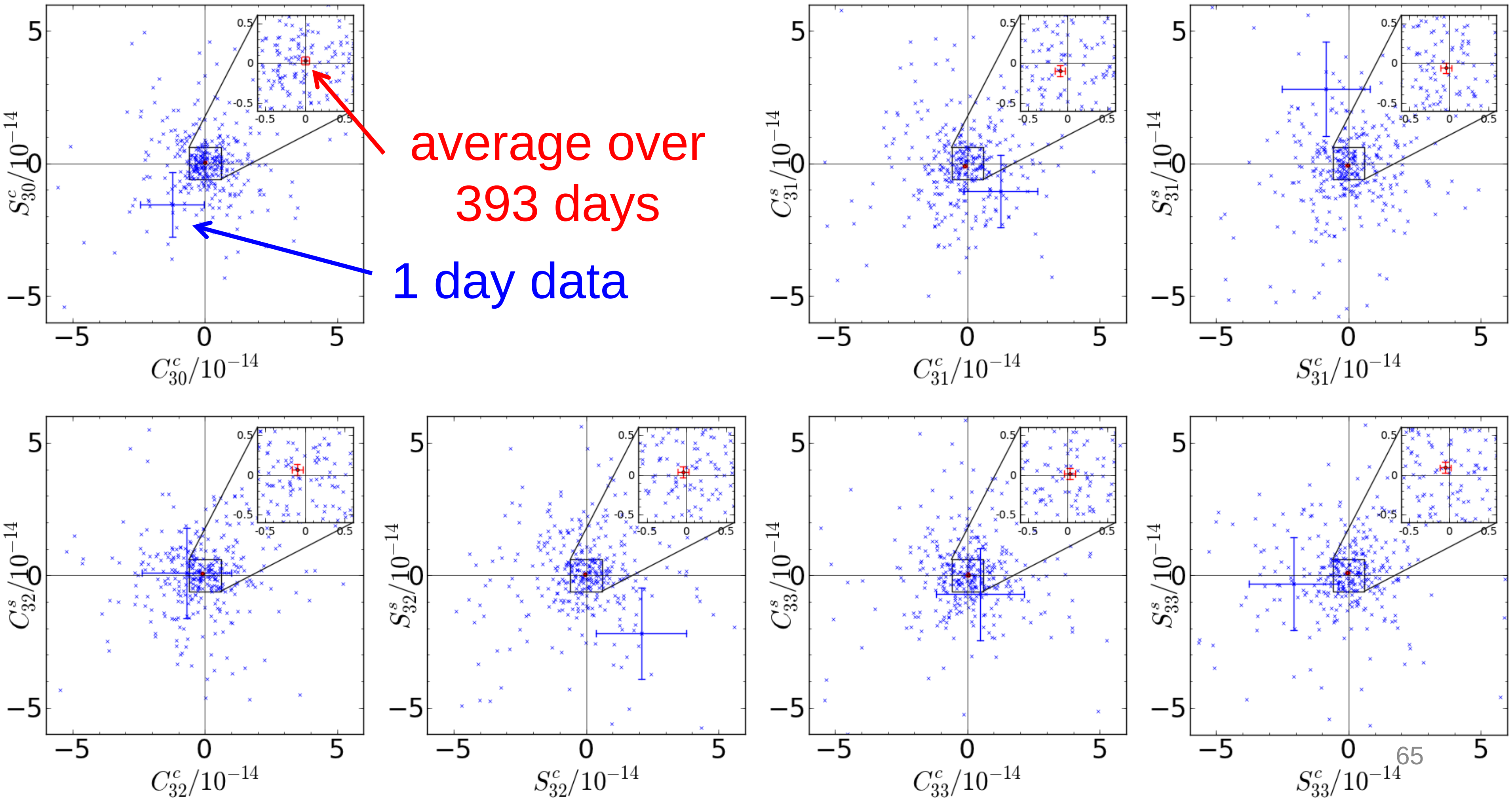

Our Limits on Anisotropy

- More than an order of magnitude improvement for dipole elements, new limits on hexapole elements

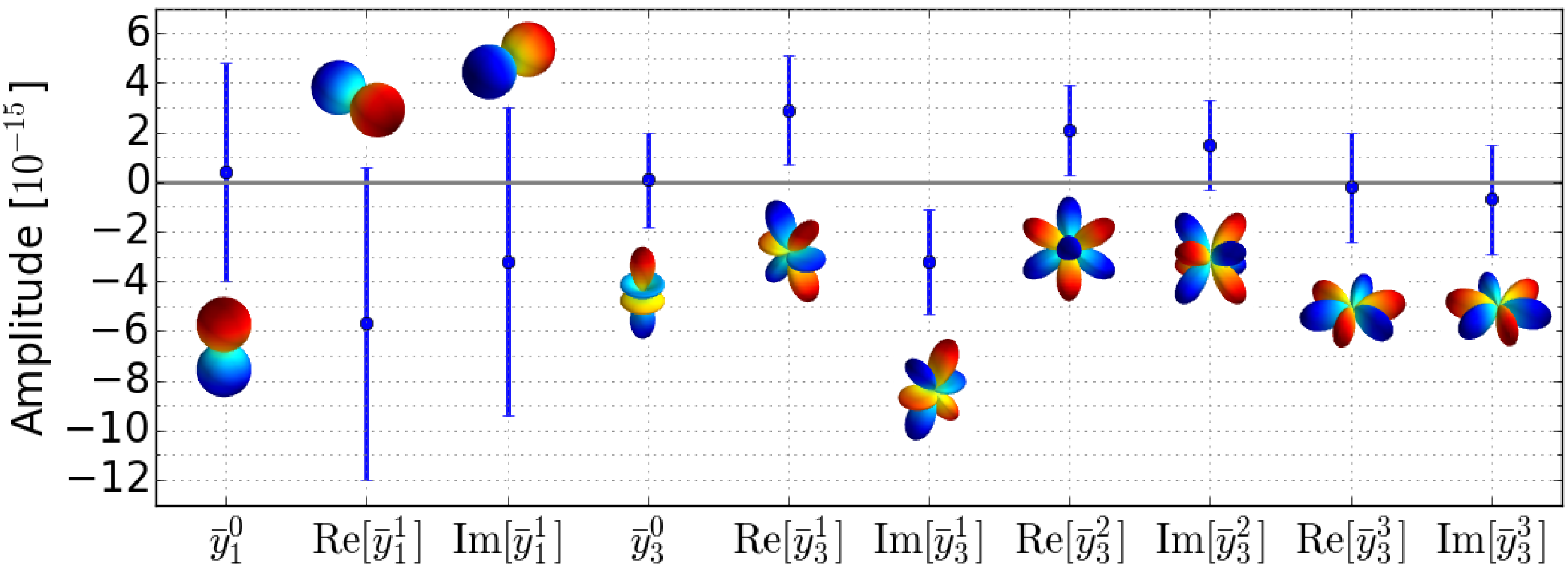

$$\left|\frac{\delta c}{c}\right| \lesssim 6 \times 10^{-15}$$
(improved limit)

$$\left|\frac{\delta c}{c}\right| \lesssim 2 \times 10^{-15}$$
(new limit)

Our Limits on SME Coefficients

- Standard Model Extension (SME)
  [D. Colladay and V. Alan Kostelecký: [PRD 58, 116002 (1998)]()]
- test theory with all realistic Lorentz violation
- our result put new limits on "camouflage coefficients" of LV in photon sector

Dimension	Coefficient	Measurement
$d=6$	$(\overline{c}_F^{(6)})^{(0E)}_{110}$	$(-0.1 \pm 1.5) \times 10^3 \text{ GeV}^{-2}$
	$\mathrm{Re}[(\overline{c}_F^{(6)})^{(0E)}_{111}]$	$(-0.8 \pm 1.1) \times 10^3 \text{ GeV}^{-2}$
	$\mathrm{Im}[(\overline{c}_F^{(6)})^{(0E)}_{111}]$	$(-0.6 \pm 1.0) \times 10^3 \text{ GeV}^{-2}$
$d=8$	$-0.020(\overline{c}_F^{(8)})^{(0E)}_{110} + (\overline{c}_F^{(8)})^{(0E)}_{310}$	$(-0.2 \pm 1.9) \times 10^{19} \text{ GeV}^{-4}$
	$\mathrm{Re}[-0.020(\overline{c}_F^{(8)})^{(0E)}_{111} + (\overline{c}_F^{(8)})^{(0E)}_{311}]$	$(1.4 \pm 1.3) \times 10^{19} \text{ GeV}^{-4}$
	$\mathrm{Re}[-0.020(\overline{c}_F^{(8)})^{(0E)}_{111} + (\overline{c}_F^{(8)})^{(0E)}_{311}]$	$(0.1 \pm 1.3) \times 10^{19} \text{ GeV}^{-4}$
	$(\overline{c}_F^{(8)})^{(0E)}_{330}$	$(-0.8 \pm 3.3) \times 10^{19} \text{ GeV}^{-4}$
	$\mathrm{Re}[(\overline{c}_F^{(8)})^{(0E)}_{331}]$	$(-0.3 \pm 1.9) \times 10^{19} \text{ GeV}^{-4}$
	$\mathrm{Im}[(\overline{c}_F^{(8)})^{(0E)}_{331}]$	$(-2.8 \pm 1.9) \times 10^{19} \text{ GeV}^{-4}$
	$\mathrm{Re}[(\overline{c}_F^{(8)})^{(0E)}_{332}]$	$(2.2 \pm 1.3) \times 10^{19} \text{ GeV}^{-4}$
	$\mathrm{Im}[(\overline{c}_F^{(8)})^{(0E)}_{332}]$	$(0.2 \pm 1.3) \times 10^{19} \text{ GeV}^{-4}$
	$\mathrm{Re}[(\overline{c}_F^{(8)})^{(0E)}_{333}]$	$(-0.1 \pm 1.6) \times 10^{19} \text{ GeV}^{-4}$
	$\mathrm{Im}[(\overline{c}_F^{(8)})^{(0E)}_{333}]$	$(-0.1 \pm 1.6) \times 10^{19} \text{ GeV}^{-4}$

limits on LV of dimension 6
10^3 GeV^{-2}

limits on LV of dimension 8
10^{19} GeV^{-4}

Higher Order Lorentz Violation

- Standard Model Extention
- add LV term in Lagrangian for electromagnetic field
- $\hat{k}_F^{(d)}$ is zero for non-LV, d is mass dimension

full SME with HOLV

minimal SME

SM

4th order LV | 6th order LV | 8th order LV

$$\mathcal{L} = -\frac{1}{4}F_{\mu\nu}F^{\mu\nu} + \frac{1}{4}F_{\kappa\lambda}(\hat{k}_F^{(4)})^{\kappa\lambda\mu\nu}F_{\mu\nu} + \frac{1}{4}F_{\kappa\lambda}(\hat{k}_F^{(6)})^{\kappa\lambda\mu\nu}F_{\mu\nu} + \frac{1}{4}F_{\kappa\lambda}(\hat{k}_F^{(8)})^{\kappa\lambda\mu\nu}F_{\mu\nu} \cdots$$

d=4
no dimension

d=6
+2nd order
differential
M^{-2} dimension

d=8
+4th order
differential
M^{-4} dimension

Higher Order LV and Anisotropy

- HOLV gives multipole anisotropy

full SME with HOLV

minimal SME

SM

4[th] order LV

6[th] order LV

8[th] order LV

$$\mathcal{L} = -\frac{1}{4}F_{\mu\nu}F^{\mu\nu} + \frac{1}{4}F_{\kappa\lambda}(\hat{k}_F^{(4)})^{\kappa\lambda\mu\nu}F_{\mu\nu} + \frac{1}{4}F_{\kappa\lambda}(\hat{k}_F^{(6)})^{\kappa\lambda\mu\nu}F_{\mu\nu} + \frac{1}{4}F_{\kappa\lambda}(\hat{k}_F^{(8)})^{\kappa\lambda\mu\nu}F_{\mu\nu} \cdots$$

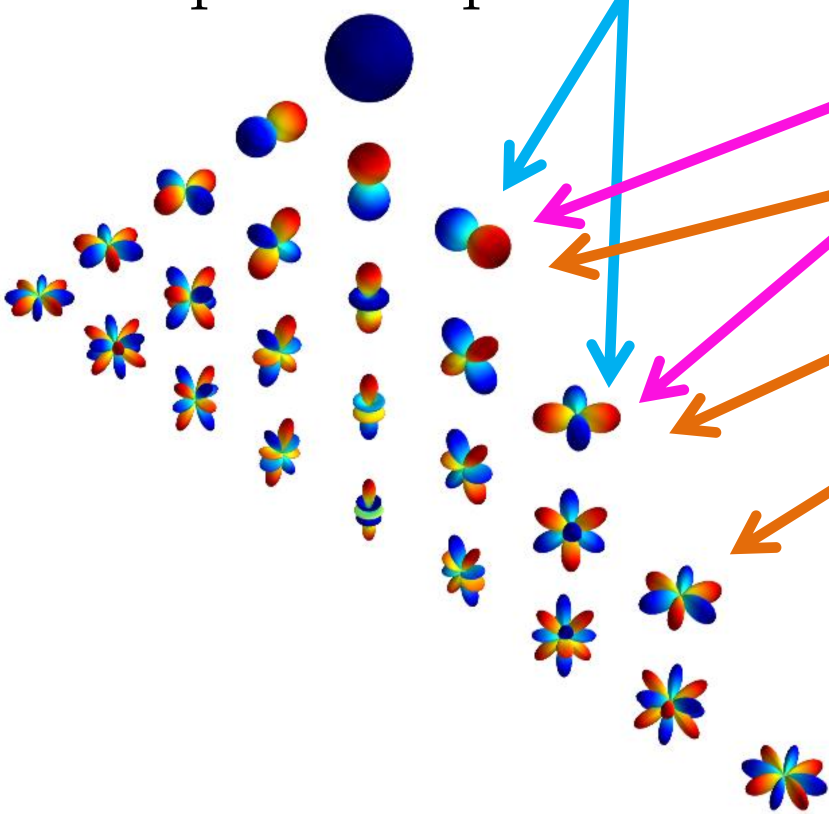

HOLV can be measured by measuring multipole anisotropy

Summary of LV Search

- Measure the speed of light difference between counter propagating directions with an optical ring cavity
  - large asymmetry with silicon
  - null measurement with double-pass configuration
  - rotated the cavity for a year
- No LV found and put limits on LV

dipole (improved)

$$\left|\frac{\delta c}{c}\right| \lesssim 6 \times 10^{-15}$$

hexapole (new)

$$\left|\frac{\delta c}{c}\right| \lesssim 2 \times 10^{-15}$$

- YM+, [PRL **110**, 200401 (2013)]()
  YM+, [PRD **88**, 111101(R) (2013)]()

Recent Updates

- Aiming for higher sensitivity by reducing noise from rotation
  - continuous rotation (by Sakai, -2017)
  - monolithic optical bench (by Takeda, -2017)
  - larger turn table, new power supply (by Takeda, -2019)

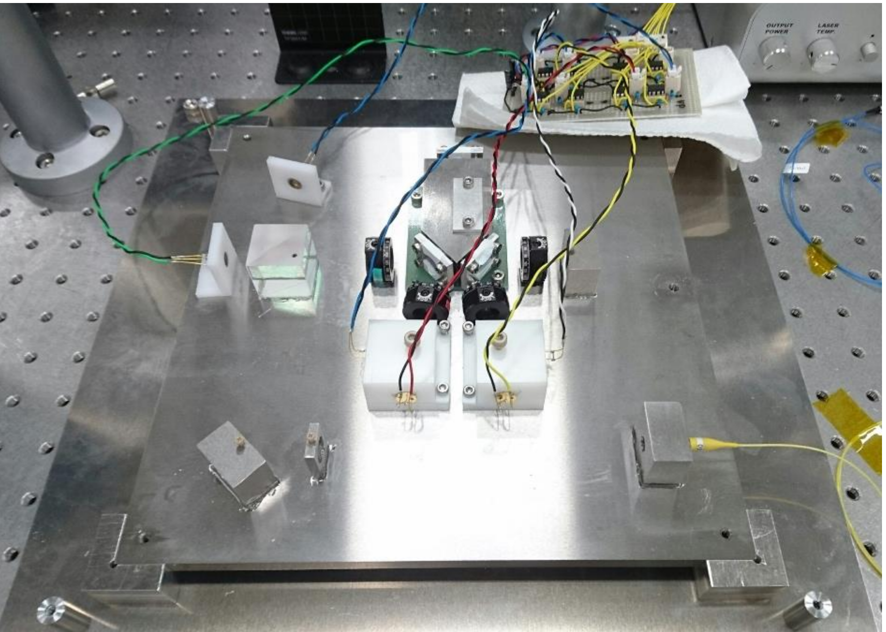

H. Takeda, [Master thesis (2017)]

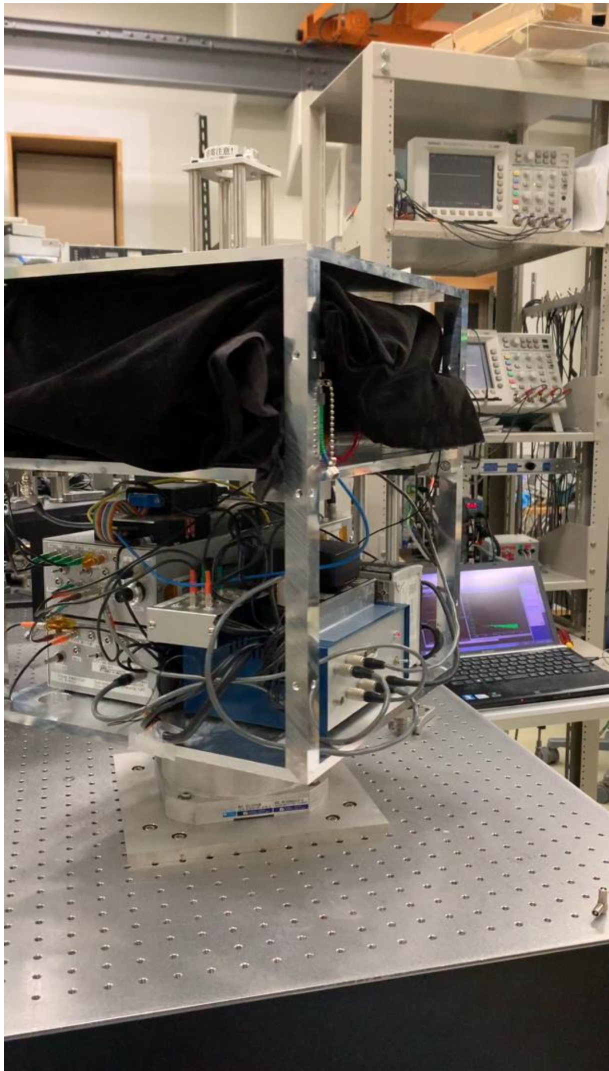

Apparatus Comparison

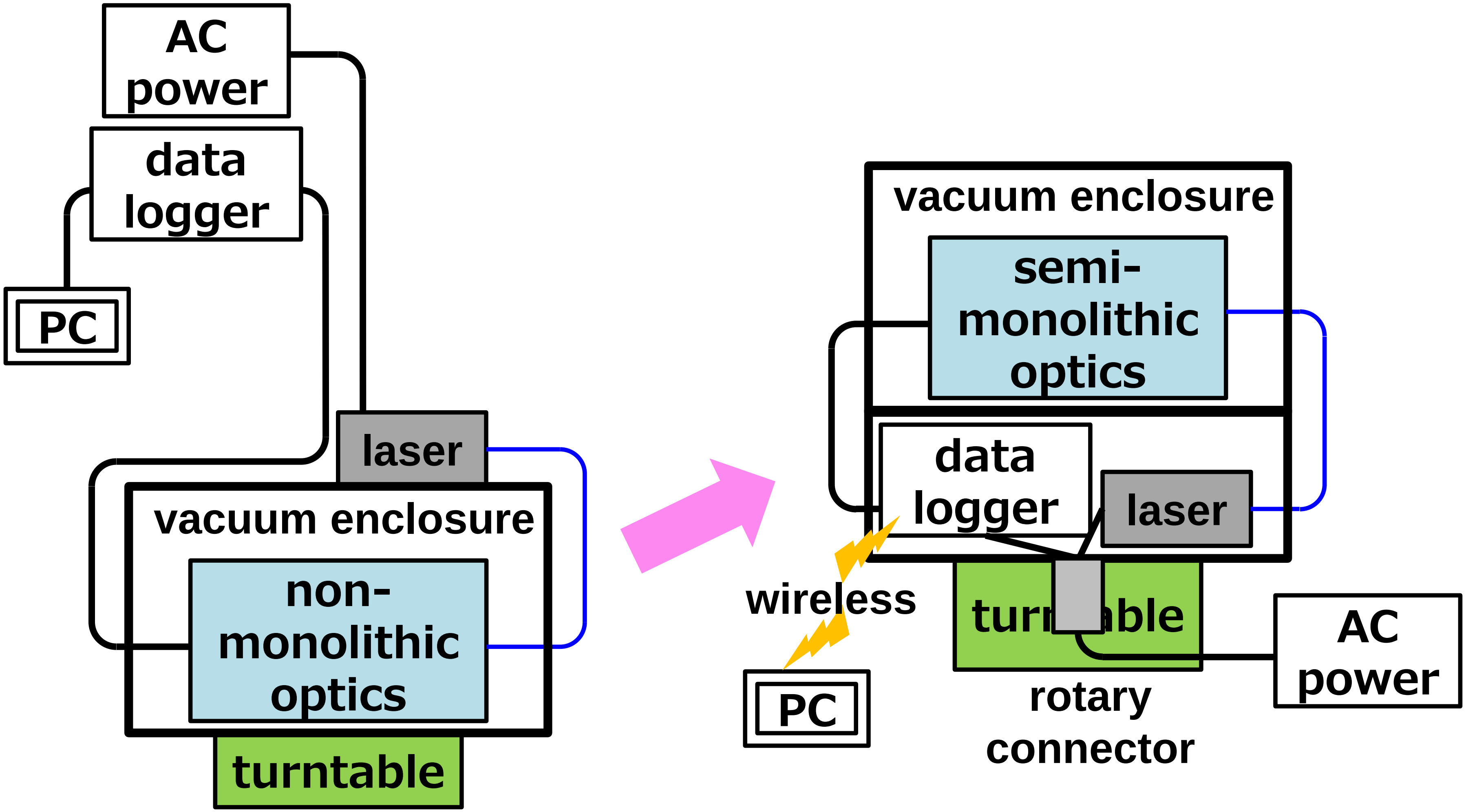

Previous Model
- non-monolithic optics
- alternative rotation

New Model
- monolithic optics
- continuous rotation

Latest Sensitivity

- Floor noise at rotation stays almost the same with that at stationary
- Noise peak at rotation frequency

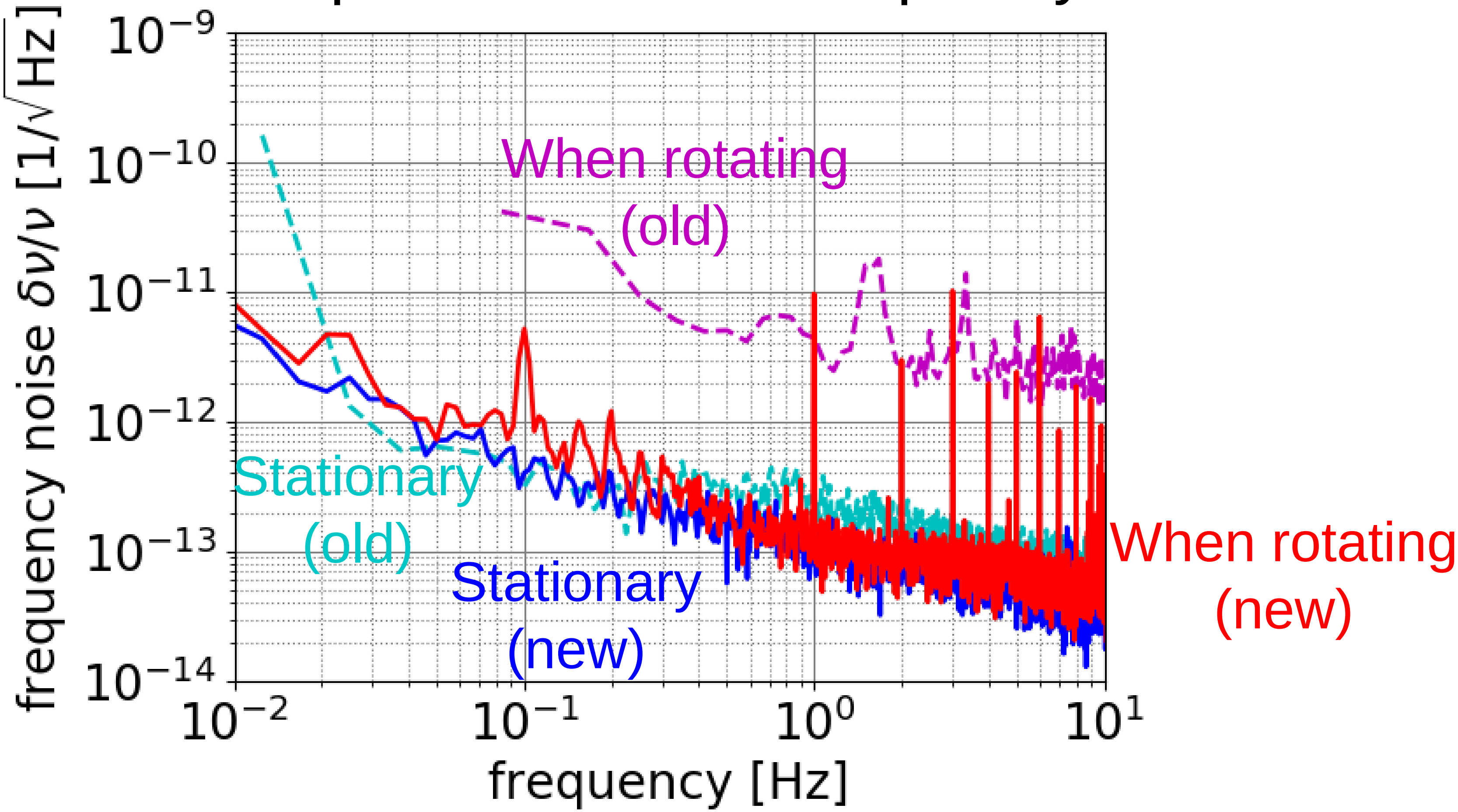

Plan of the Talk

- **Basics of Laser Interferometry** (60 min)
  - Michelson interferometer
  - Fabry-Perot cavity
  - Quantum noise and other classical noises
- **Test of Lorentz Invariance** (30 min)
- **Search for Axion Dark Matter** (30 min)
- **Macroscopic Quantum Mechanics** (40 min)
- **KAGRA Gravitational Wave Telescope** (20 min)

- Slides available at https://tinyurl.com/YM20200109

Axion and Axion-Like Particles

- Pseudo-scalar particle originally introduced to solve strong CP problem (QCD axion)
- Axion-like particles also predicted by string theory and supergravity
- Leading candidate of dark matter (m << keV, tiny interaction with matter)
- Search through axion-photon coupling is popular (especially by using magnetic fields)

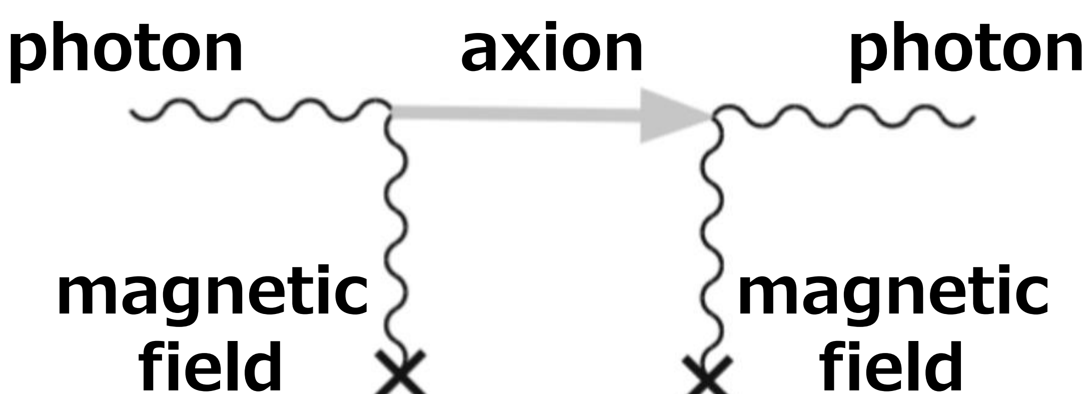

Primakoff effect

Search for Axion-Photon Coupling

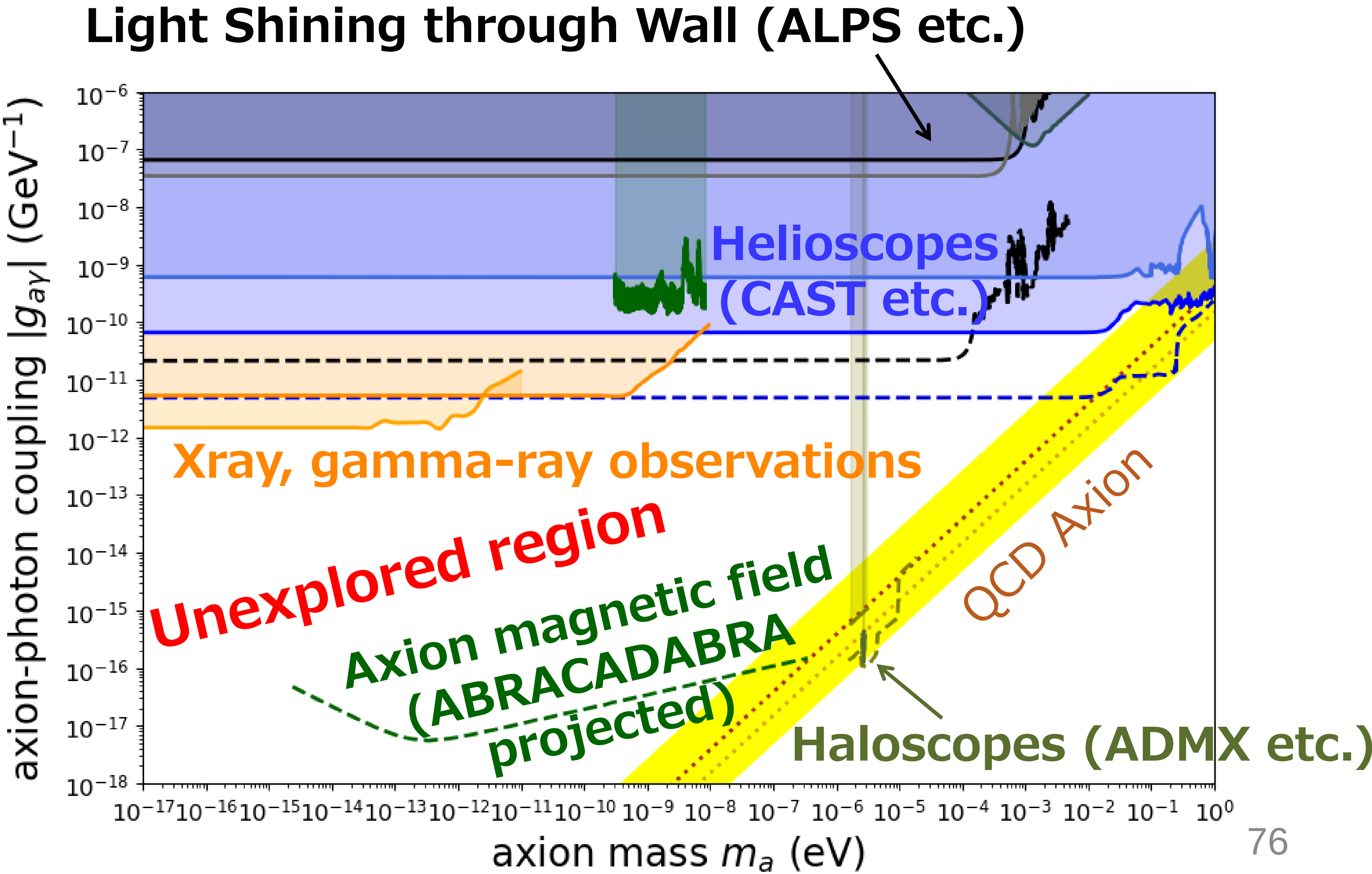

Velocity of Circular Polarizations

- Axion-photon coupling ($\frac{g_{a\gamma}}{4} a F_{\mu\nu} \tilde{F}^{\mu\nu}$) gives different phase velocity between left-handed and right-handed circular polarizations

$$c_{\mathrm{L/R}} = \sqrt{1 \pm \frac{g_{a\gamma} a_0 m_a}{k} \sin(m_a t + \delta_\tau)}$$

coupling constant axion field axion mass

- Measure the difference as resonant frequency difference in an optical cavity

$$\frac{\delta c}{c} = \frac{\nu_{\mathrm{L}} - \nu_{\mathrm{R}}}{\nu}$$

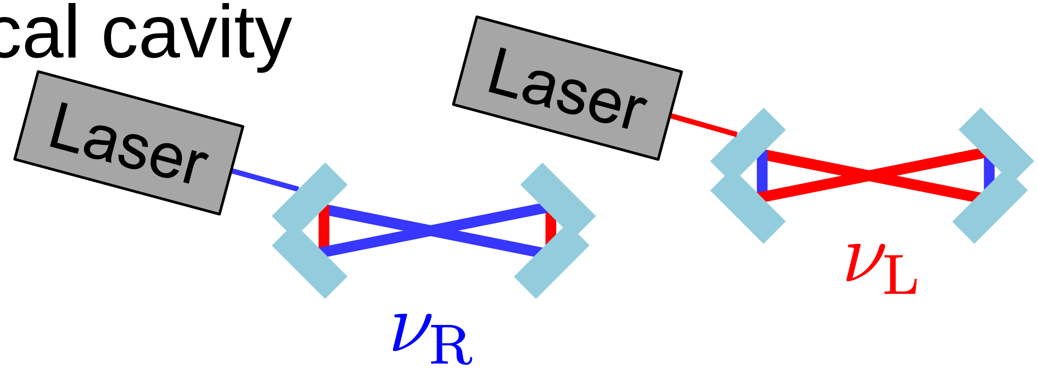

- Search can be done without magnetic field

Our Ideas

- Use of bow-tie cavity

The effect is canceled in a linear cavity

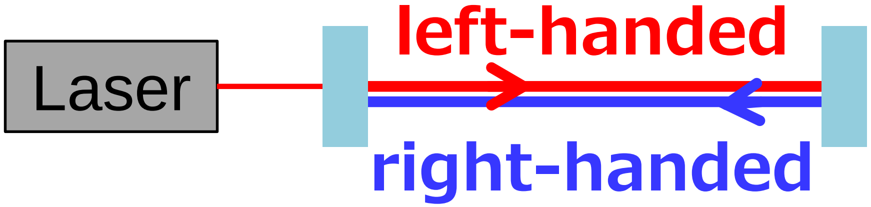

Not canceled in a bow-tie cavity

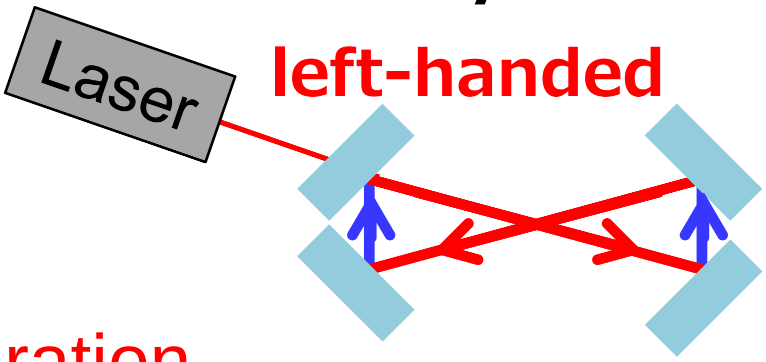

- Use of double-pass configuration

  Transmitted beam is reflected back into the same cavity as different polarization to realize a null measurement of the resonant frequency difference

Y. Michimura+, [PRL 110, 200401 (2013)]

Double-Pass Configuration 1/4

- Inject left-handed polarization

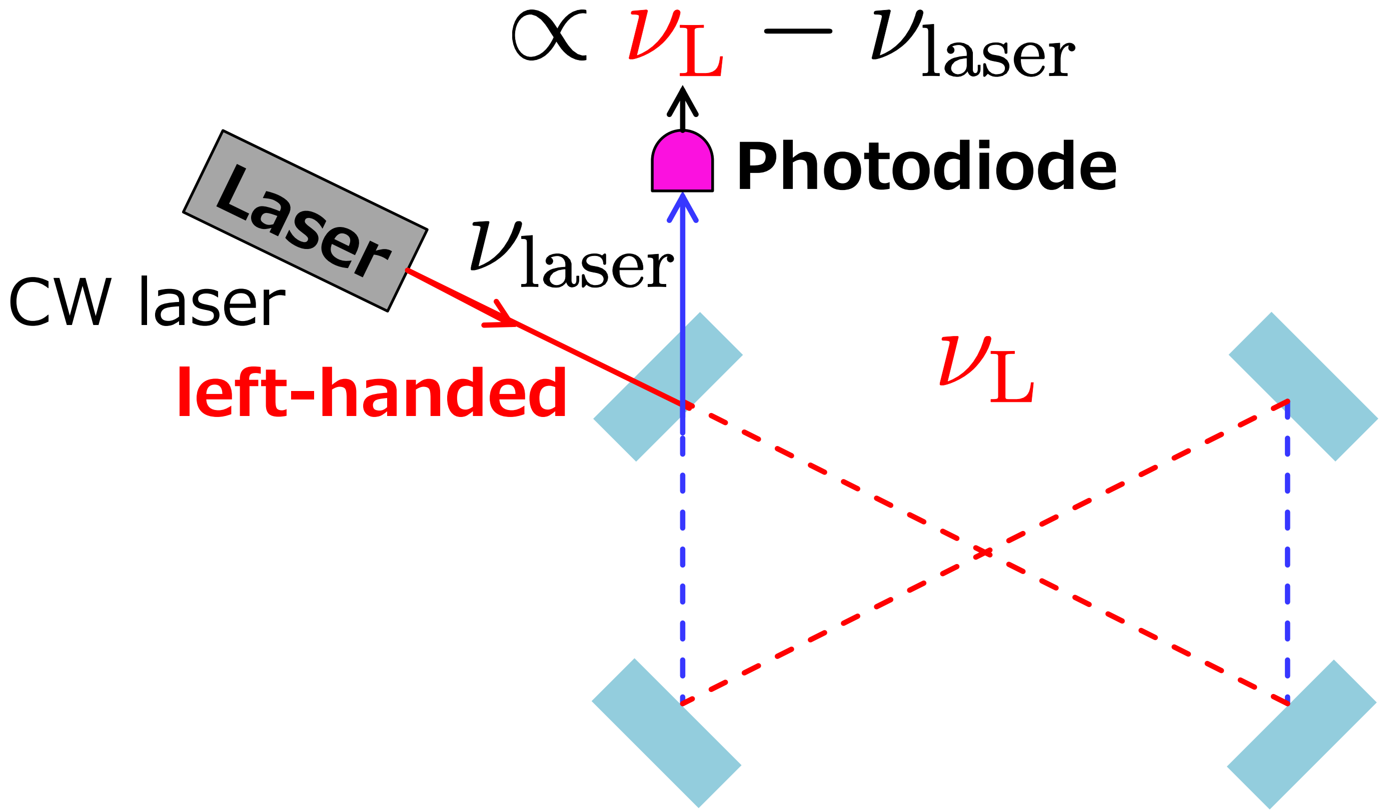

Double-Pass Configuration 2/4

- Lock the frequency of the laser to left-handed resonant frequency (ν_L)

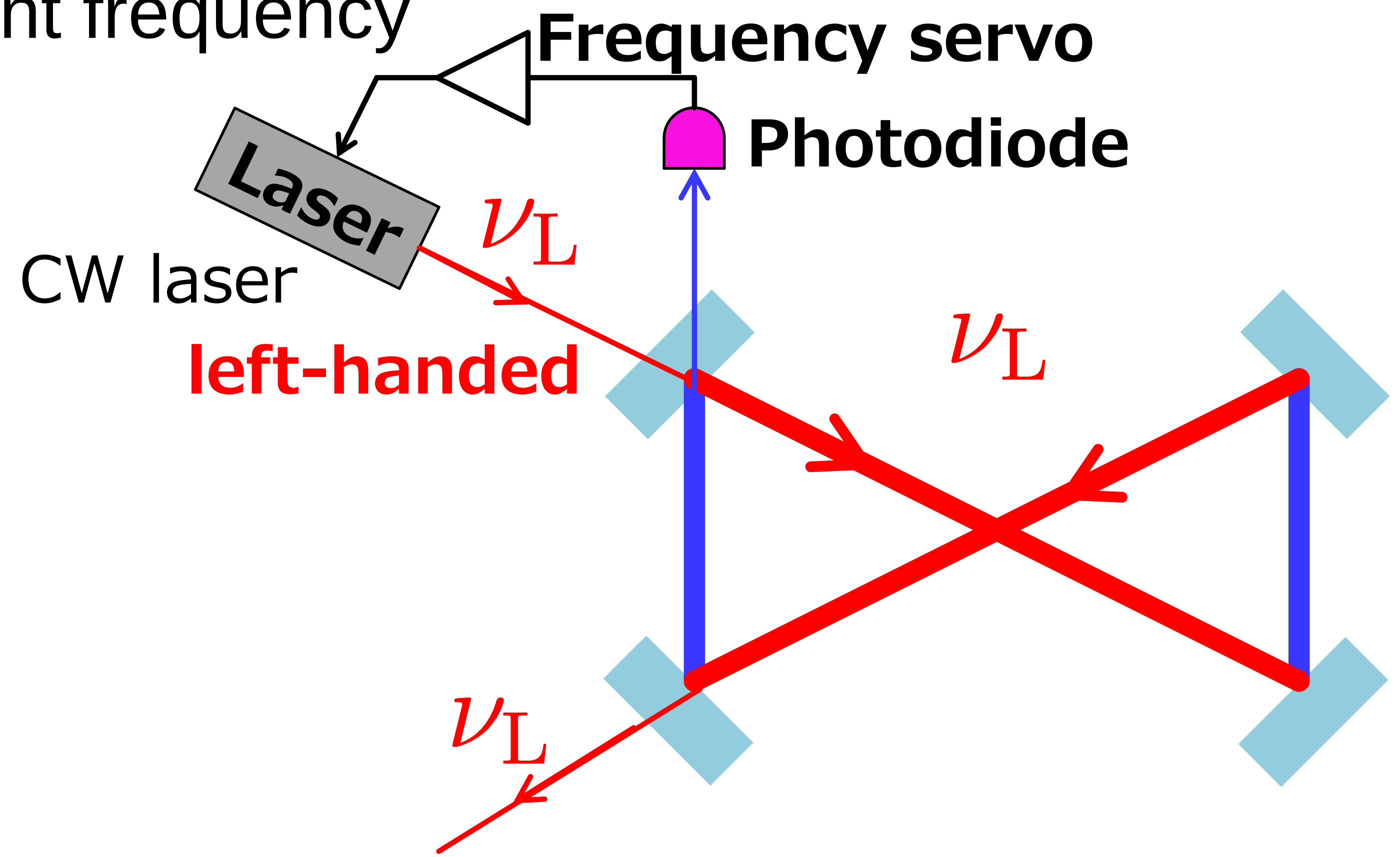

Double-Pass Configuration 3/4

- Transmitted beam is reflected back into the cavity as right-handed polarization

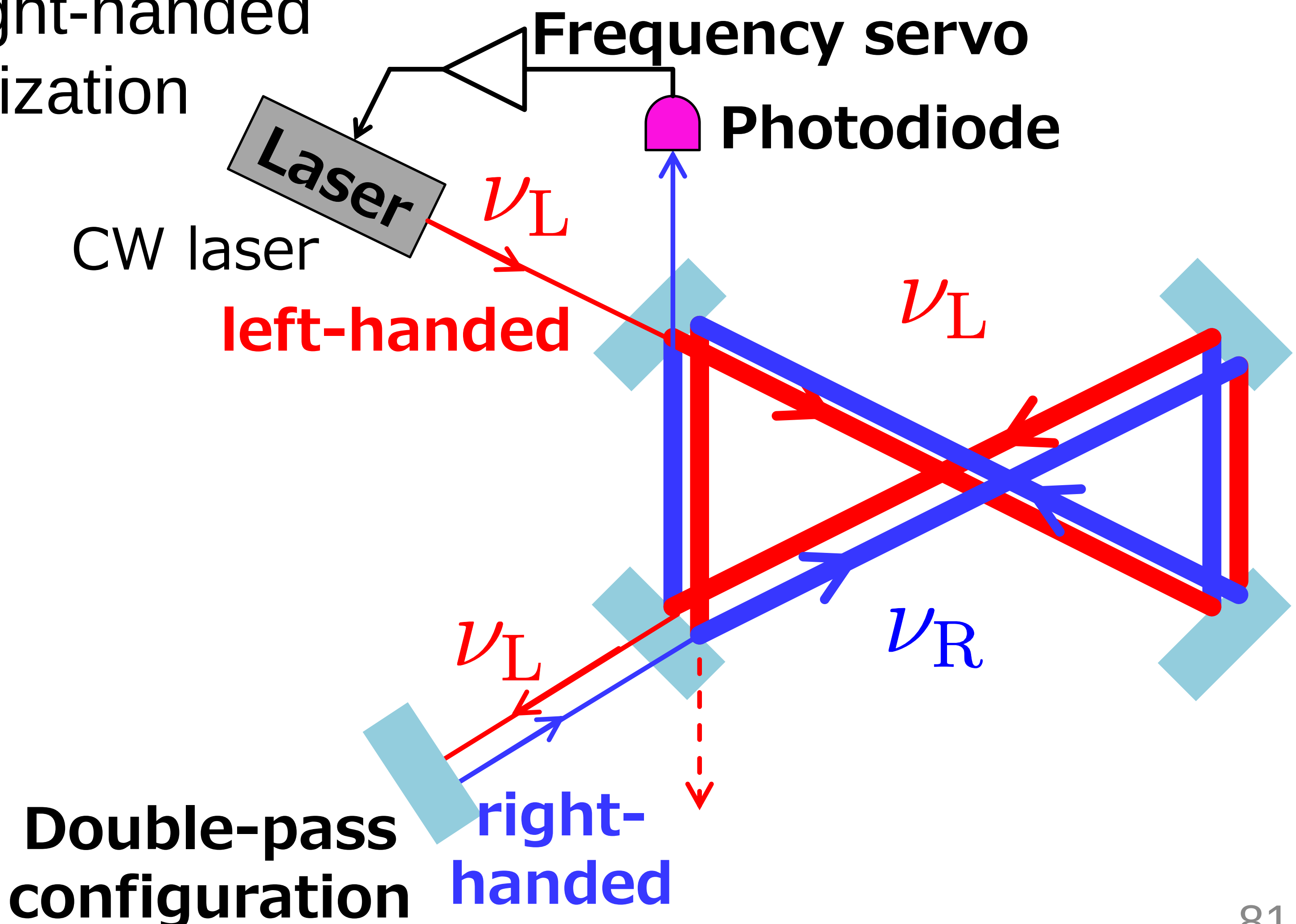

Double-Pass Configuration 4/4

- Axion signal is extracted from the cavity reflection (null measurement)

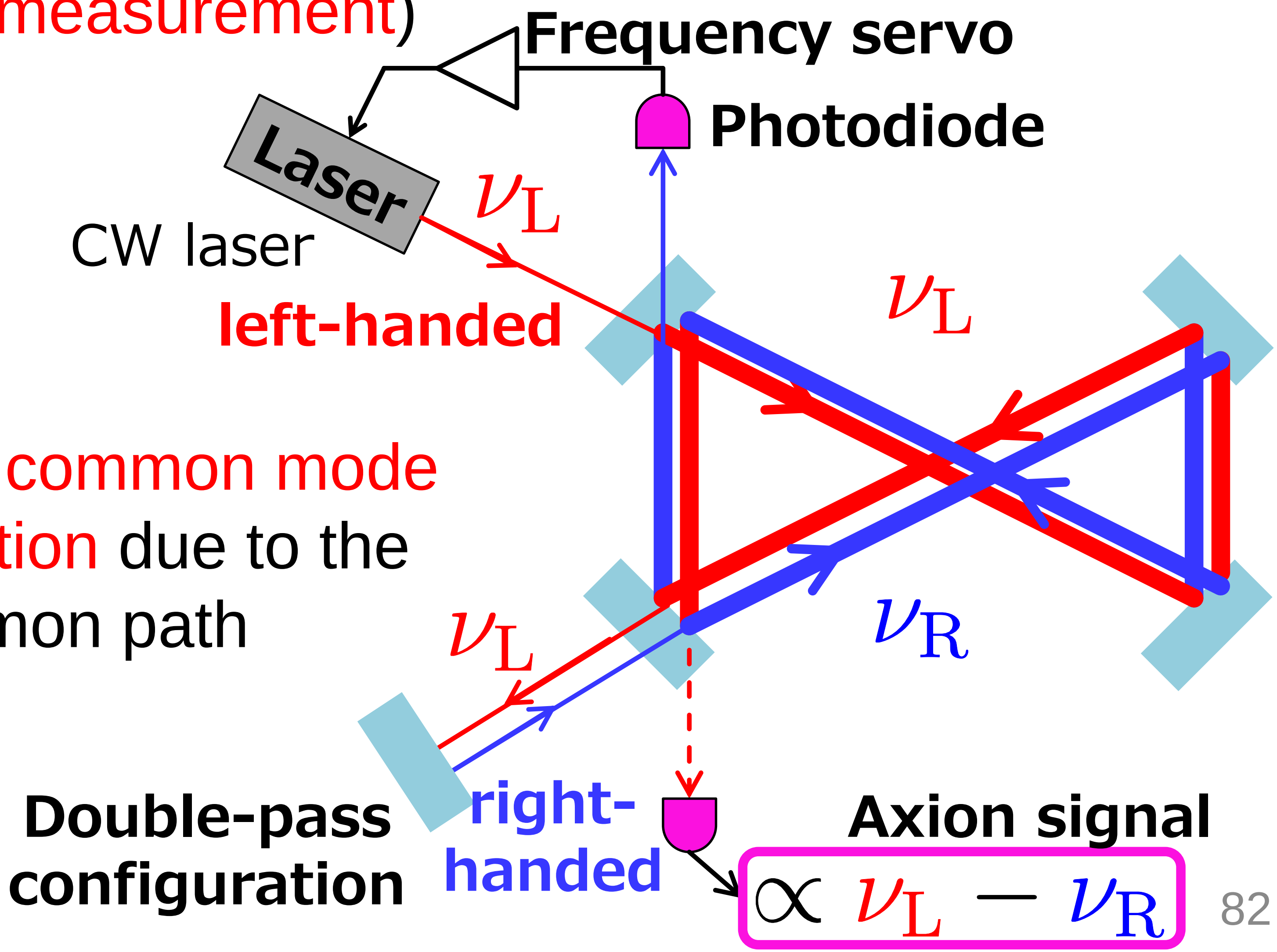

- High common mode rejection due to the common path

Sensitivity Calculation

- Cavity length changes (displacement noises) will not be a fundamental noise due to common mode rejection
- Ultimately limited by quantum shot noise

$$\sqrt{S_{\mathrm{shot}}} = \sqrt{\frac{\lambda}{4\pi P}\left(\frac{\pi^2}{L^2\mathcal{F}^2} + m_a^2\right)}$$

input laser power

cavity length

finesse

axion mass

- Sensitivity to axion-photon coupling can be calculated by assuming

  axion density = dark matter density

Search for Unexplored Region

Dark matter Axion search with riNg Cavity Experiment

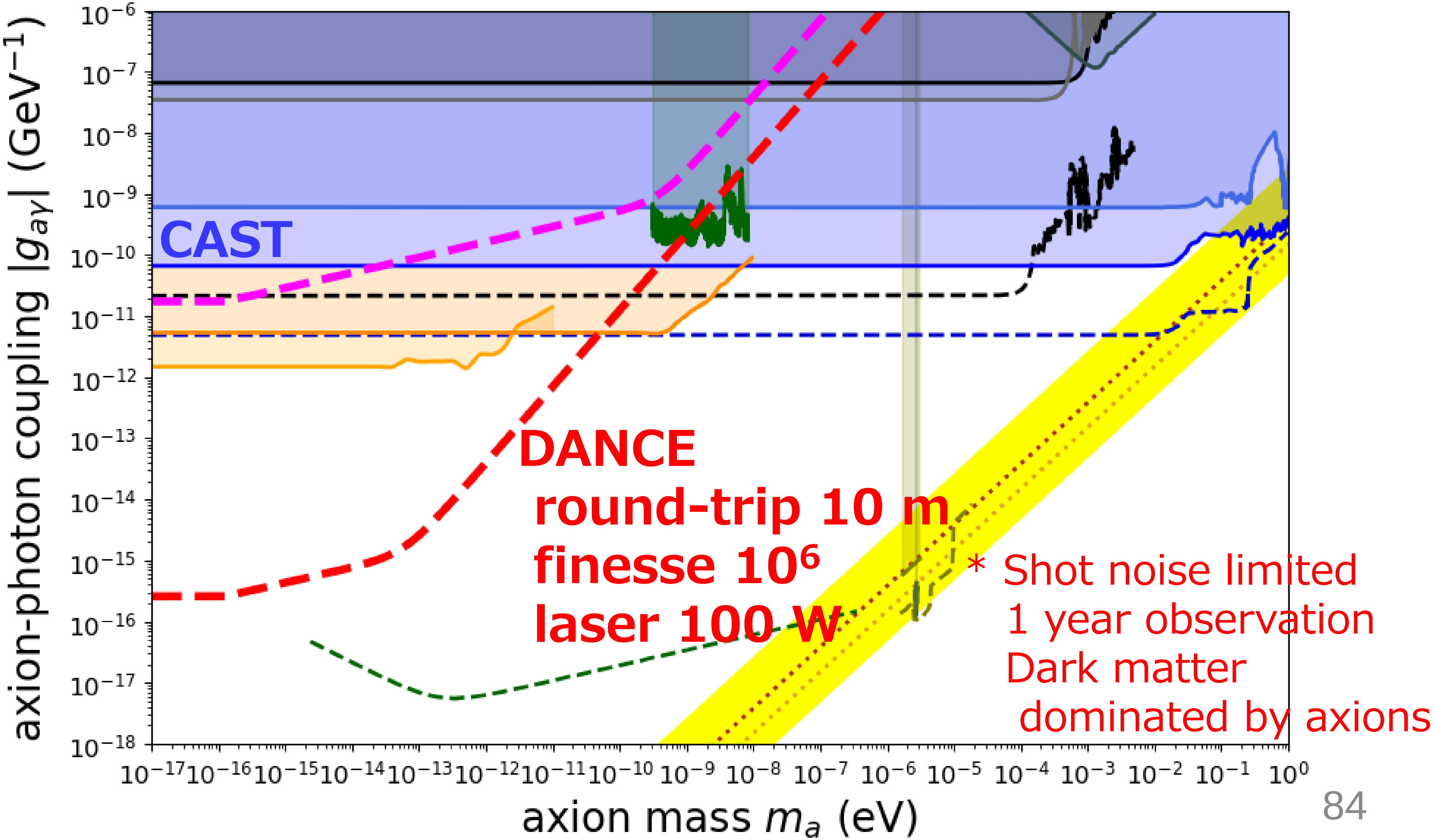

Prototype Experiment

Dark matter Axion search with riNg Cavity Experiment

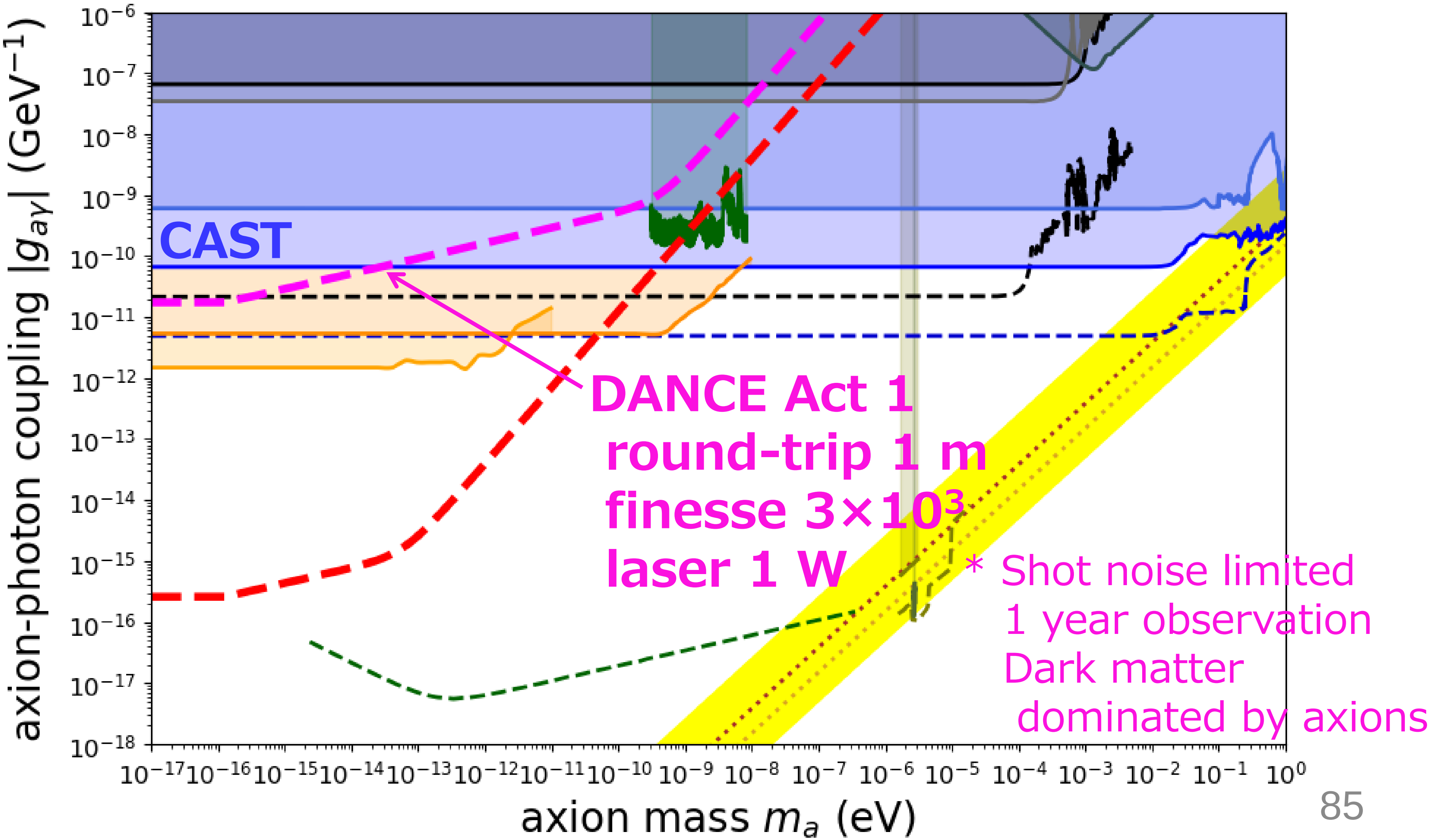

Schematic of DANCE Act 1

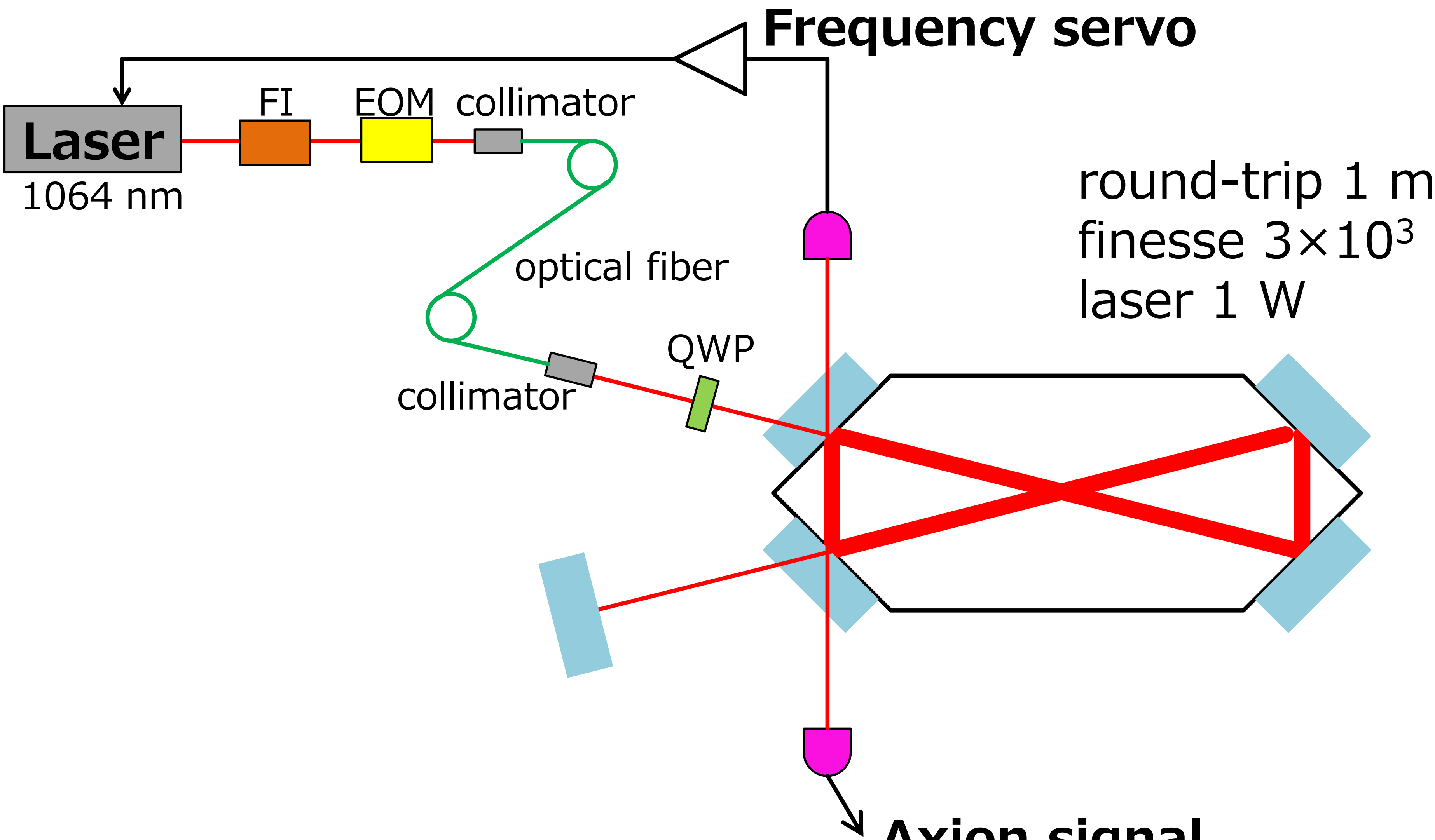

$\propto \nu_L - \nu_R$

DANCE Act 1

- Completed the assembly of optics
- Finesse measured to be 515 +/- 6 (design: 3×10^3)
- Having trouble with stable lock now

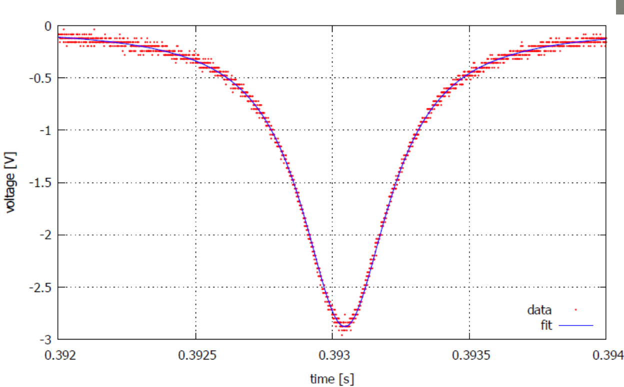

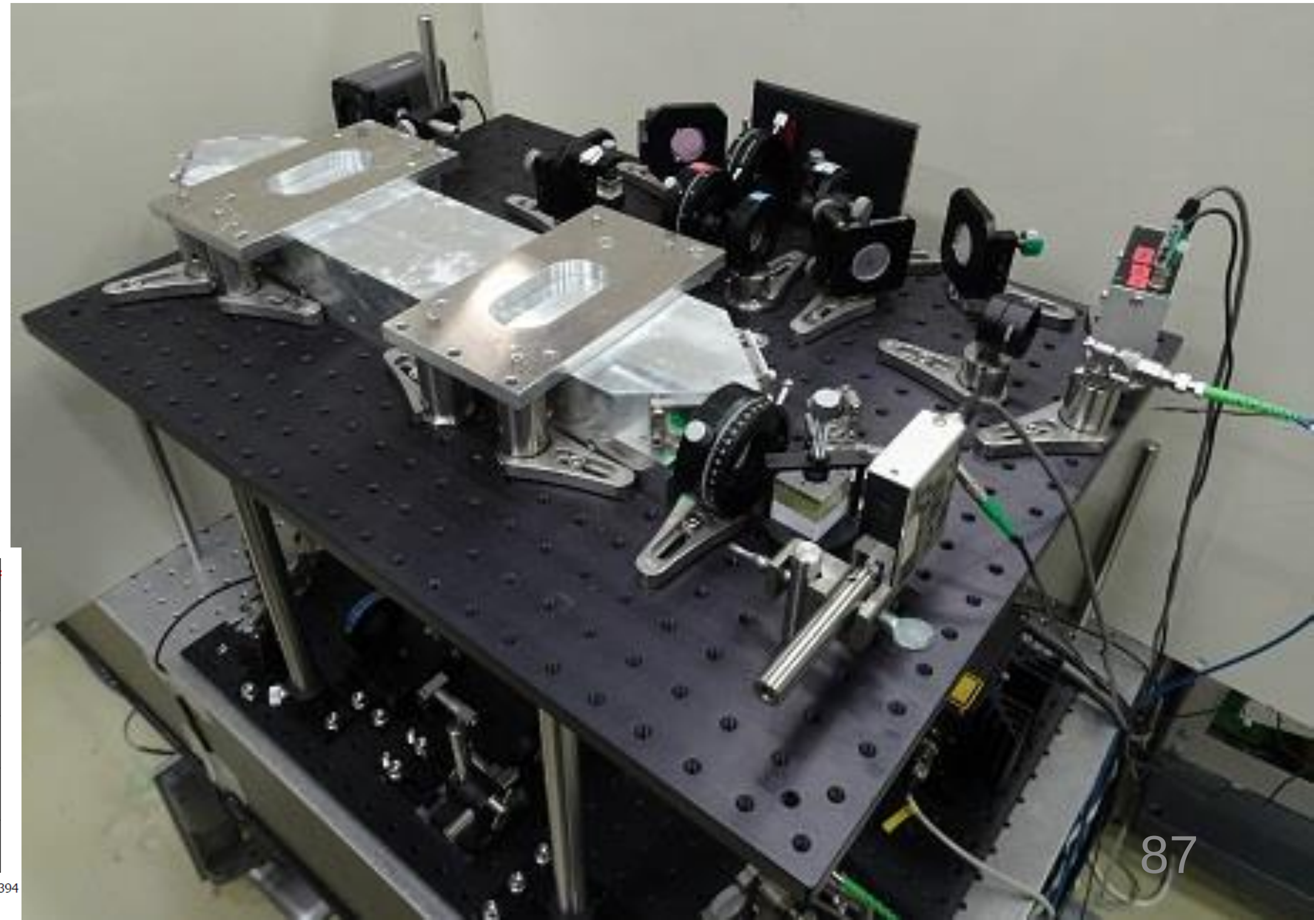

DANCE Act 1

- Completed the assembly of optics
- Finesse measured to be 515 +/- 6 (design: 3×10^3)
- Having trouble with stable lock now

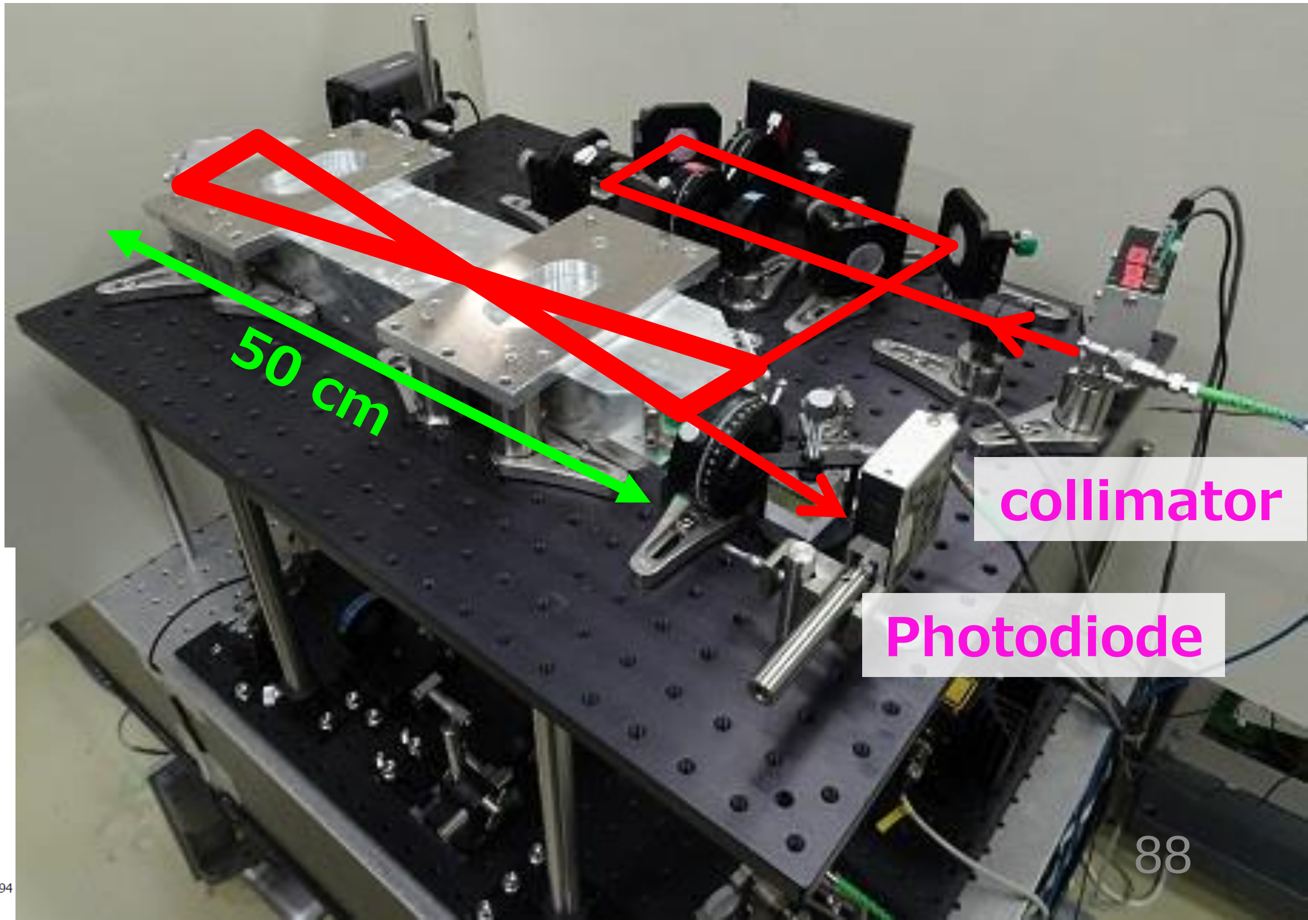

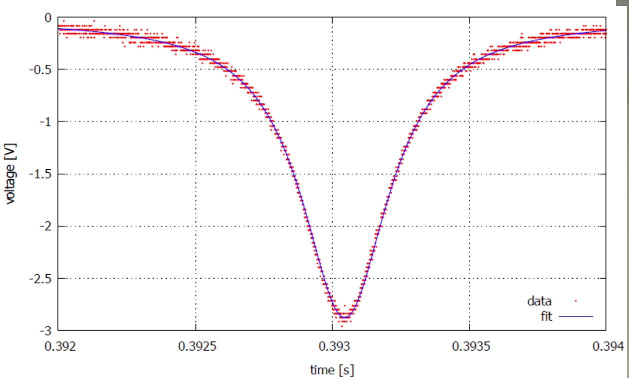

Search with Linear Cavity

- Linear polarization rotates at axion frequency

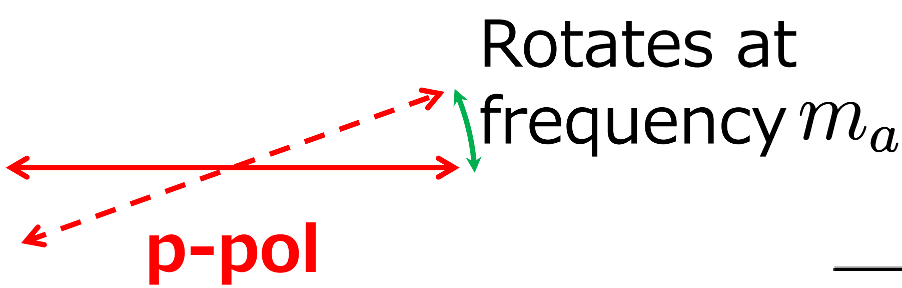

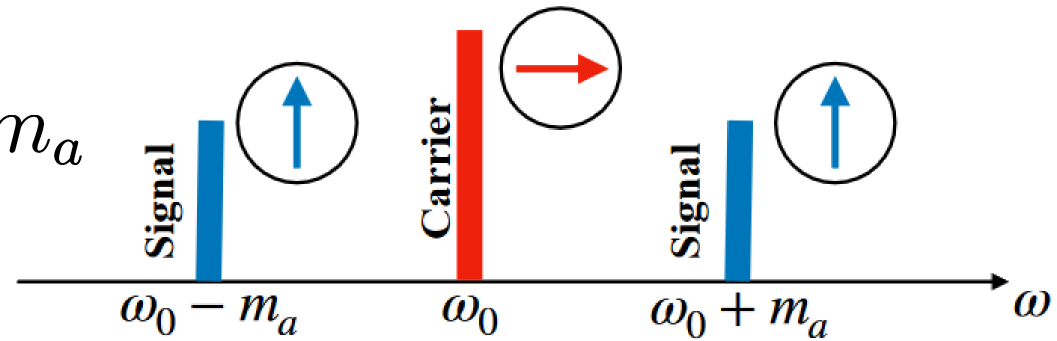

Liu+, PRD **100**, 023548 (2019)

- Sensitive when axion oscillation period and round-trip time of optical cavity is the same

Search with Linear Cavity

- Linear polarization rotates at axion frequency

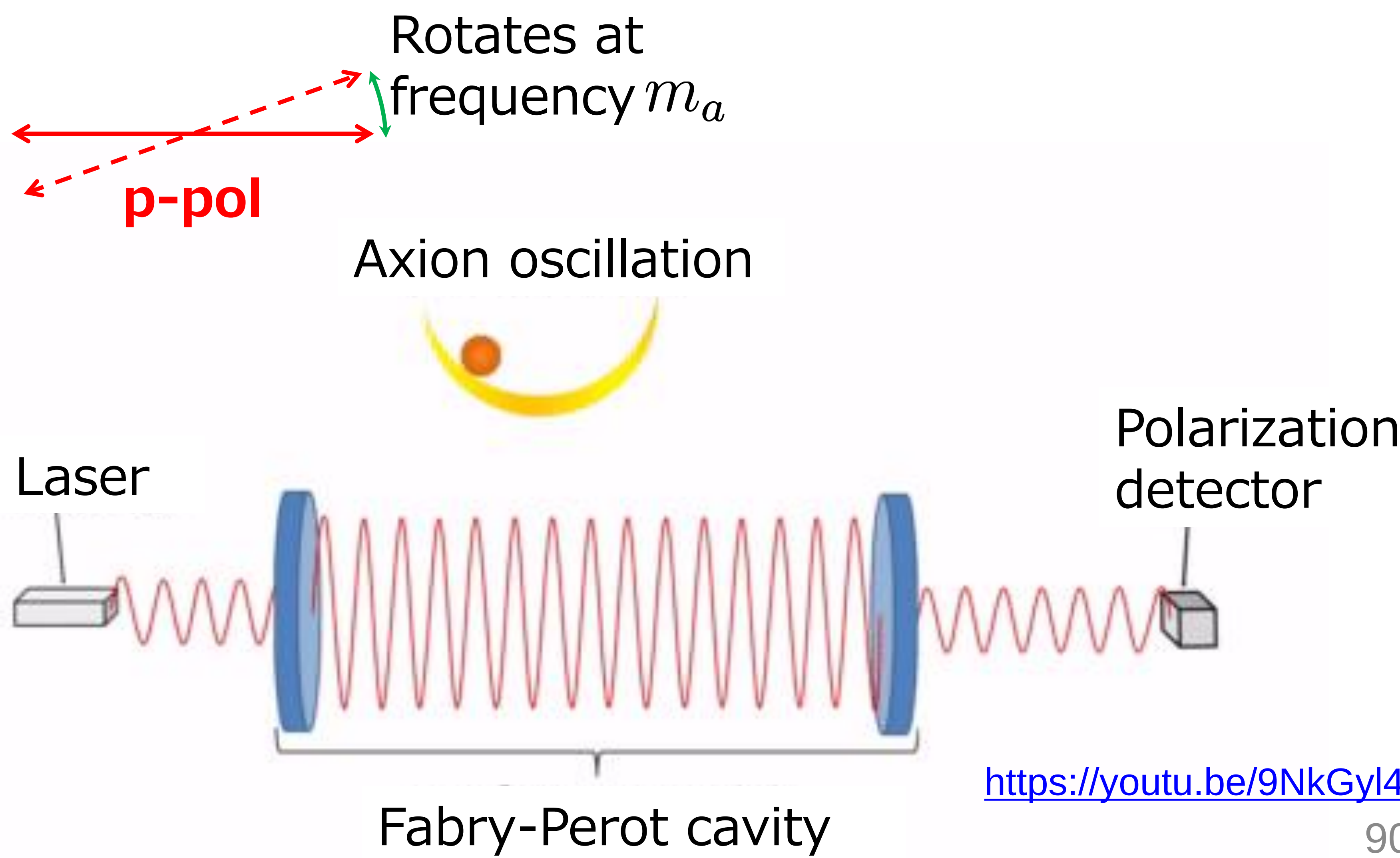

https://youtu.be/9NkGyl4cEks

Linear Cavity in GW Detectors

- Suitable because of long arms and high power
- Can be done simultaneously with GW observation
- Considering of applying to KAGRA

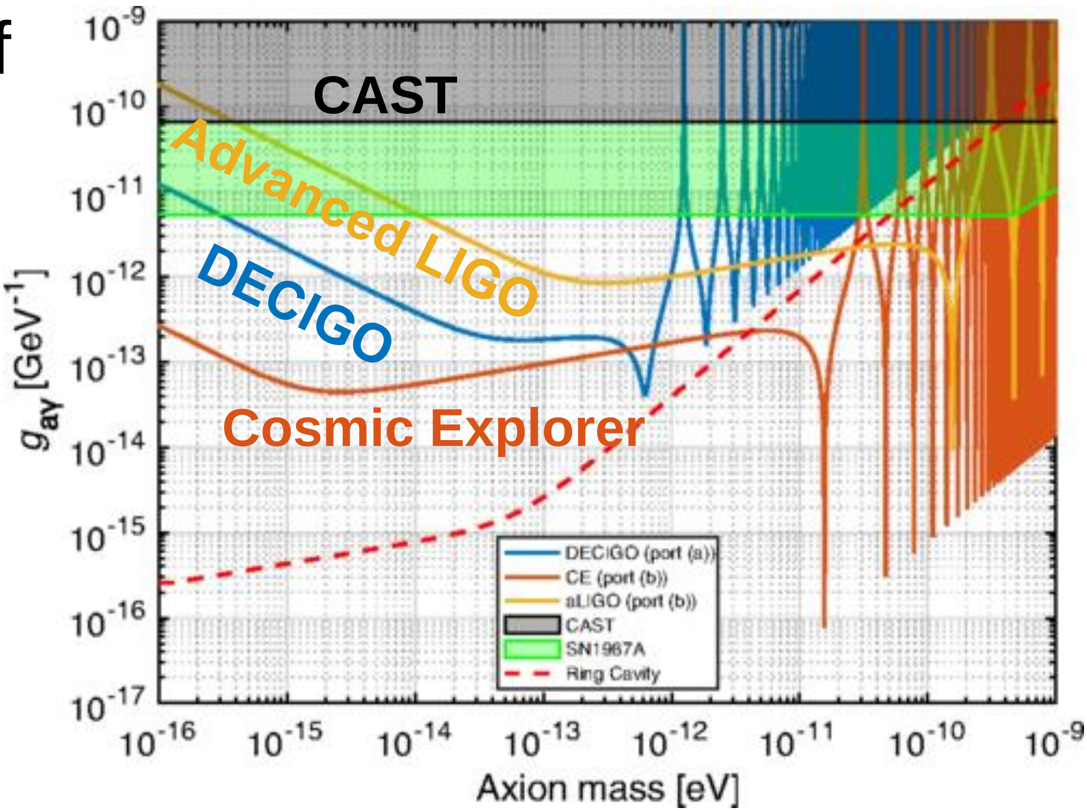

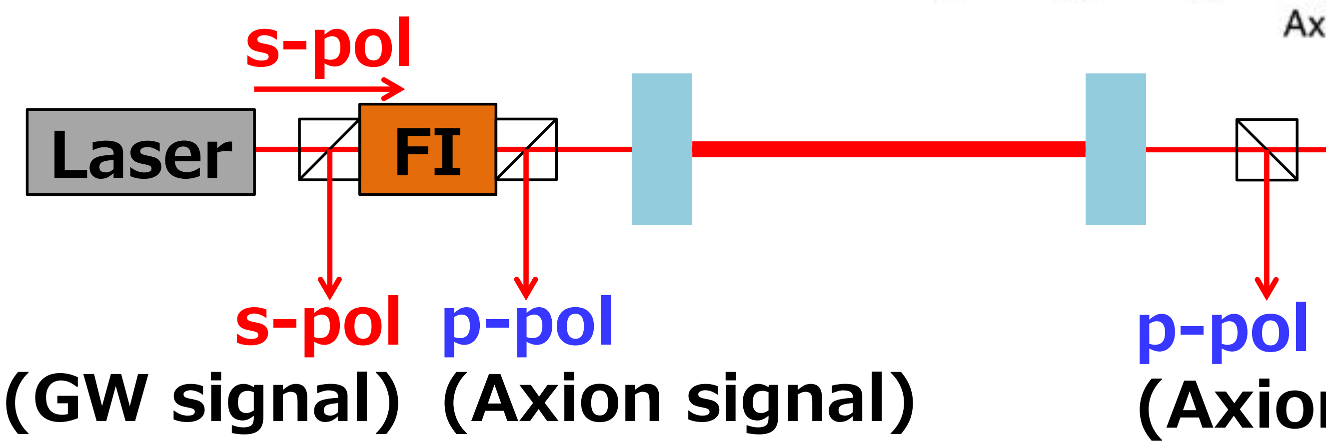

Nagano+, [PRL **123**, 111301 (2019)]

Other Recent Proposals

- There are also different proposals for axion dark matter search with laser interferometers

DeRocco & Hook, PRD **98**, 035021 (2018)

Liu+, PRD **100**, 023548 (2019) ; Martynov & Miao, arXiv:1911.00429

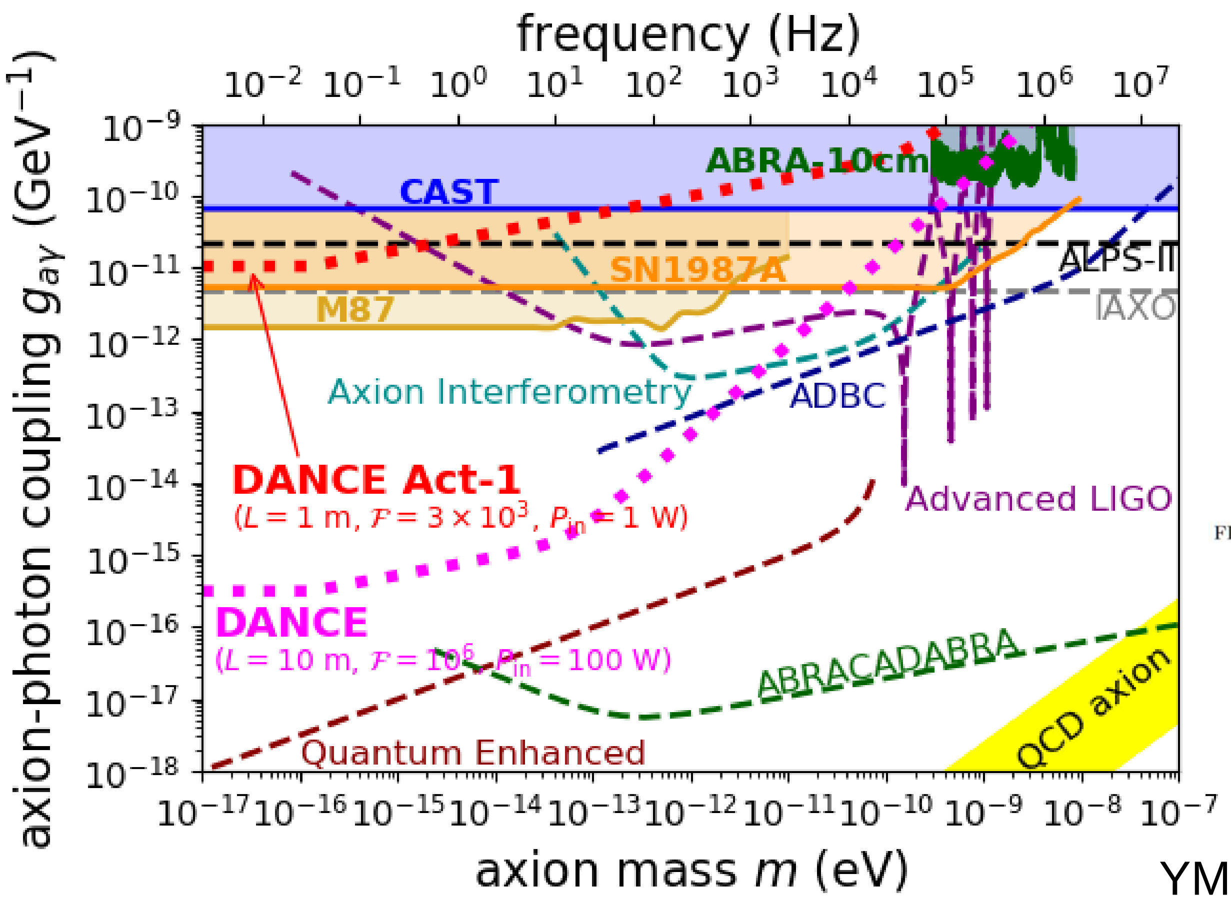

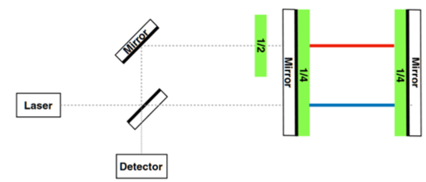

FIG. 3. A diagram of our proposed axion interferometer where

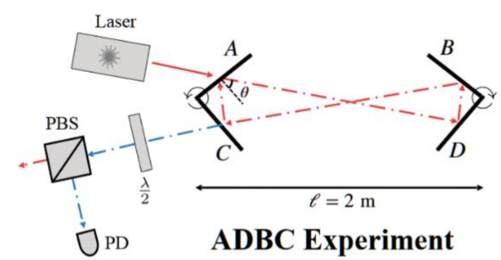

FIG. 2: Schematic of the ADBC experiment. The red optical

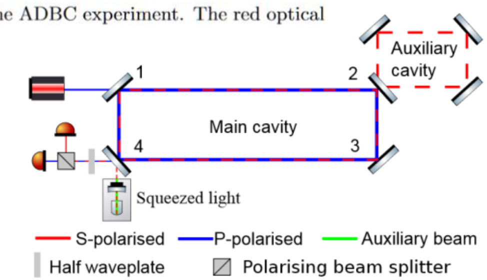

YM+, arXiv:1911.05196

Summary of Axion Search

- Proposed a new method to search for axion dark matter using a ring cavity
  Obata, Fujita, YM, PRL **121**, 161301 (2018)
- Measure phase velocity difference between two circular polarizations
  Bow-tie cavity and double-pass configuration
- Sensitivity to axion-photon coupling can be improved by several orders of magnitude for axion masses $m_a \lesssim 10^{-10}\,\mathrm{eV}$
- Prototype experiment DANCE Act 1 is on-going
- Also proposed a new method using laser interferometric gravitational wave detectors
  Nagano, Fujita, YM, Obata, PRL **123**, 111301 (2019)

Plan of the Talk

- **Basics of Laser Interferometry** (60 min)
  - Michelson interferometer
  - Fabry-Perot cavity
  - Quantum noise and other classical noises
- **Test of Lorentz Invariance** (30 min)
- **Search for Axion Dark Matter** (30 min)
- **Macroscopic Quantum Mechanics** (40 min)
- **KAGRA Gravitational Wave Telescope** (20 min)

- Slides available at https://tinyurl.com/YM20200109

Quantum Gravity?

- Whether photon goes X-arm or Y-arm is in quantum superposition

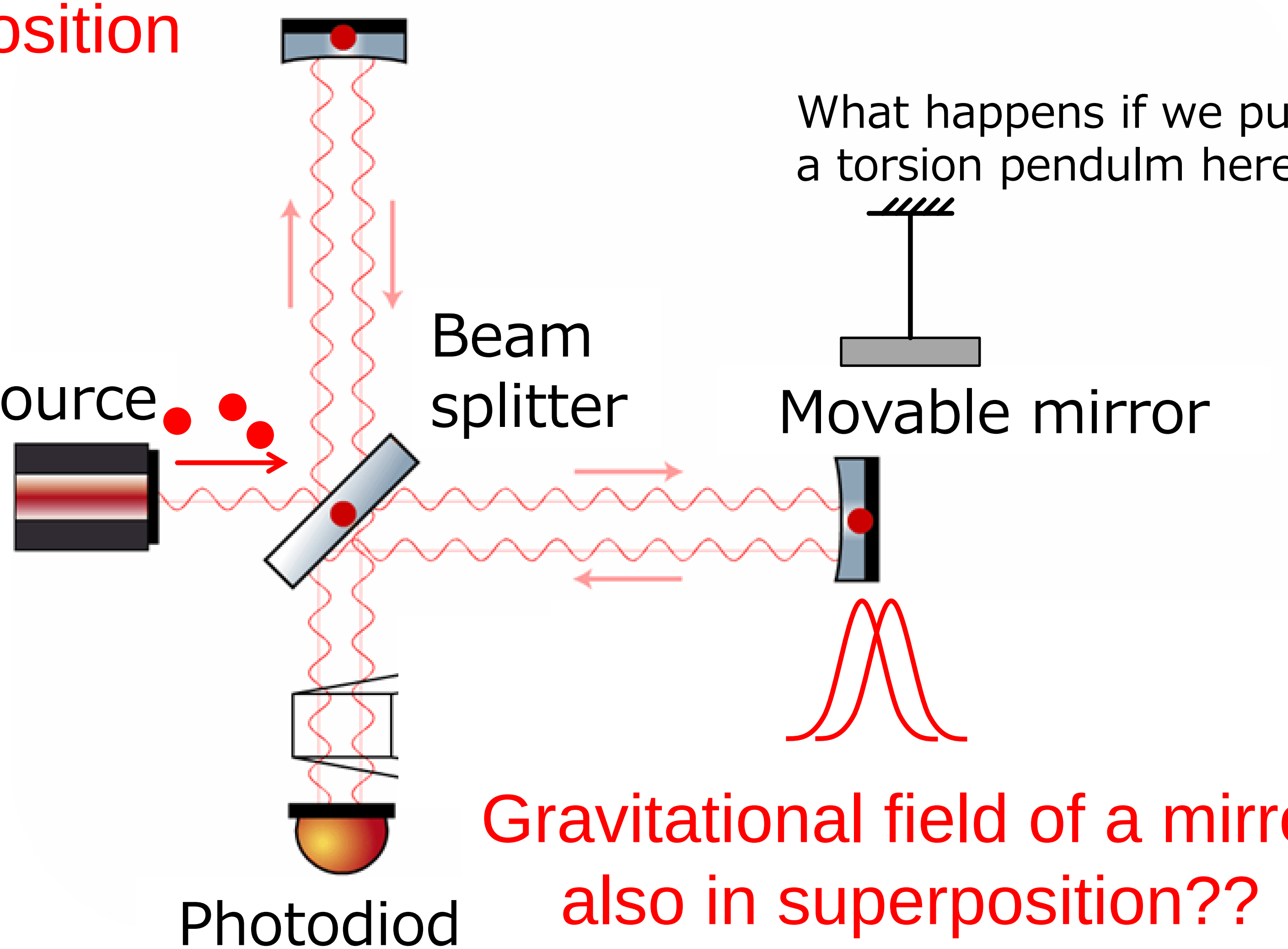

Gravitational field of a mirror also in superposition??

Macroscopic Quantum Mechanics

- Quantum mechanics do not depend on scales
- But macroscopic quantum superposition has never been observed (double-slit experiment upto 25 kDa (4e-23 kg)) [Nature Physics **15**, 1242 (2019)]

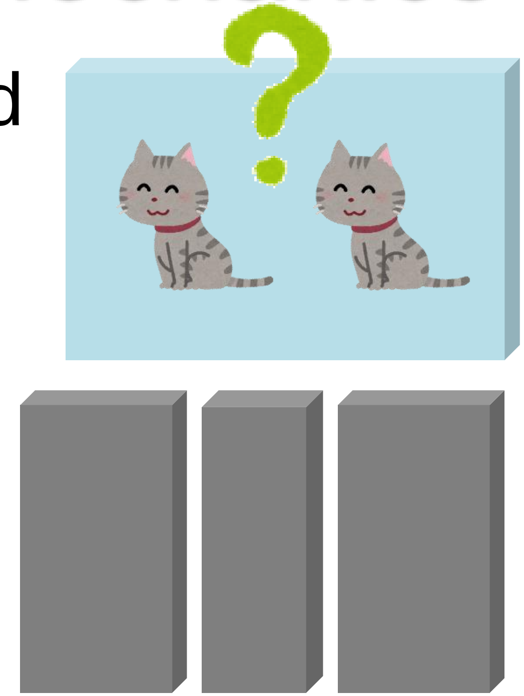

- Two possibilities at macroscopic scales
  - Quantum mechanics is valid, but too much classical decoherence
  - Quantum mechanics should be modified (e.g. non-linear Schrödinger Eq., Gravitational decoherence …)

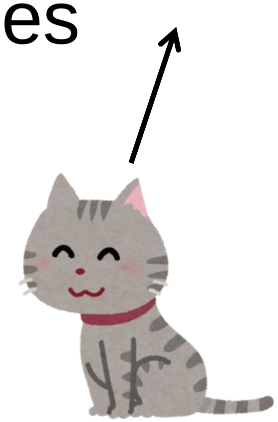

Experimental Proposals 1 / 4

- Towards Quantum Superpositions of a Mirror
  Marshall+, [PRL 91, 130401 (2003)]
- If no decoherence, photon interference fringe should revive at the period of mirror oscillation
- Ground state and ultra-strong coupling necessary

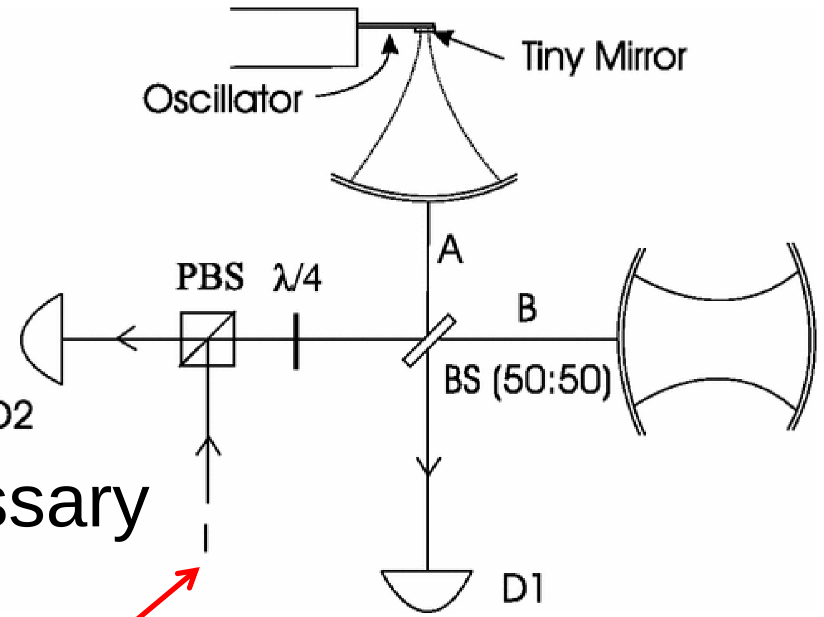

Single photon source

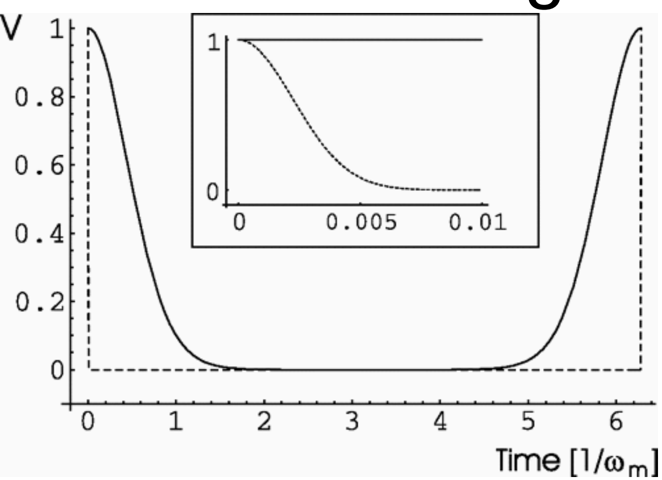

Photon path and mirror motion is entangled
If mirror has decoherence, photon interference fringe will also disappear

Experimental Proposals 2 / 4

- Entanglement of Macroscopic Test Masses and the Standard Quantum Limit in Laser Interferometry Muller-Ebhardt+, [PRL 100, 013601 (2008)]
- Quantum correlation between mirror common mode and differential mode
- Need to reach SQL for common/differential measurement

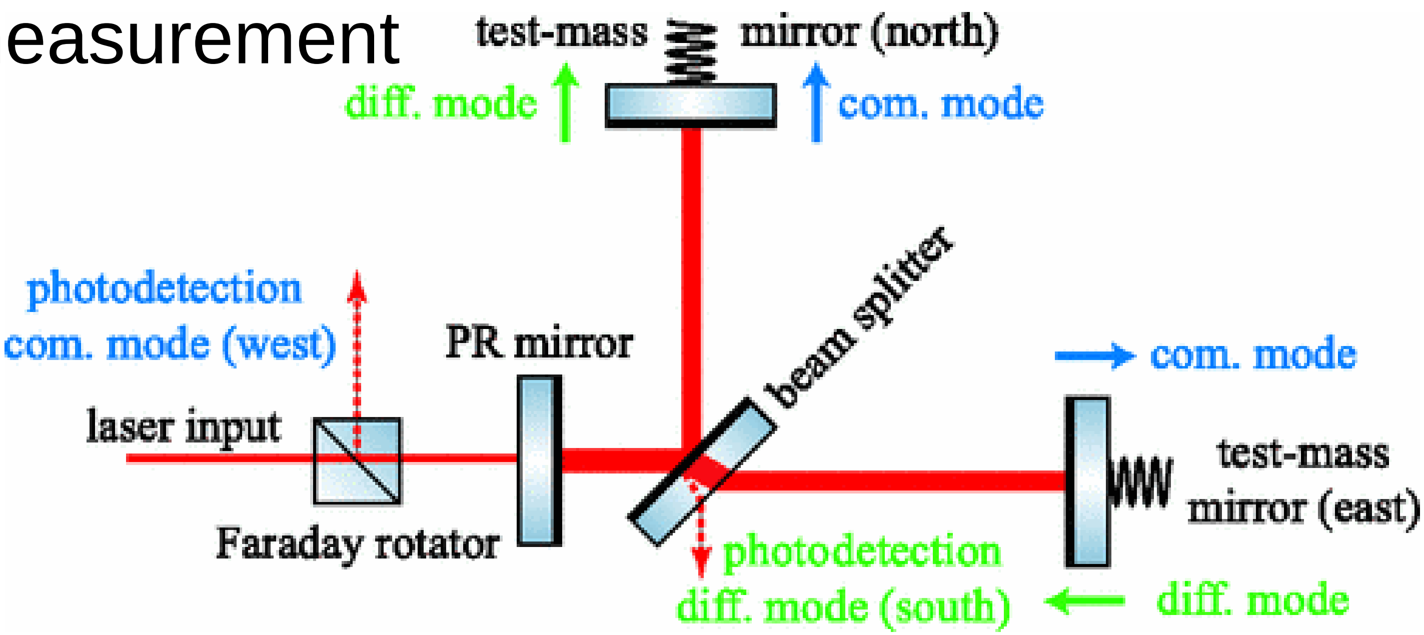

Experimental Proposals 3 / 4

- Large Quantum Superpositions and Interference of Massive Nanometer-Sized Objects
  Romero-Isart+, [PRL 107, 020405 (2011)]
- Prepare superposition of nanoparticle at left or right (not at the center), and drop it to see the interference pattern

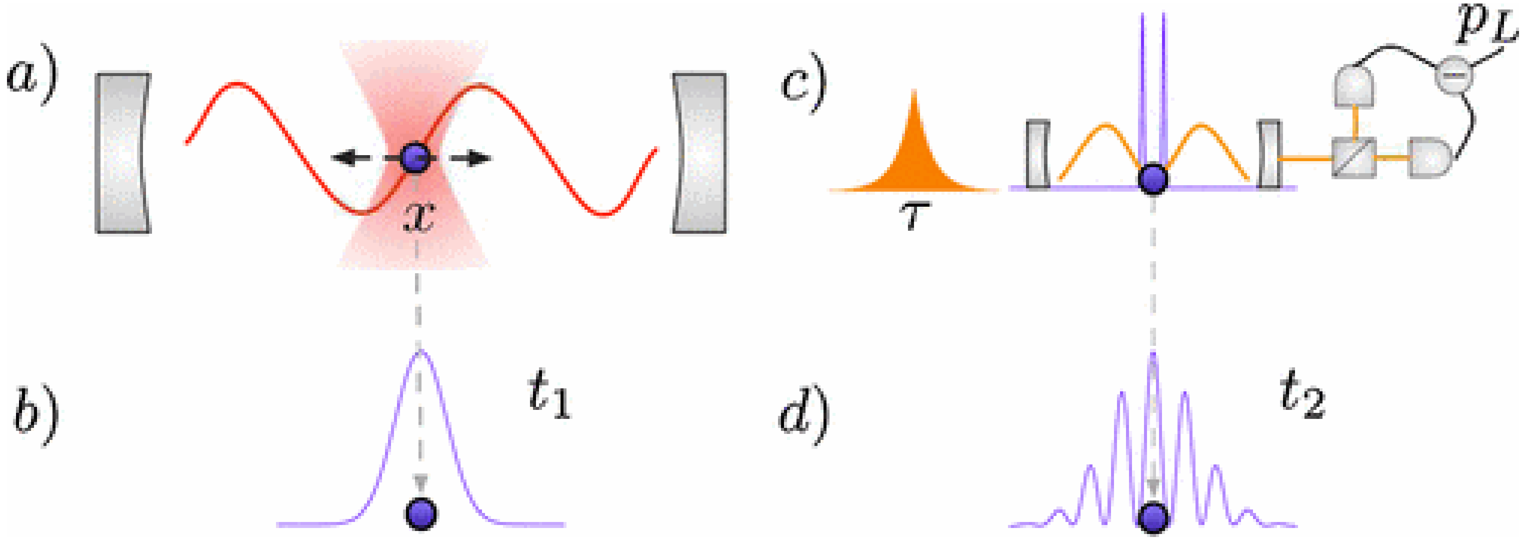

Experimental Proposals 4 / 4

- Quantum correlation of light mediated by gravity Miao+, arXiv:1901.05827
- Search for quantum correlation between two beams mediated by gravitational coupling of two mirrors
- Thermal noise should be smaller than quantum radiation pressure noise

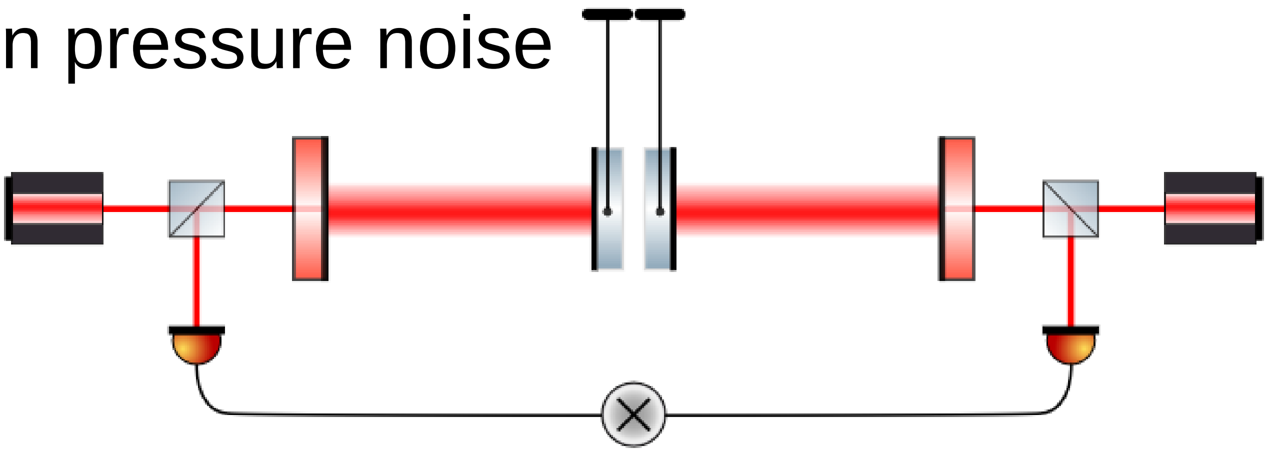

FIG. 1. Schematics showing the setup of two optomechanical cavities with their end mirrors coupled to each other through gravity. The quantum correlation of light is inferred by cross-correlating the readouts of two photodiodes.

Requirements to Optomechanics

- These systems are called optomechanical systems
  Interaction between light and mechanical oscillator

- Common requirements
  - Make thermal fluctuation smaller than quantum radiation pressure fluctuation (make quantum cooperativity larger than 1)
  - Reach standard quantum limit
  - Ground state cooling of mirror (make photon number smaller than ~1)

Optomechanical Systems

- SQL not yet reached above Planck mass scale

Double-slit

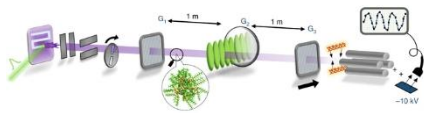

molecules, 40 zg
Fein+ (2019)

Planck mass (22 ug)

Factor of ~3 to SQL

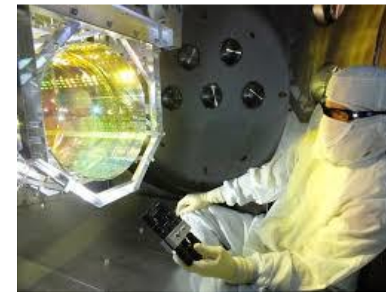

suspended disk, 40 kg
Advanced LIGO

Quantum radiation pressure

cantilever, 50 ng
Cripe+ (2019)

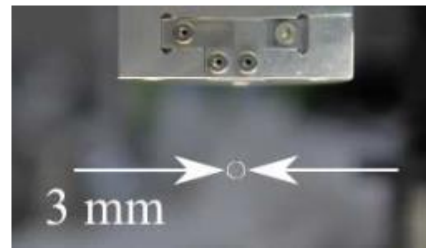

suspended disk, 7 mg
Matsumoto+ (2019)

Ground state cooling

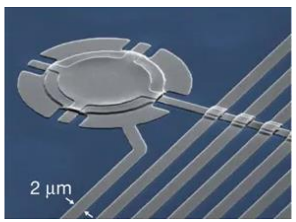

membrane, 48 pg
Taufel+ (2011)

suspended bar, 10 mg
Komori+ (2019)

Ground state cooling

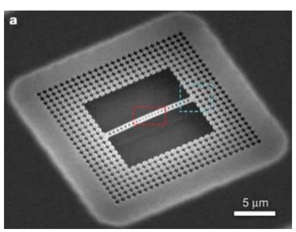

nanobeam, 331 fg
Chan+ (2011)

Ground state cooling

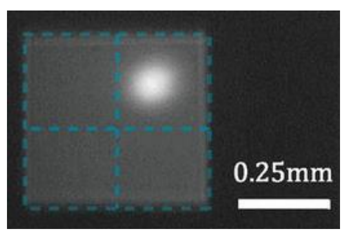

membrane, 7 ng
Peterson+ (2016)

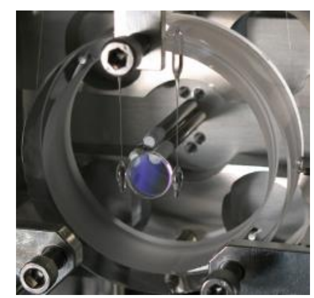

suspended disk, 1 g
Neben+ (2012)

fg pg ng ug mg g kg

Optomechanical Systems

- SQL not yet reached above Planck mass scale

Double-slit

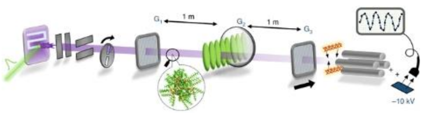

molecules, 40 zg
Fein+ (2019)

Planck mass (22 ug)

Factor of ~3 to SQL

Quantum radiation pressure

Ground state cooling

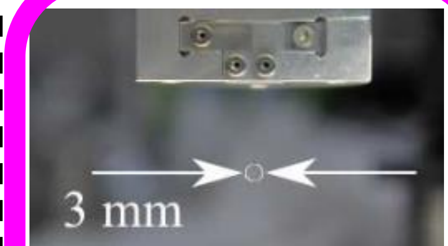

suspended disk, 7 mg
Matsumoto+ (2019)

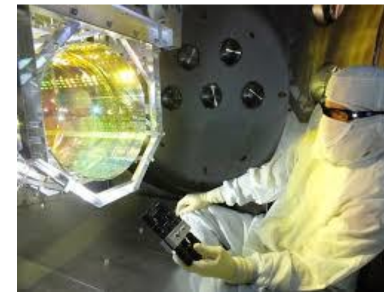

suspended disk, 40 kg
Advanced LIGO

We are focusing on mg-scale experiments to probe boundary between quantum world and gravitational world

suspended bar, 10 mg
Komori+ (2019)

nanobeam, 331 fg
Chan+ (2011)

membrane, 7 ng
Peterson+ (2016)

suspended disk, 1 g
Neben+ (2012)

fg pg ng ug mg g kg

Three Approaches

- Simple pendulum (suspended disk)
  Reduce thermal noise by use of very thin wire
- Torsion pendulum (suspended bar)
  Reduce thermal noise by lowering mechanical resonant frequency
- Optical levitation
  Remove suspension thermal noise

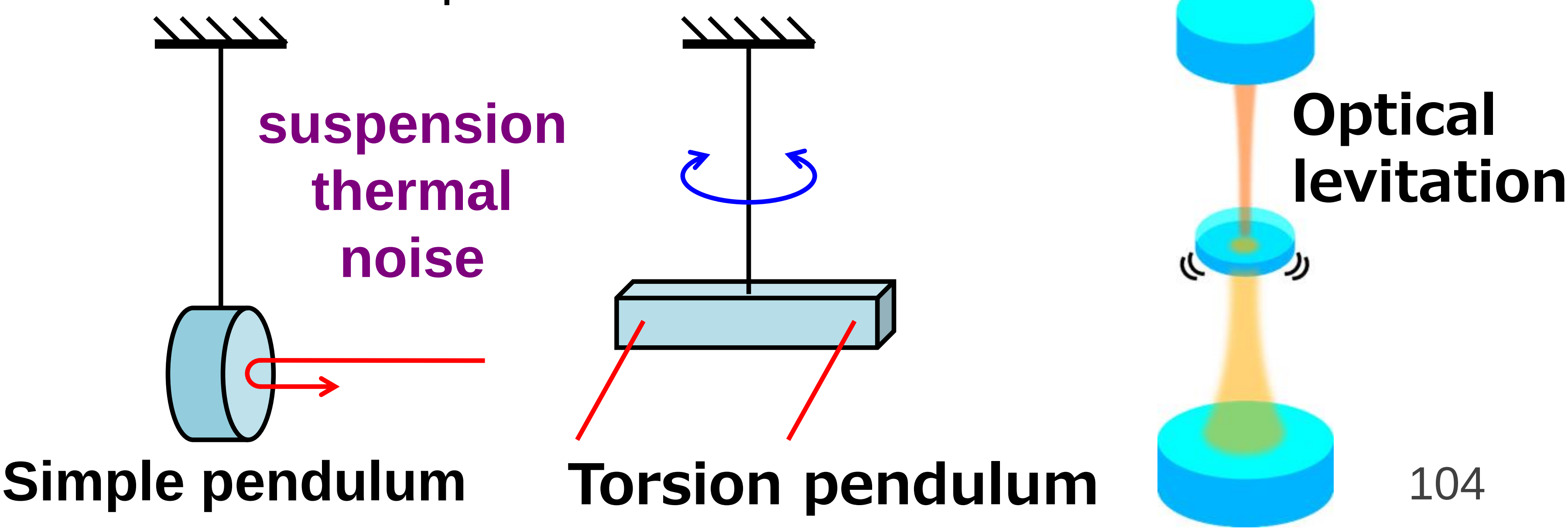

7 mg Suspended Disk

- Displacement sensitivity at 3e-14 m/√Hz @ 280 Hz
- Thermal noise limited
- Possible to measure 100 mg gravity in a second

TOHOKU UNIVERSITY

(c)

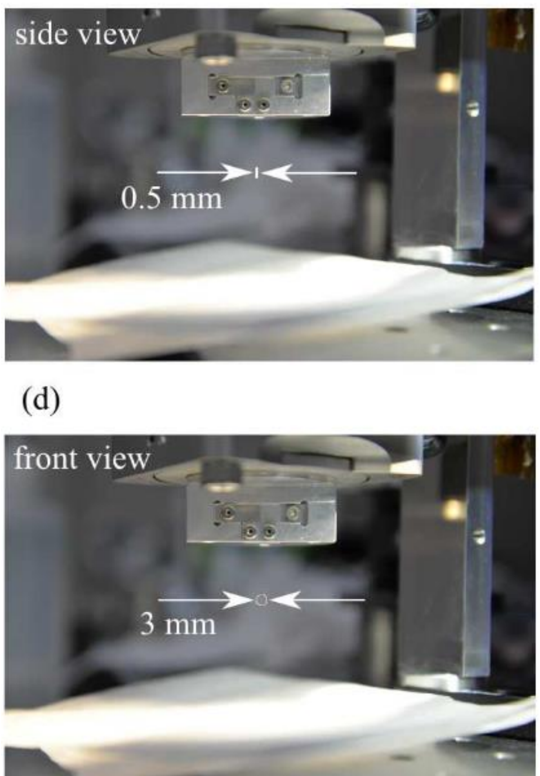

(d)

Matsumoto, …, YM+, PRL 122, 071101 (2019)

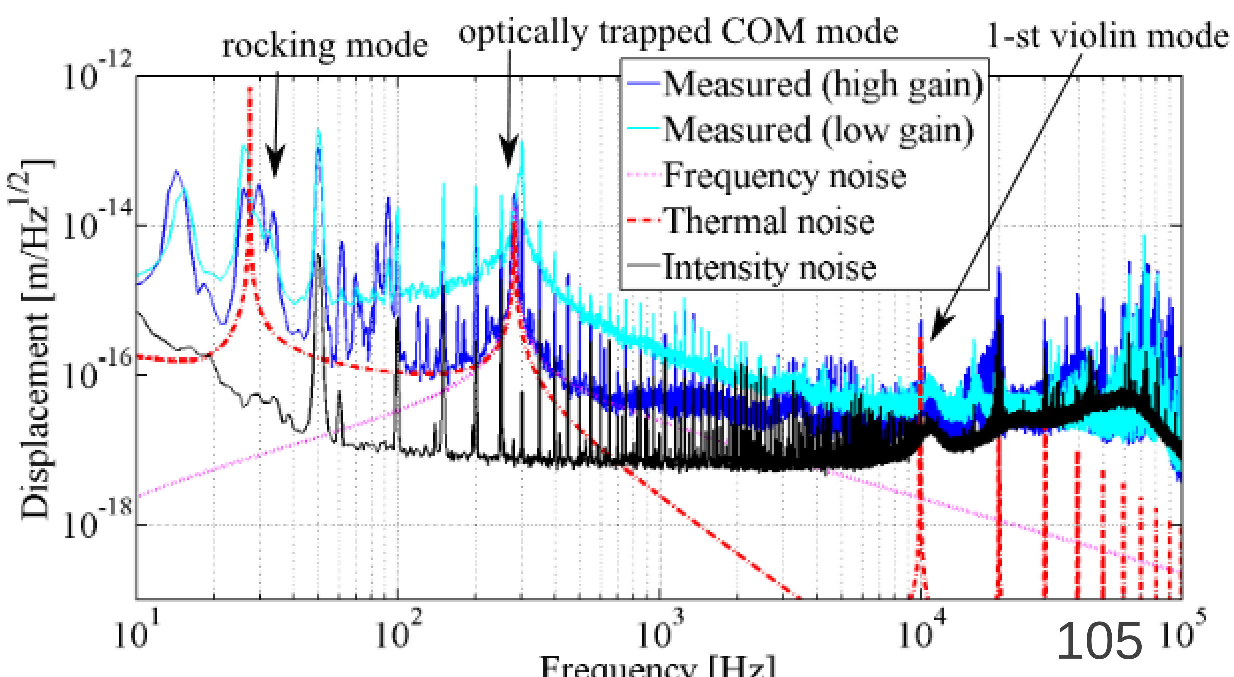

Monolithic Suspension

- Currently developing a suspension with lower mechanical loss

Cataño-Lopez+, arXiv:1912.12567

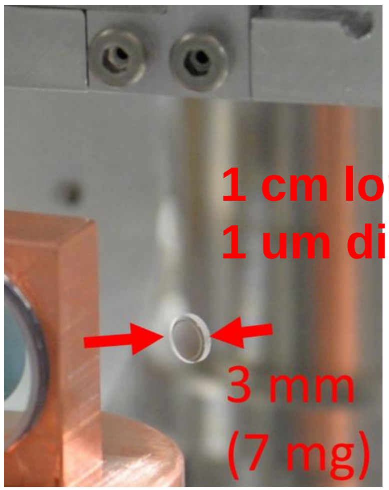

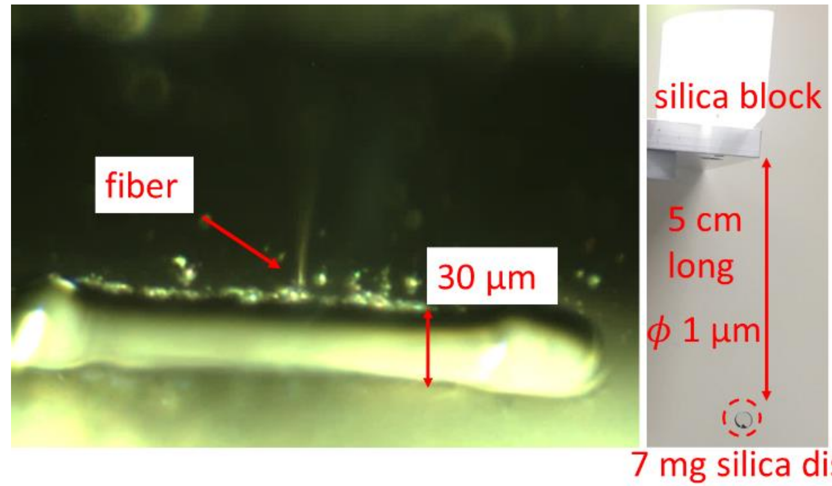

Fused silica fiber attached with epoxy

Pendulum
  resonant frequency 4.4 Hz
  Qm=1e5
After optical trap
  resonant frequency 280 Hz
  Qeff=1e8

⇨

Fused silica fiber welded

Pendulum
  resonant frequency 2.2 Hz
  Qm=2e6
After optical trap (planned)
  resonant frequency 300 Hz
  Qeff=4e10

Possible Application to DM Search

- As a force sensor, optomechanical system can be used for dark matter search
- Already sensitive enough to search for ultralight vector dark matter which couples to B-L charge

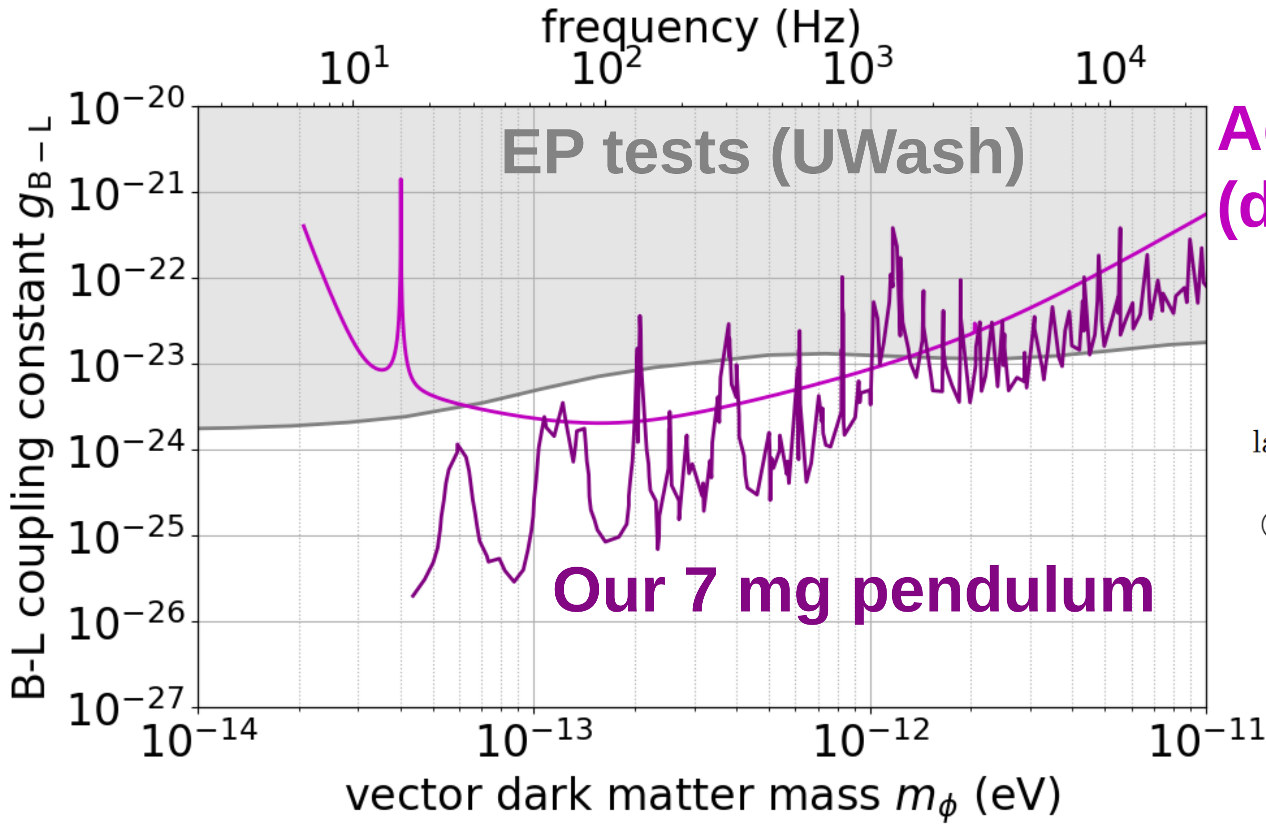

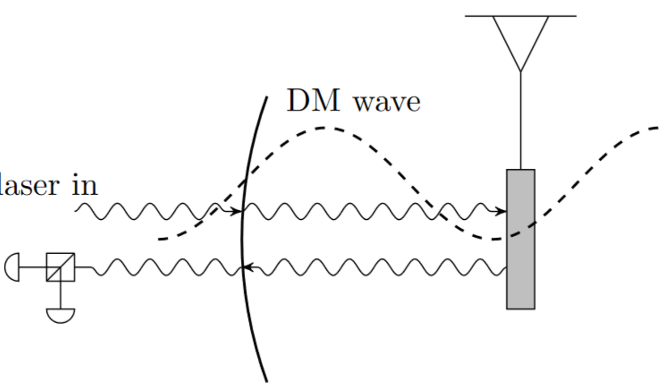

Carney+, arXiv:1908.04797

10 mg Torsion Pendulum

- Torque sensitivity
  2e-17 Nm/√Hz @ 100 Hz
  (2e-15 N/√Hz in force)

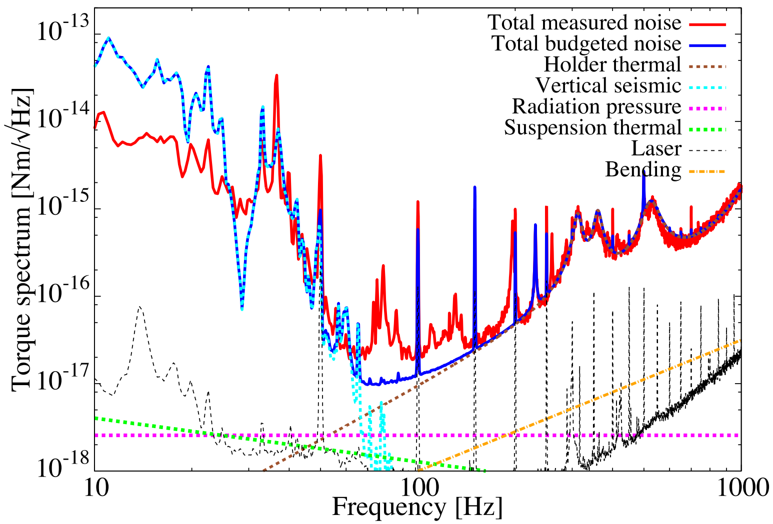

- Most sensitive mg-scale torsion pendulum
  Komori, …, YM+, arXiv:1907.13139

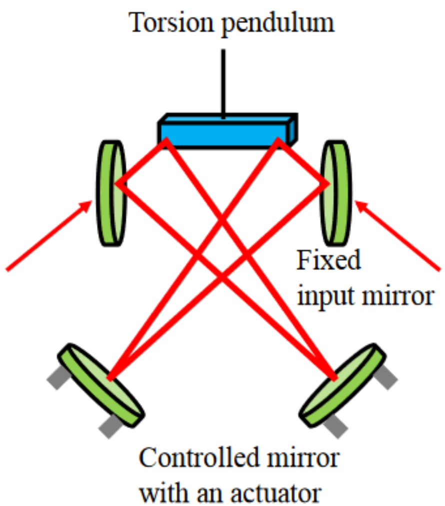

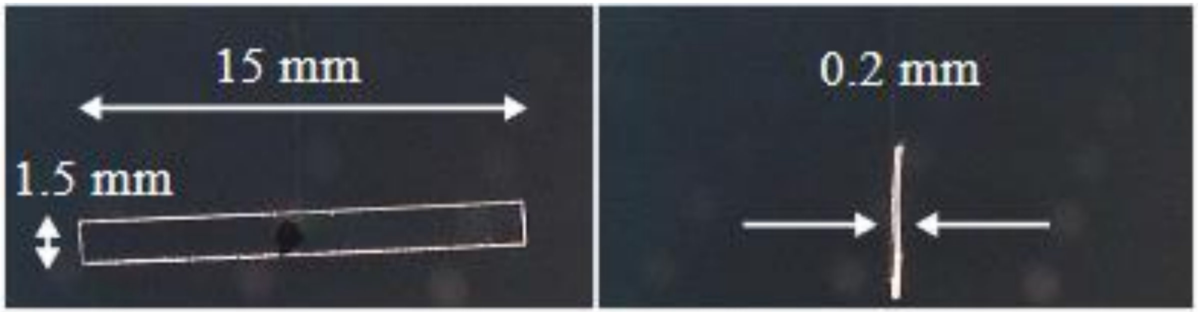

Front view

Side view

Optical Levitation

- Alternative approach is to support a mirror with radiation pressure alone
- Both suspended mirror and levitated mirror will be ultimately limited by thermal noise from residual gas and mirror coating

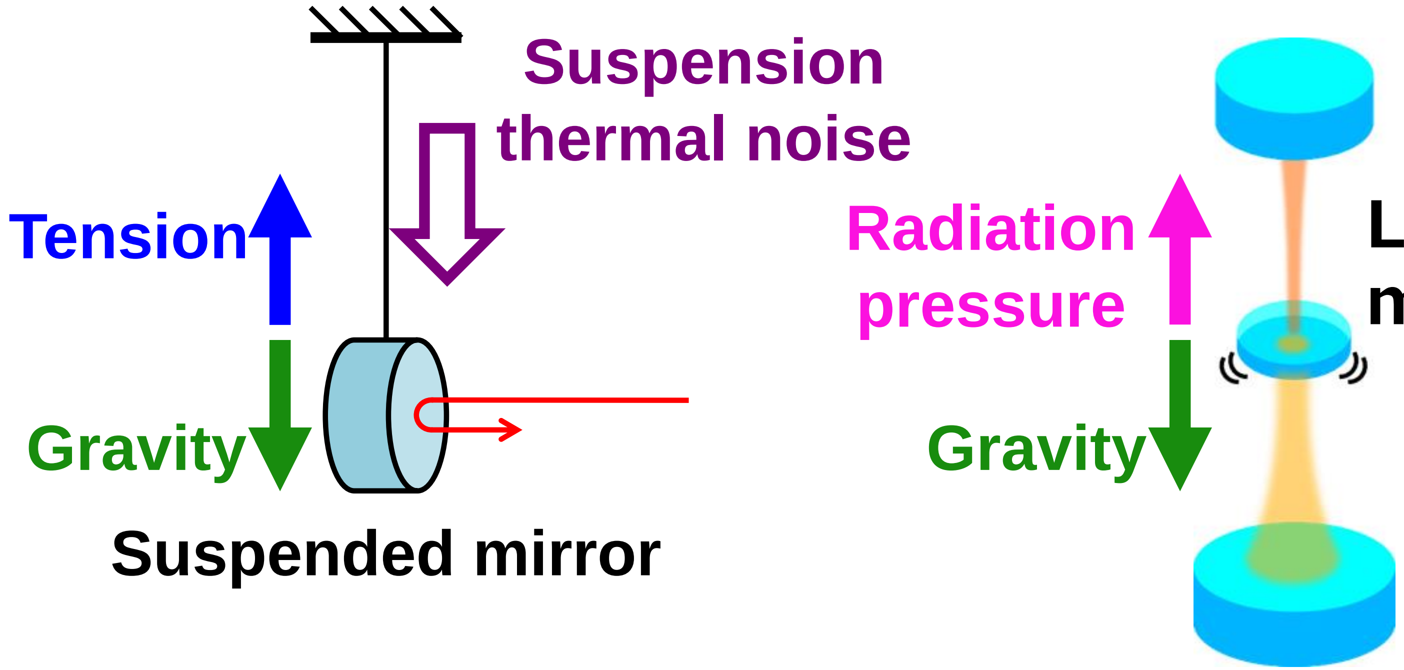

Sandwich Configuration

- Optical levitation have never been realized
- Simpler configuration than previous proposals

  YM, Kuwahara+, [Optics Express 25, 13799 (2017)]
- Proved that stable levitation is possible and SQL can be reached

Levitated mirror

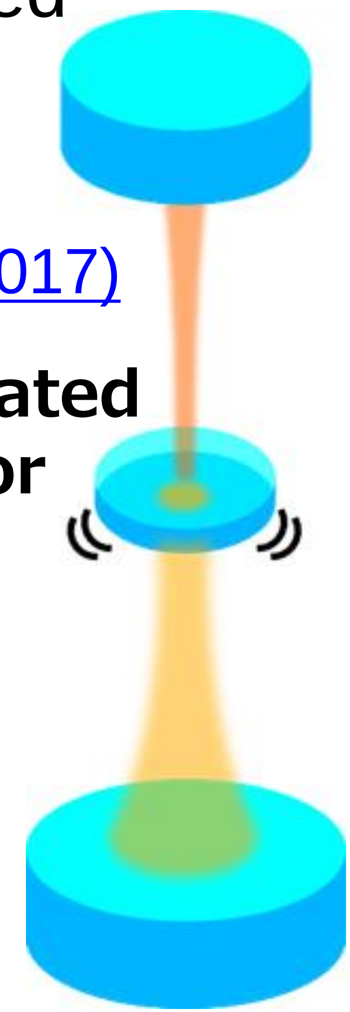

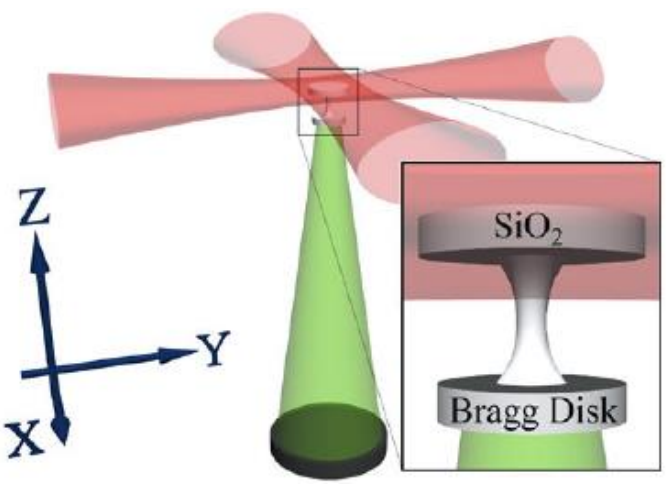

S. Singh+: PRL 105, 213602 (2010)

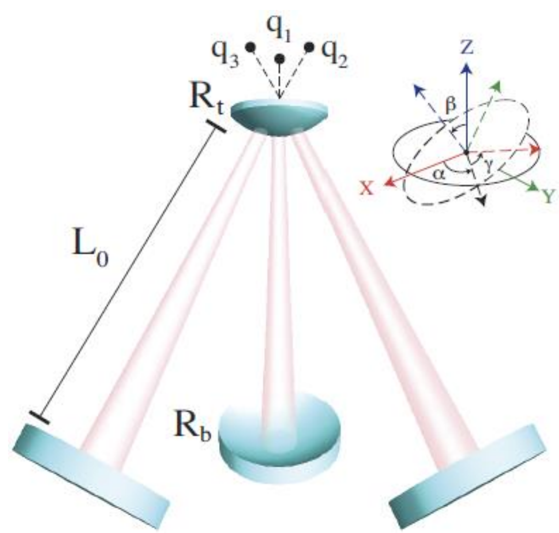

G. Guccione+: PRL 111, 183001 (2013)

Stability of Levitation

- Rotational motion is stable with gravity
- Vertical motion is stable with optical spring
- Horizontal motion is stable with cavity axis change

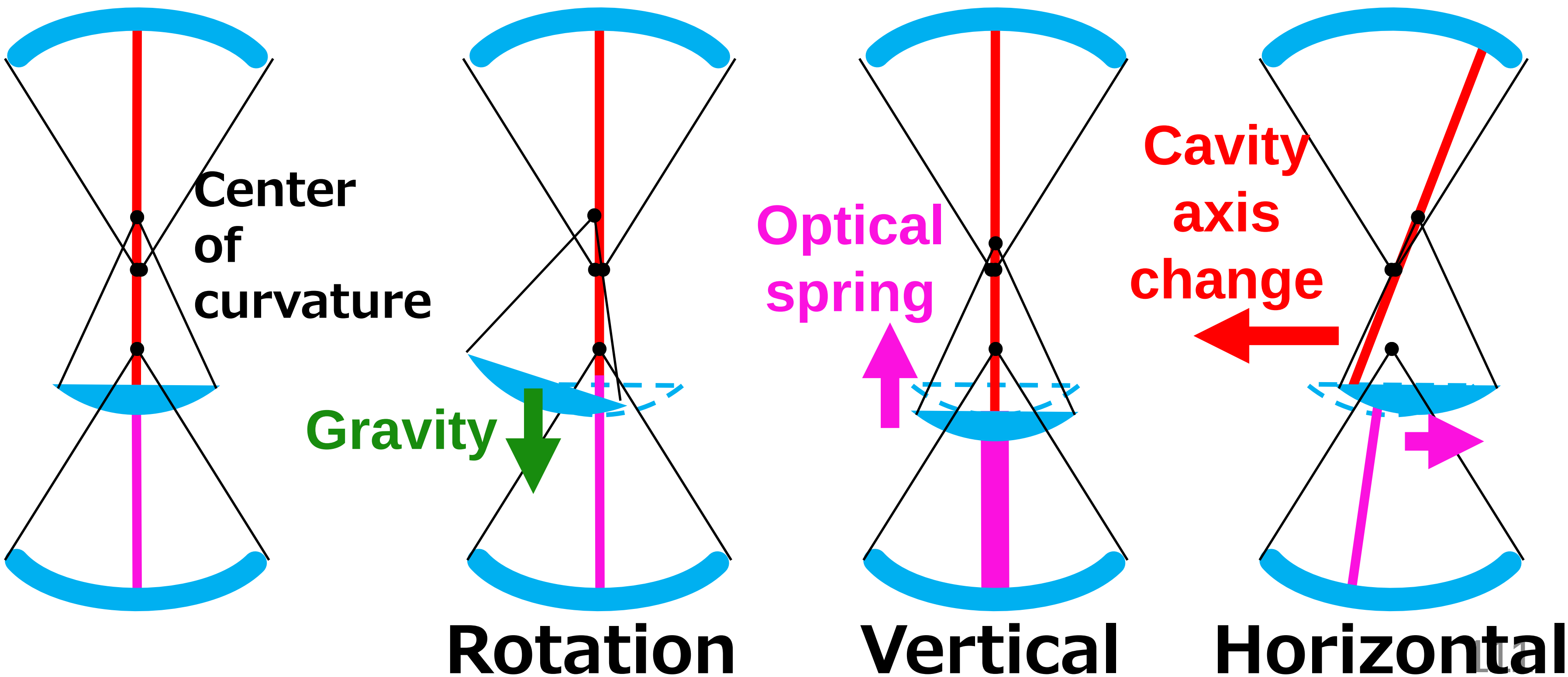

Reaching SQL

- 0.2 mg fused silica mirror, Finesse of 100, 13 W + 4 W input

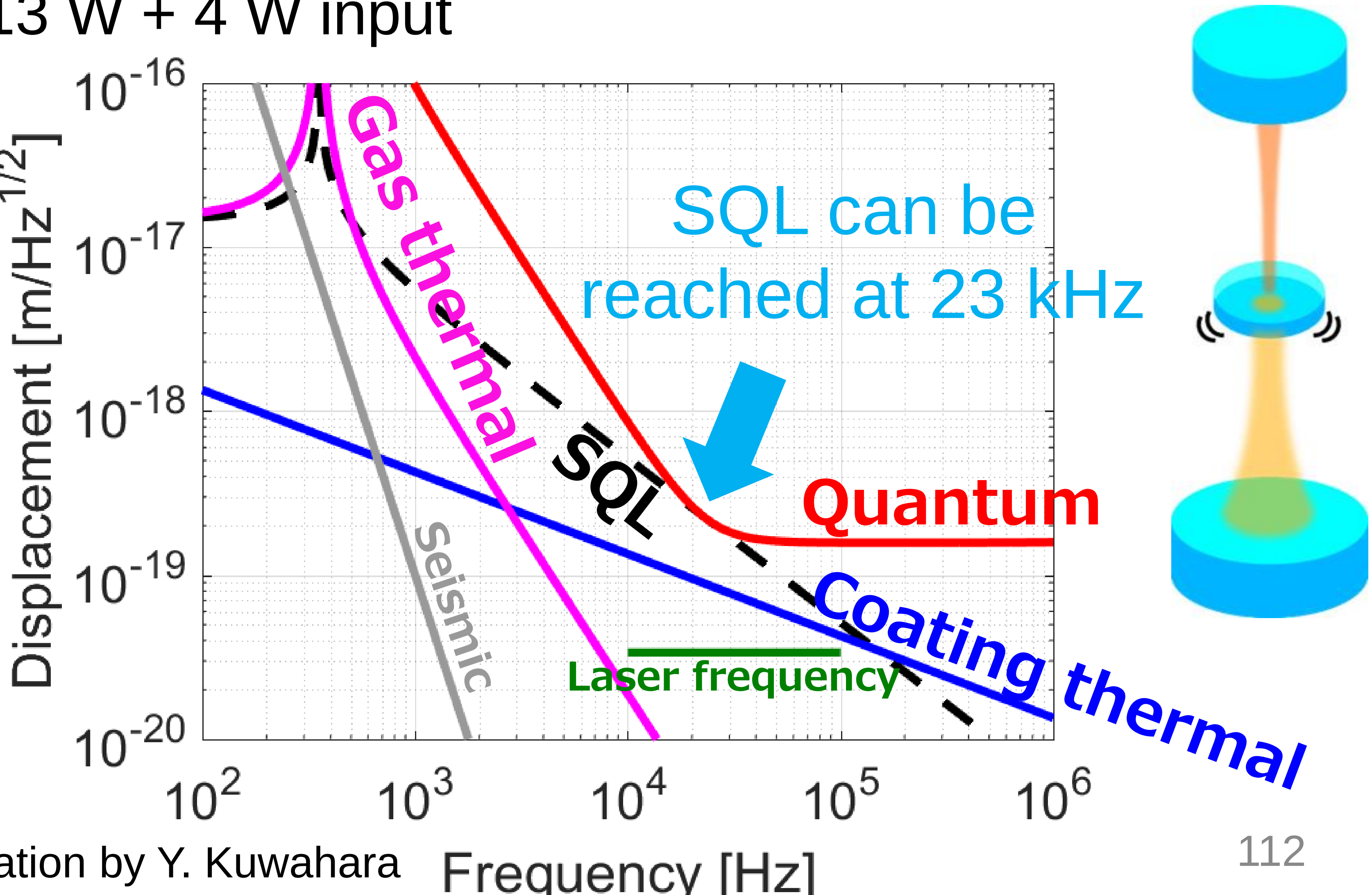

Calculation by Y. Kuwahara

Experiment to Verify the Stability

- Especially, stability of the horizontal motion is special for this sandwich configuration
- Experiment with torsion pendulum is underway to measure the restoring force

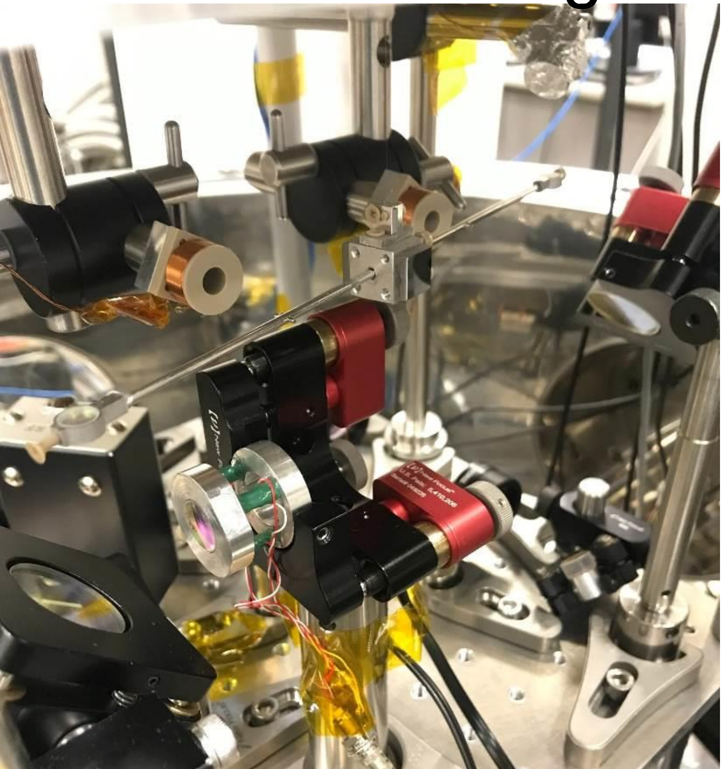

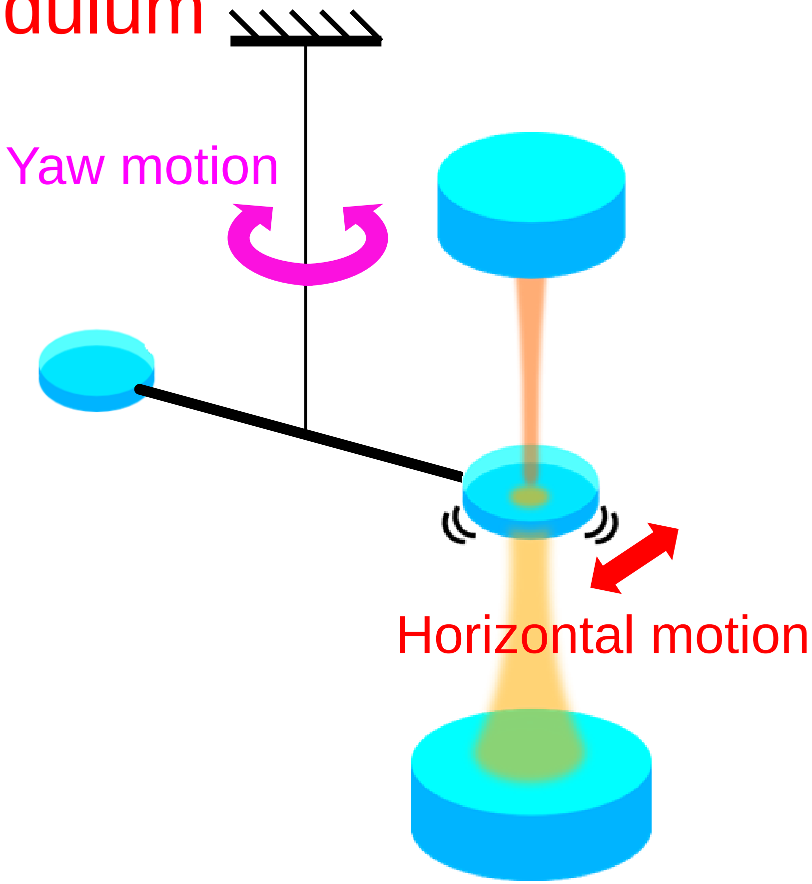

Experiment to Verify the Stability

- Resonant frequency of torsion pendulum increased when optical cavity is locked

→ Successfully measured the restoring force

Spring constant increase with power

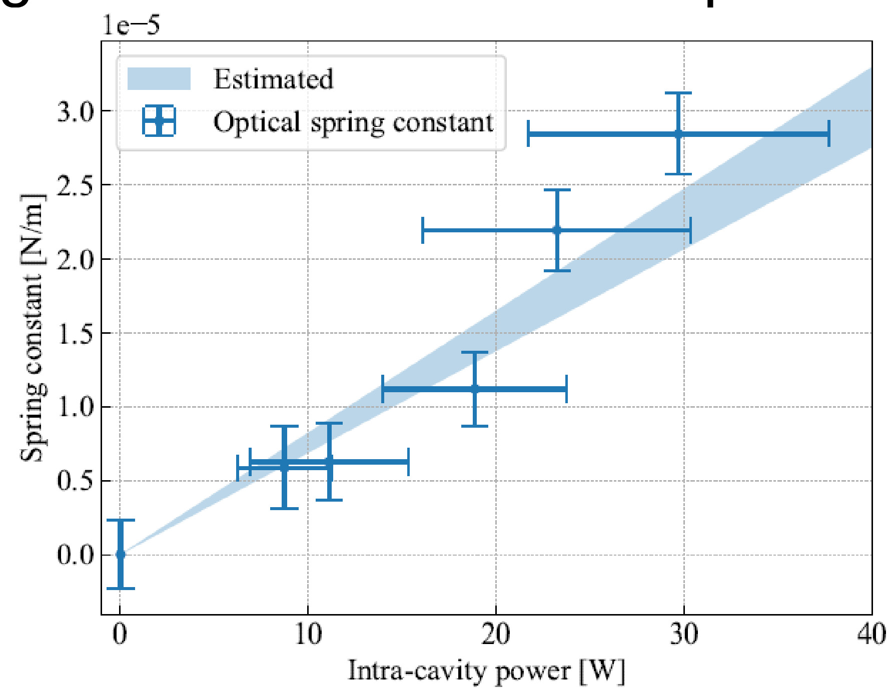

Resonant frequency measurement

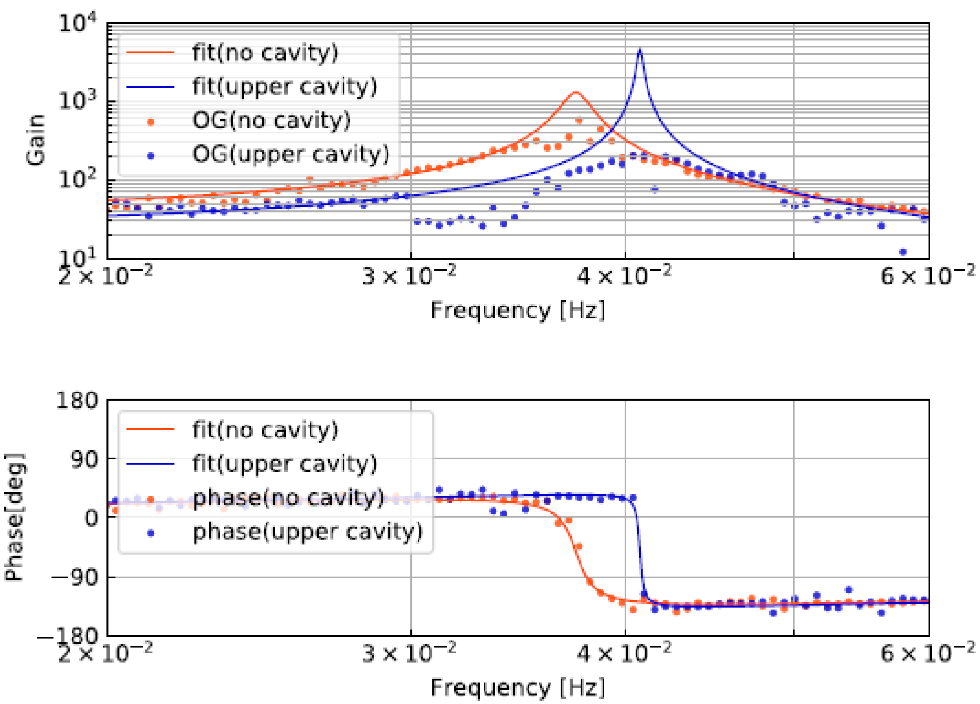

plot by N. Kita

Fabrication of Levitation Mirrors

- Fused silica mirror with dielectric multilayer coating have been tried, but cracks due to coating stress
- Looking for alternative methods

	For SQL	Prototype	For suspended experiment
Mass	0.2 mg	~1.6 mg	~ 7 mg
Size (mm)	φ 0.7 mm t 0.23 mm	φ 3 mm t 0.1 mm	φ 3 mm t 0.5 mm
RoC	30 mm convex	30±10 mm convex (measured: 15.9±0.5 mm)	100 mm concave (previously flat ones were used)
Reflectivity	97 % (finesse 100)	>99.95 % (measured: >99.5%)	99.99%
Comment	[Optics Express 25, 13799 (2017)]()	Only one out of 8 without big cracks	Succeeded

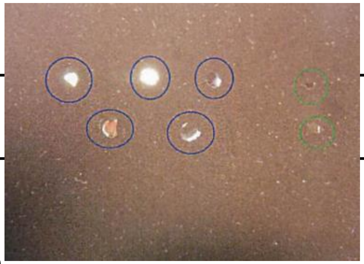

Photonic Crystal Mirror ?

- M. S. Seghilani+, [Optics Express 22, 5962 (2014)]()

R > 99%

RoC = 20 mm

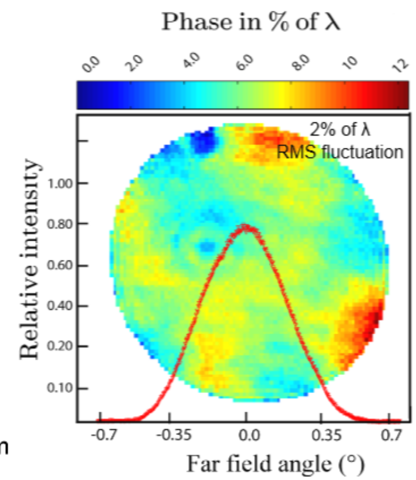

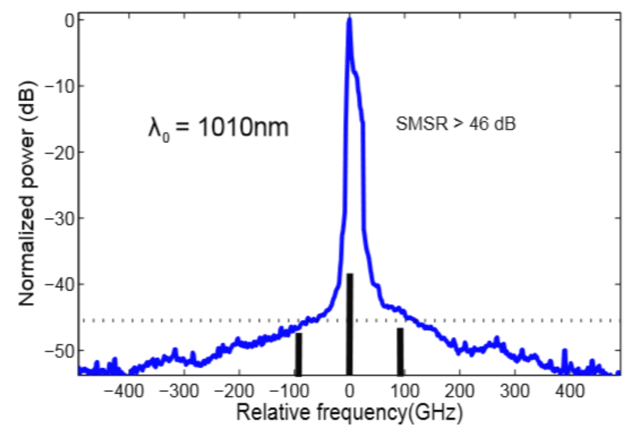

Distributed Bragg reflector (DBR) for high reflectivity

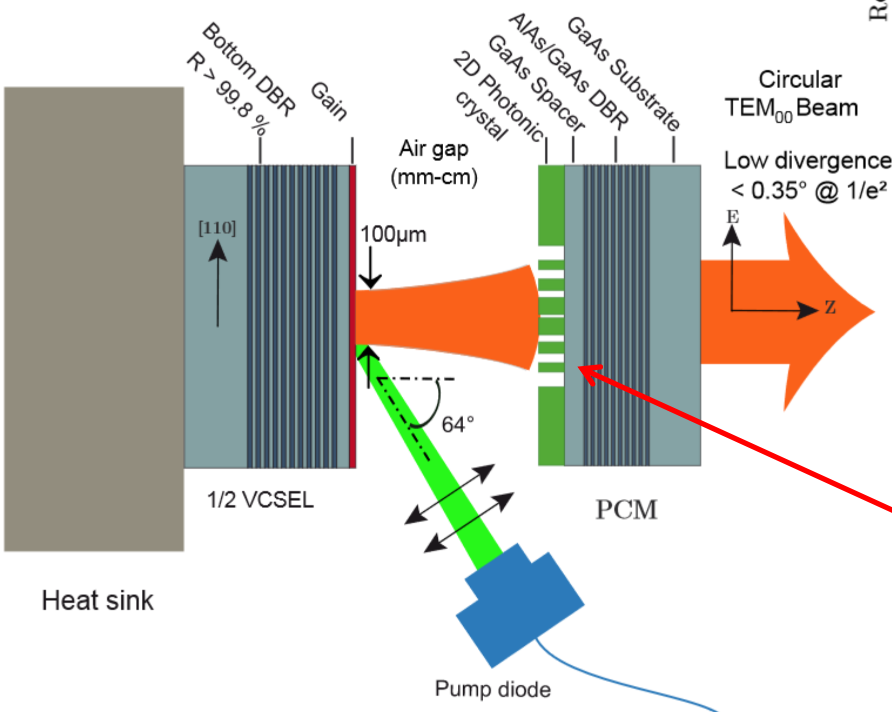

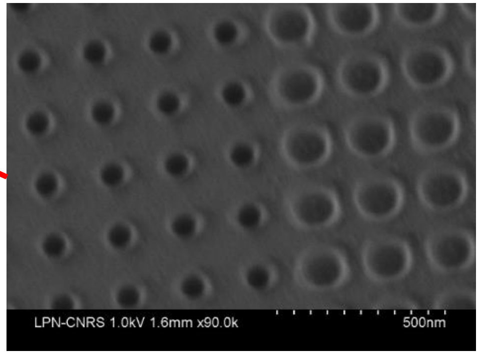

Summary of MQM Experiments

- Working on milligram scale experiments to test quantum mechanics at macroscopic scales
- Three approaches
  - **Simple pendulum**

    Sensitivity of 3e-14 m/rtHz achieved

    Fabricating monolithic suspension with Qeff~4e10
  - **Torsion pendulum**

    Sensitivity of 2e-15 N/rtHz achieved
  - **Optical levitation**

    Successfully demonstrated the stability

    Trying to make a levitation mirror
- Also interested in dark matter search using these systems

Plan of the Talk

- **Basics of Laser Interferometry** (60 min)
  - Michelson interferometer
  - Fabry-Perot cavity
  - Quantum noise and other classical noises
- **Test of Lorentz Invariance** (30 min)
- **Search for Axion Dark Matter** (30 min)
- **Macroscopic Quantum Mechanics** (40 min)
- **KAGRA Gravitational Wave Telescope** (20 min)

- Slides available at https://tinyurl.com/YM20200109

Gravitational Waves

- Ripples in space-time
- Stretches and squeezes length
- Strain amplitude:
  fraction of length change
- Two polarizations
  (plus and cross)

$$h = \frac{\delta L}{L}$$

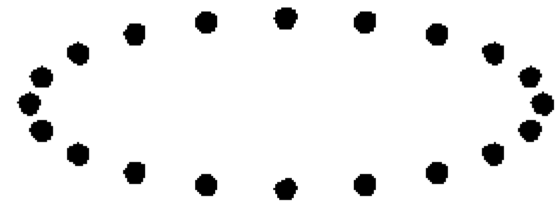

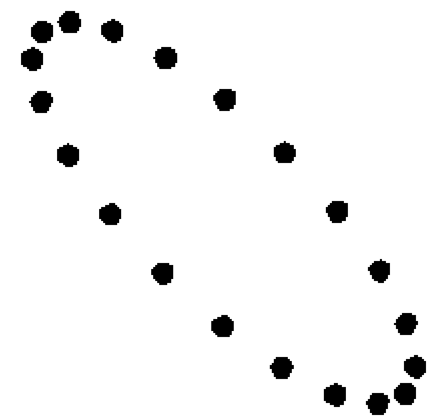

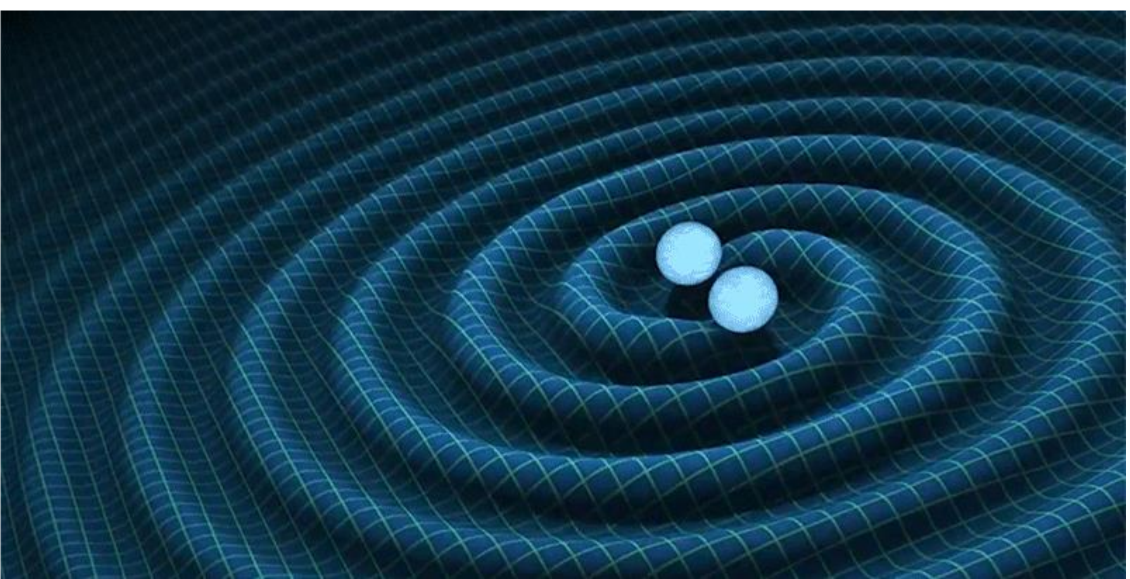

Global Network of GW Detectors

- Network of ground-based Advanced interferometric gravitational wave detectors

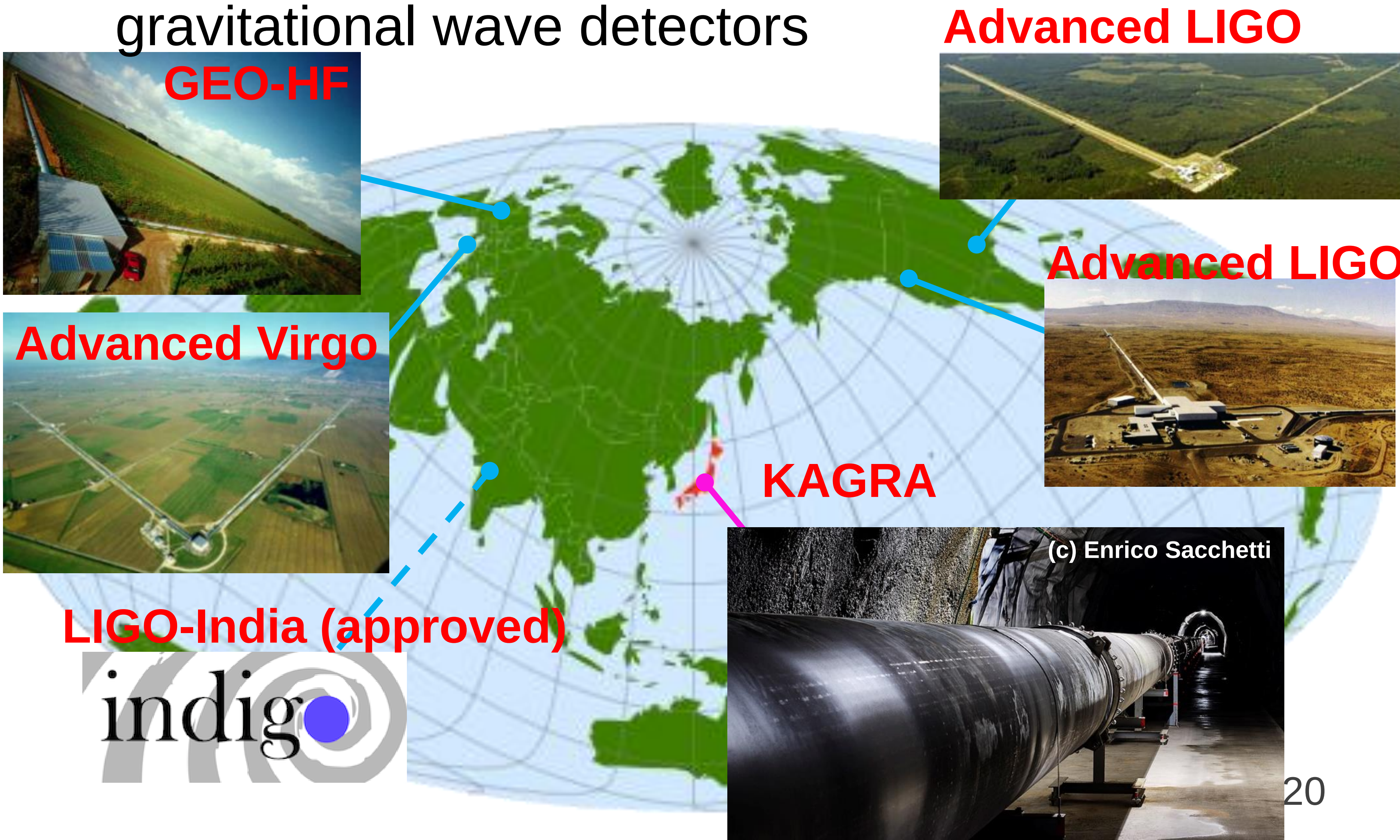

Designed Sensitivity

- aLIGO, AdV and KAGRA has similar designed sensitivity

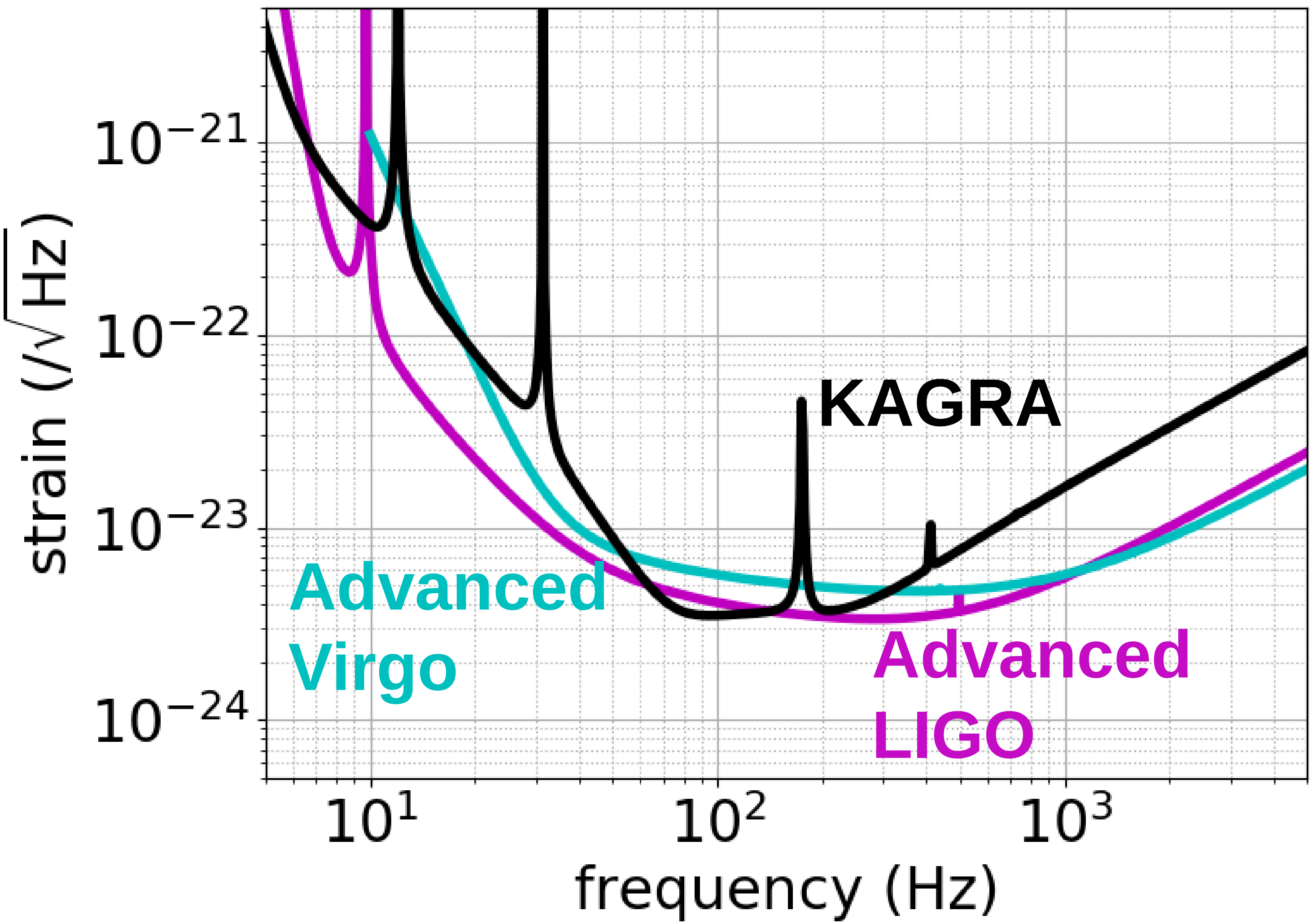

Noise Sources

- Sensitivity is limited by seismic noise, suspension and mirror thermal noise, and quantum noise

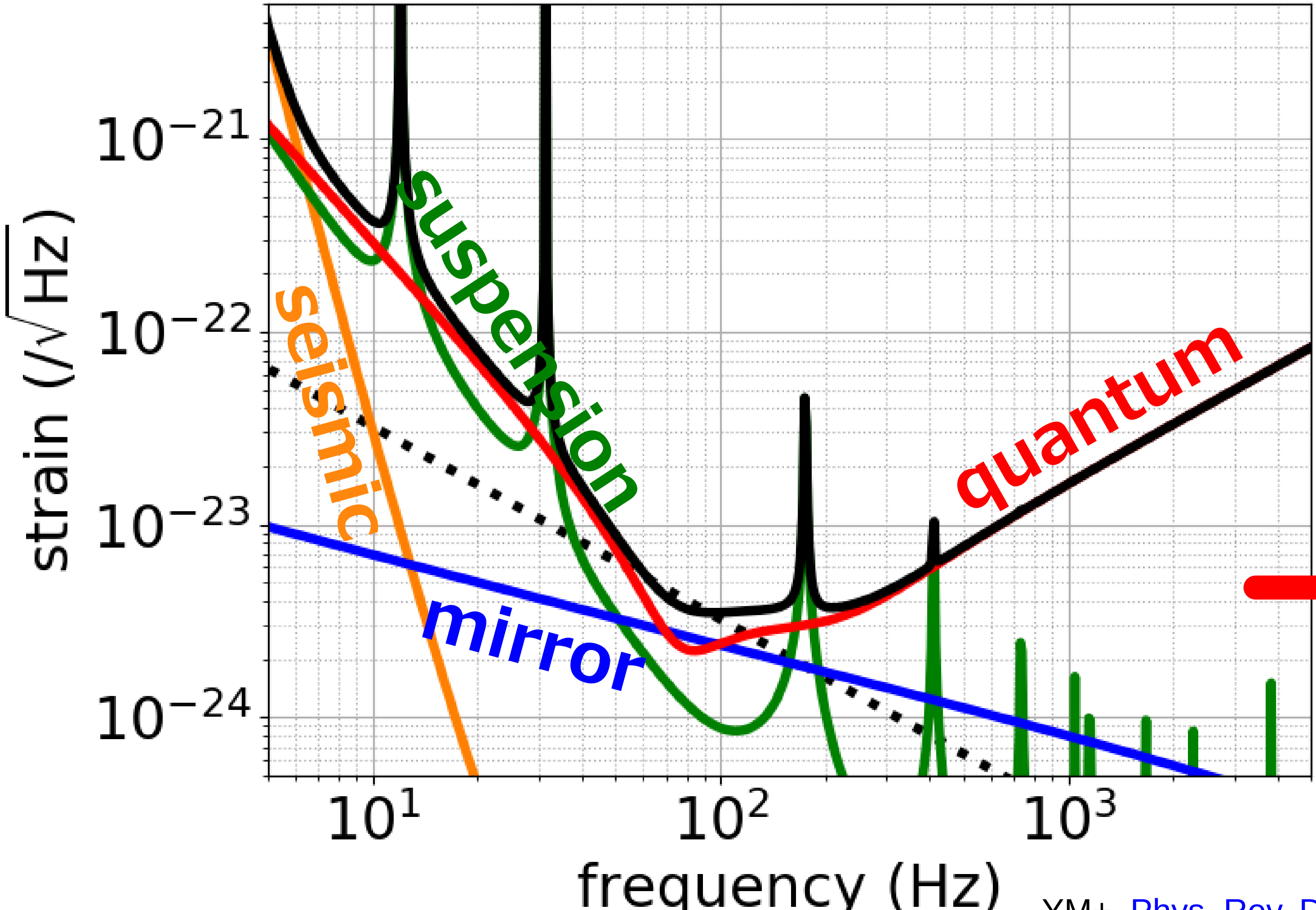

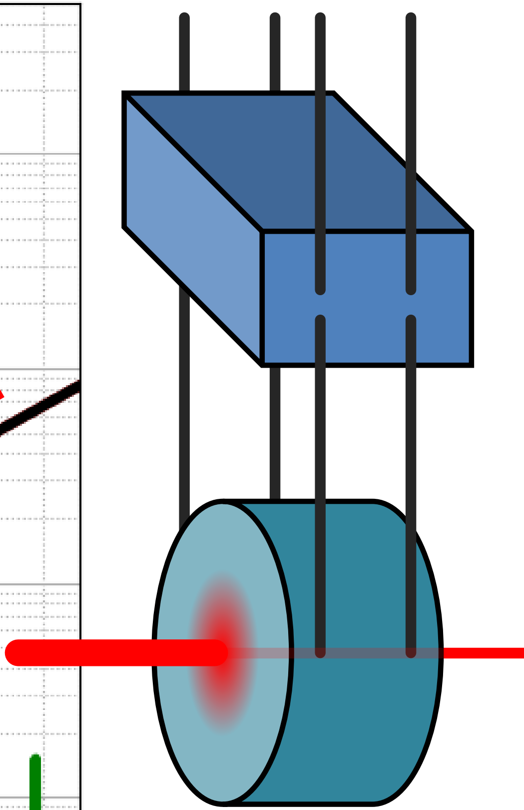

YM+, Phys. Rev. D 97, 122003 (2018)

Differences from aLIGO/AdV

- Built underground for lower seismic noise
- 23 kg sapphire test masses at 20 K
  (aLIGO and AdV uses 40 kg fused silica test masses at room temperature)
- Compared with aLIGO and AdV
  - suspension thermal noise is higher due to thick and short suspension to extract heat
  - mirror thermal noise is lower due to cryogenic
- Interferometer topology is similar

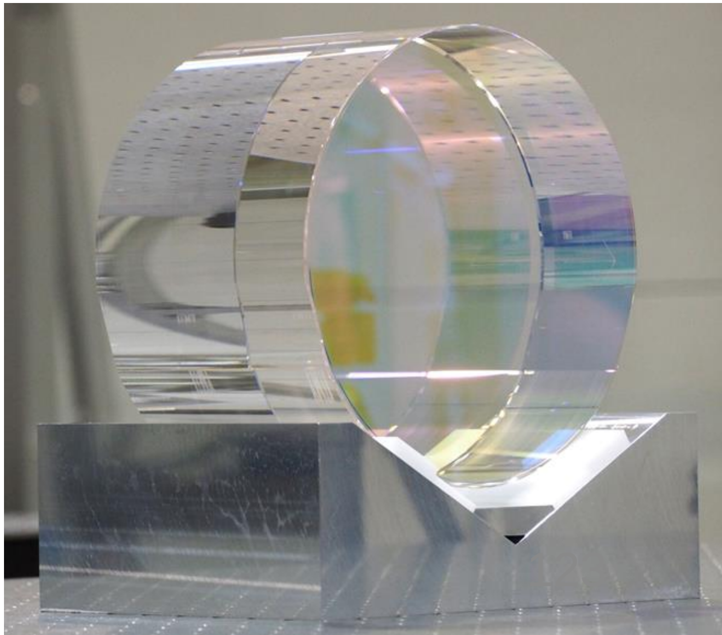

Interferometer Topology

- Dual-recycled Fabry-Perot Michelson Interferometer (DRFPMI)

Power recycling mirror
to effectively increase the input power by reflecting the beam back into the interferometer

Arm cavities
to effectively increase the arm length

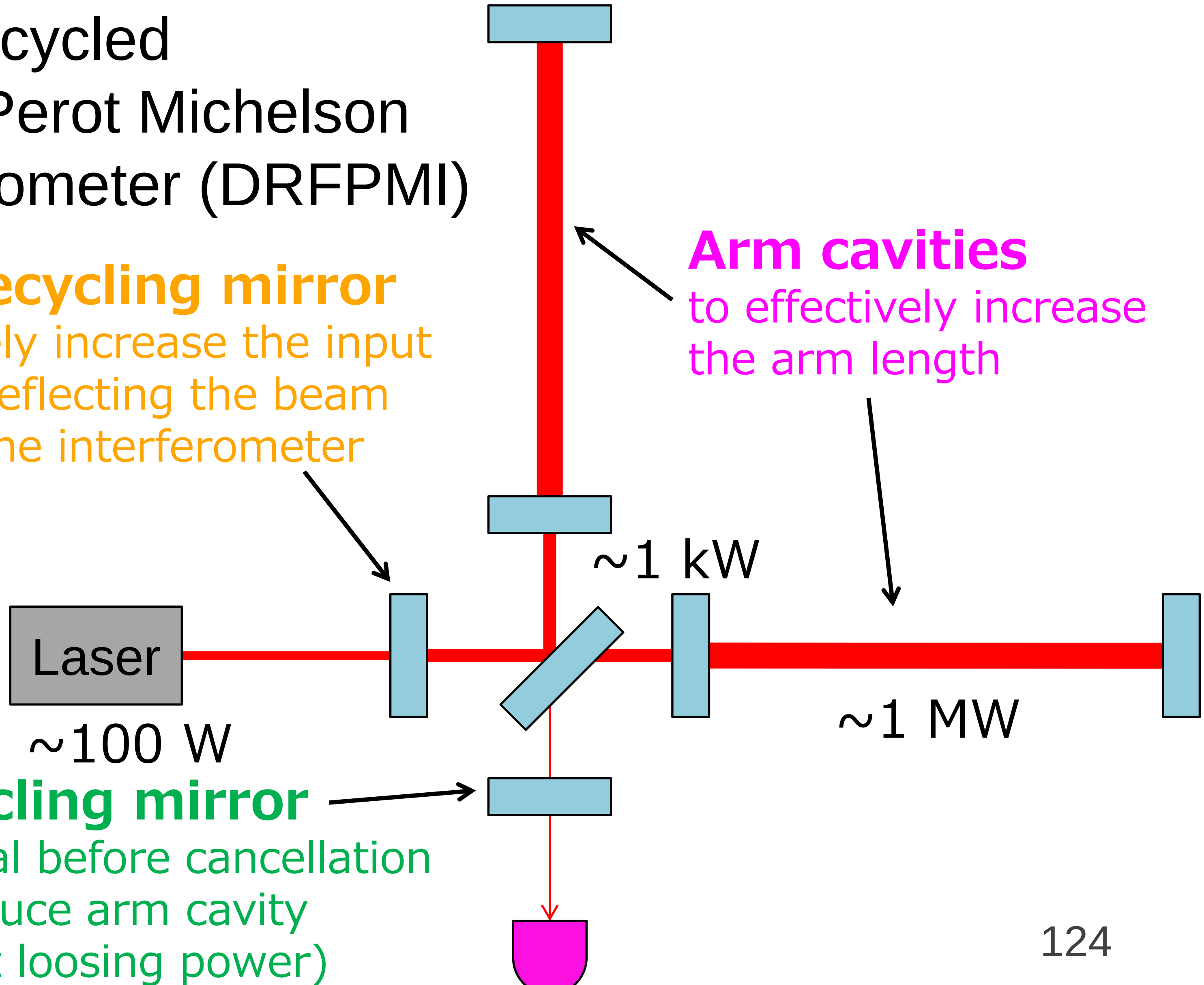

Signal recycling mirror
to extract signal before cancellation (effectively reduce arm cavity finesse without loosing power)

Figure of Merit for Sensitivity

- Usually use binary neutron star inspiral range
- Sky-averaged distance to which SNR > 8

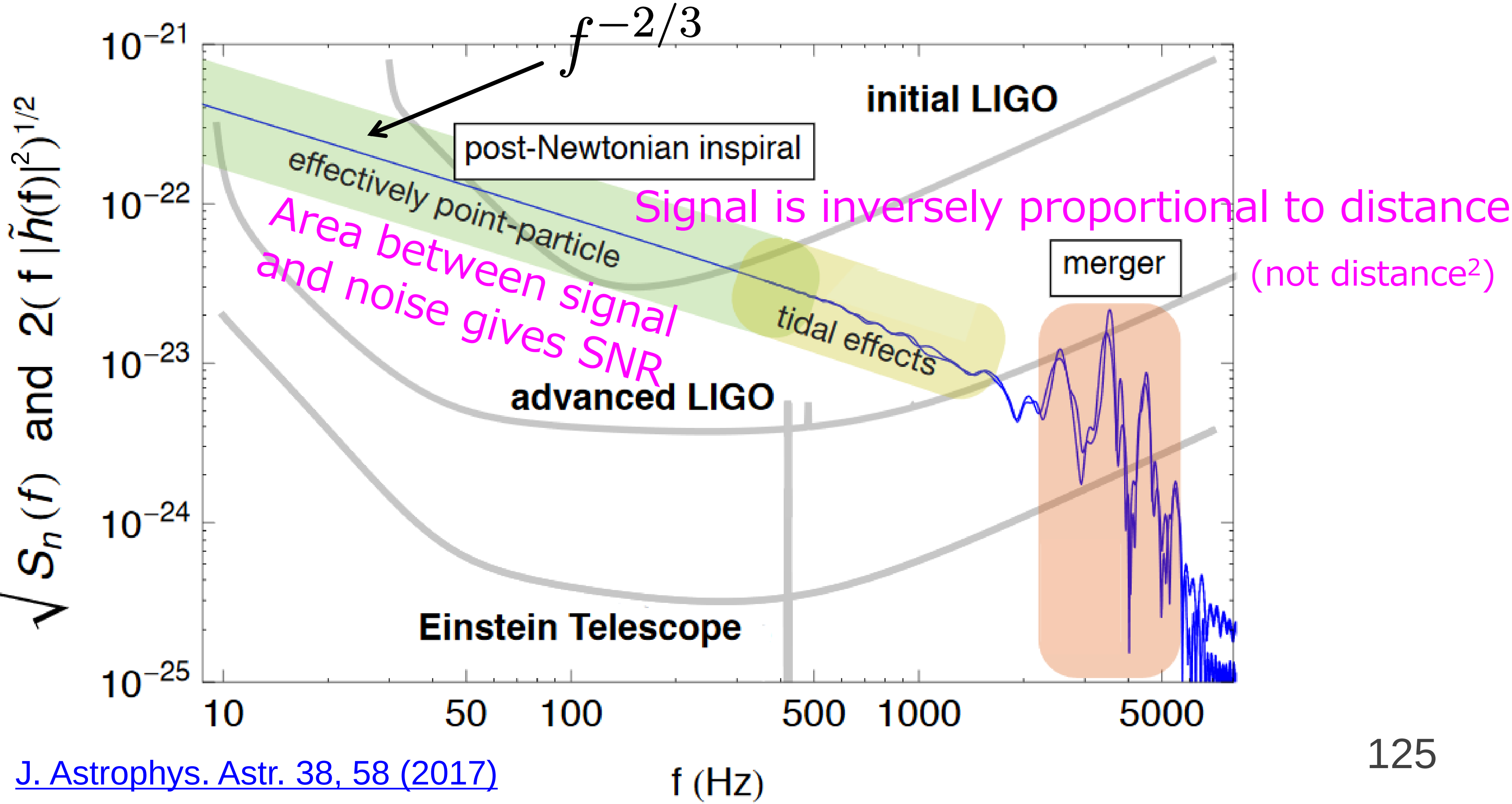

J. Astrophys. Astr. 38, 58 (2017)

Observing Scenario of LVK

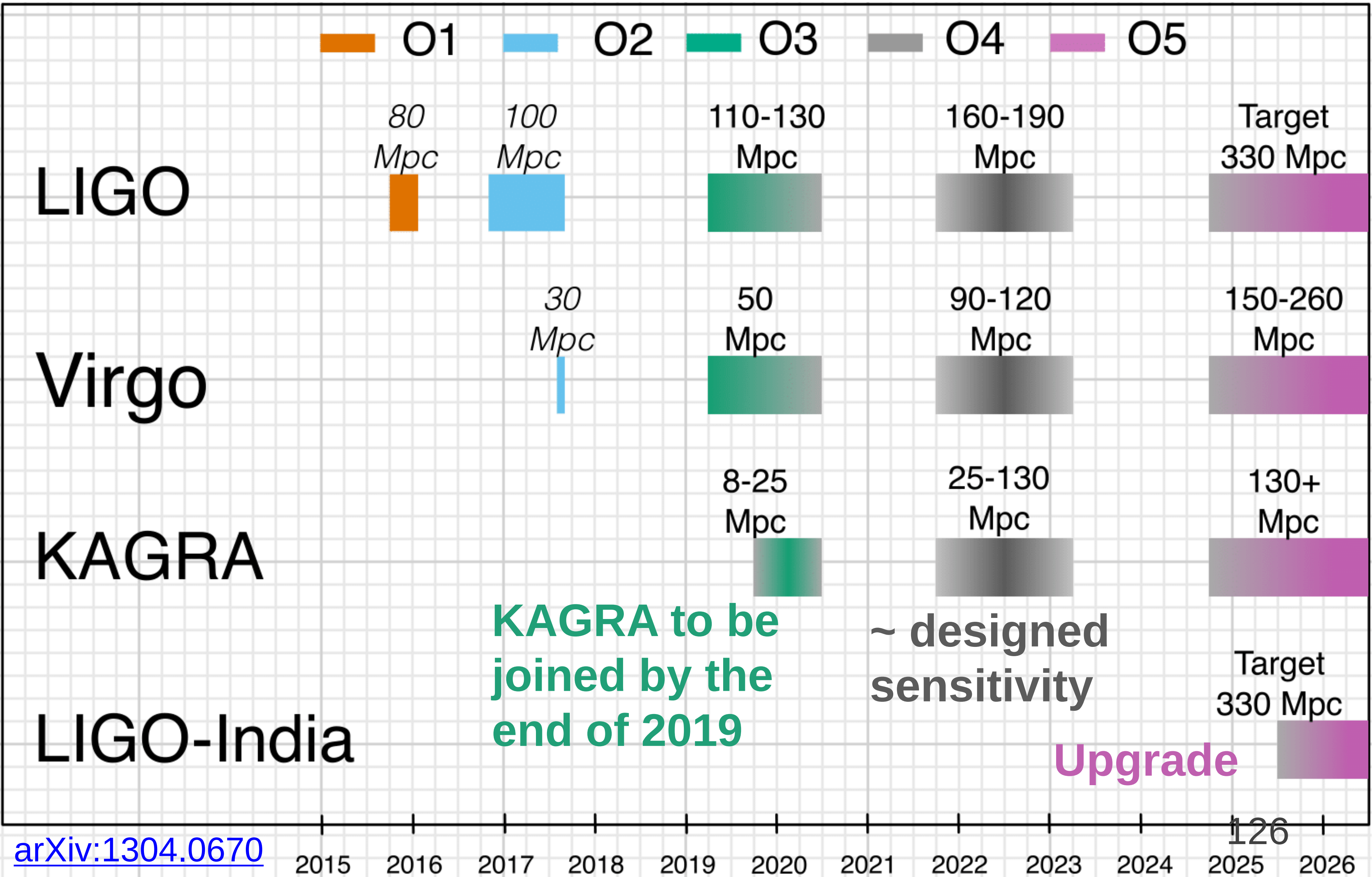

arXiv:1304.0670

KAGRA Project

- Budget approved in 2010
- 110 institutes, 360+ collaborators (200 authors)
- Cryogenic and underground

Join us!

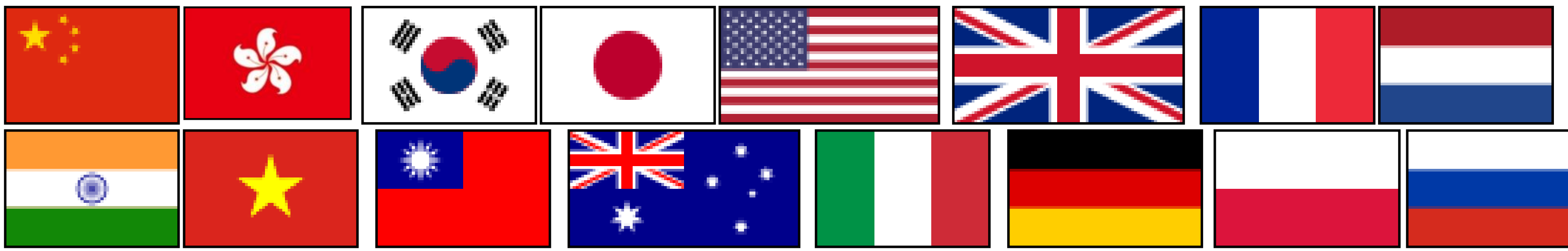

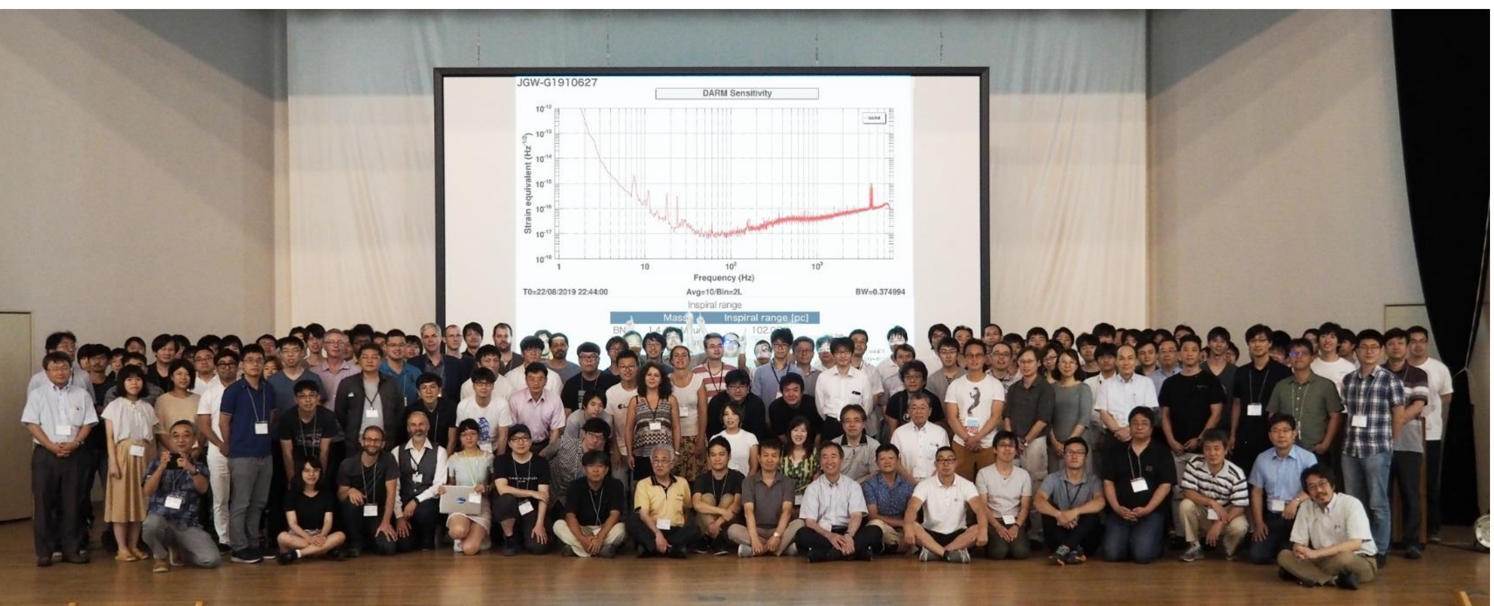

Aug 2019
F2F meeting
@ Toyama

KAGRA Location

- 1 hour drive south from Toyama station

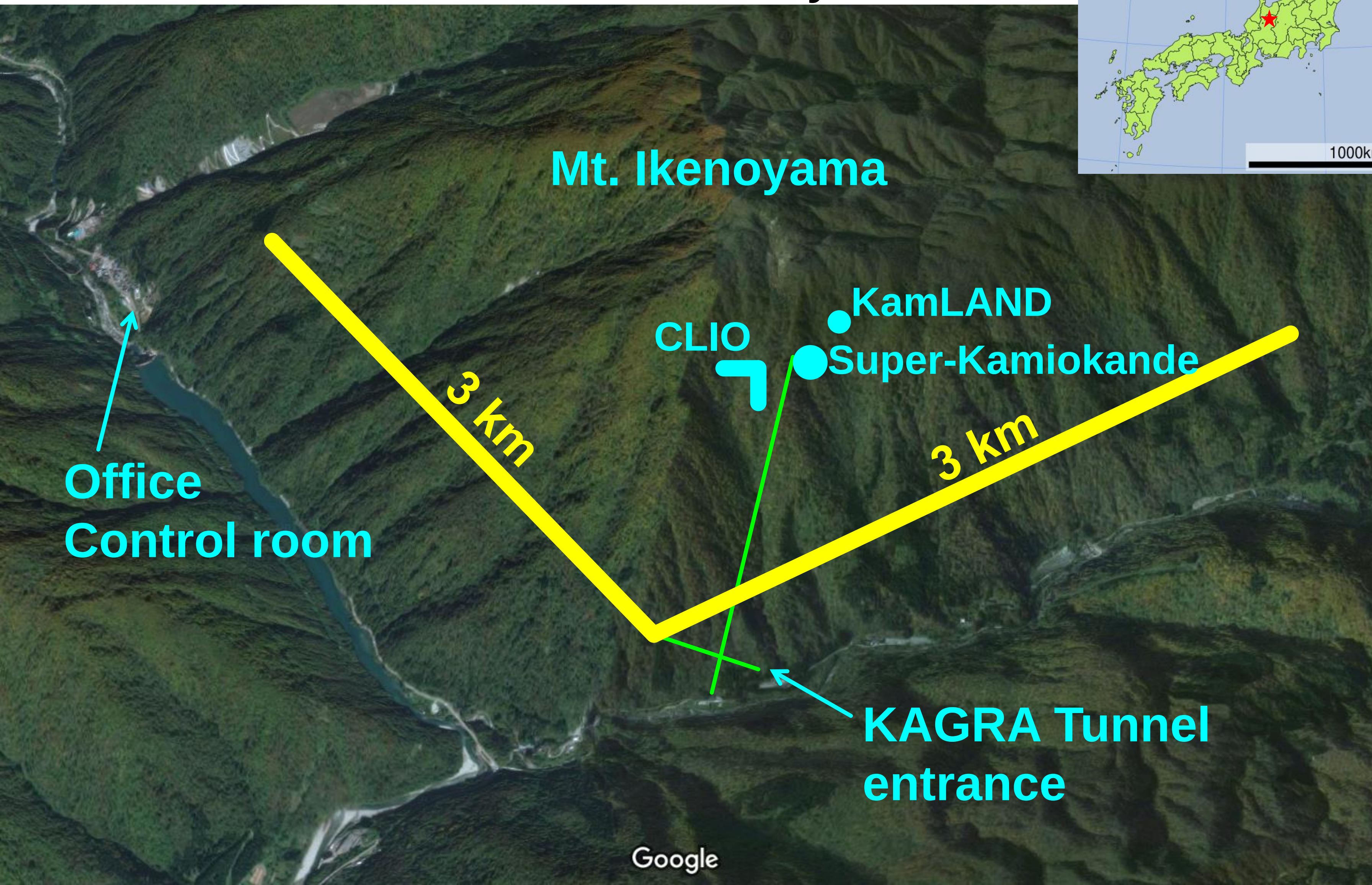

KAGRA Tunnel

- Laser beam goes back and forth inside two 3 km vacuum tubes

Entrance
(2016.2.8)

KAGRA Timeline

- 2014: Tunnel excavation done
- 2015: Inauguration of initial-phase facility
- 2016: First test run at room temp. (iKAGRA)
  KAGRA Collaboration, [PTEP 2018, 013F01 (2018)]
- 2017
- 2018: First cryogenic test run (Phase 1)
  KAGRA Collaboration, [arXiv:1901.03569]
- 2019: MoA between LIGO and Virgo signed
- 2020: Expect to join observing run O3

Completion Ceremony on Oct 4

- Almost all components installed
- Agreement between LIGO/Virgo signed

https://www.u-tokyo.ac.jp/focus/ja/articles/z0508_10010.html

KAGRA Joining Observation

- Improves 3+ detector duty factor
  LHV 34 % → LHVK 65 %
  (assuming 70 % duty factor for single detector)
- Improves sky localization
  (roughly by factor of ~3)
- Enables better GW polarization measurements, distinguish non-GR polarization

S. Haino,
JGW-G1808212
(designed sensitivity)

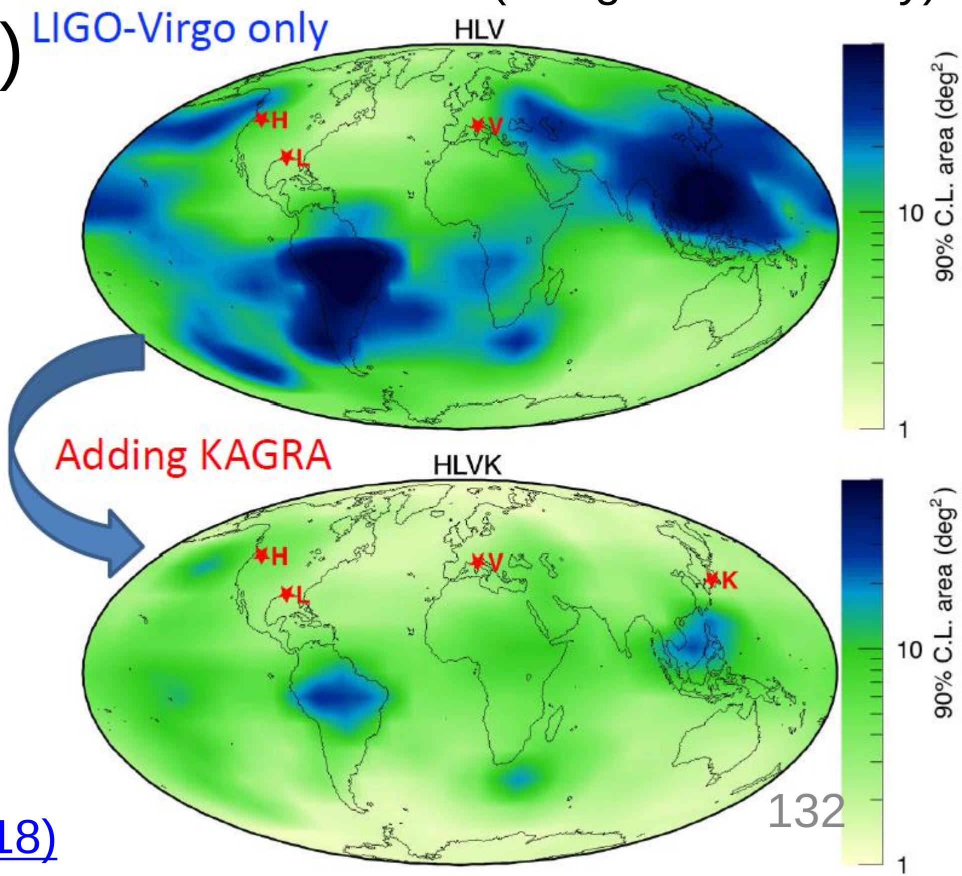

H. Takeda+, [PRD 98, 022008 (2018)]

KAGRA Status

- Maximum range upto ~30 kpc
- Expect to start the run by Feb 2020 (will be "joint" observing run with LV if more than 1 Mpc)
- Two issues
  - Mirror frosting
  - Birefringence
- Maximum sensitivity at O3 will be ~2 Mpc

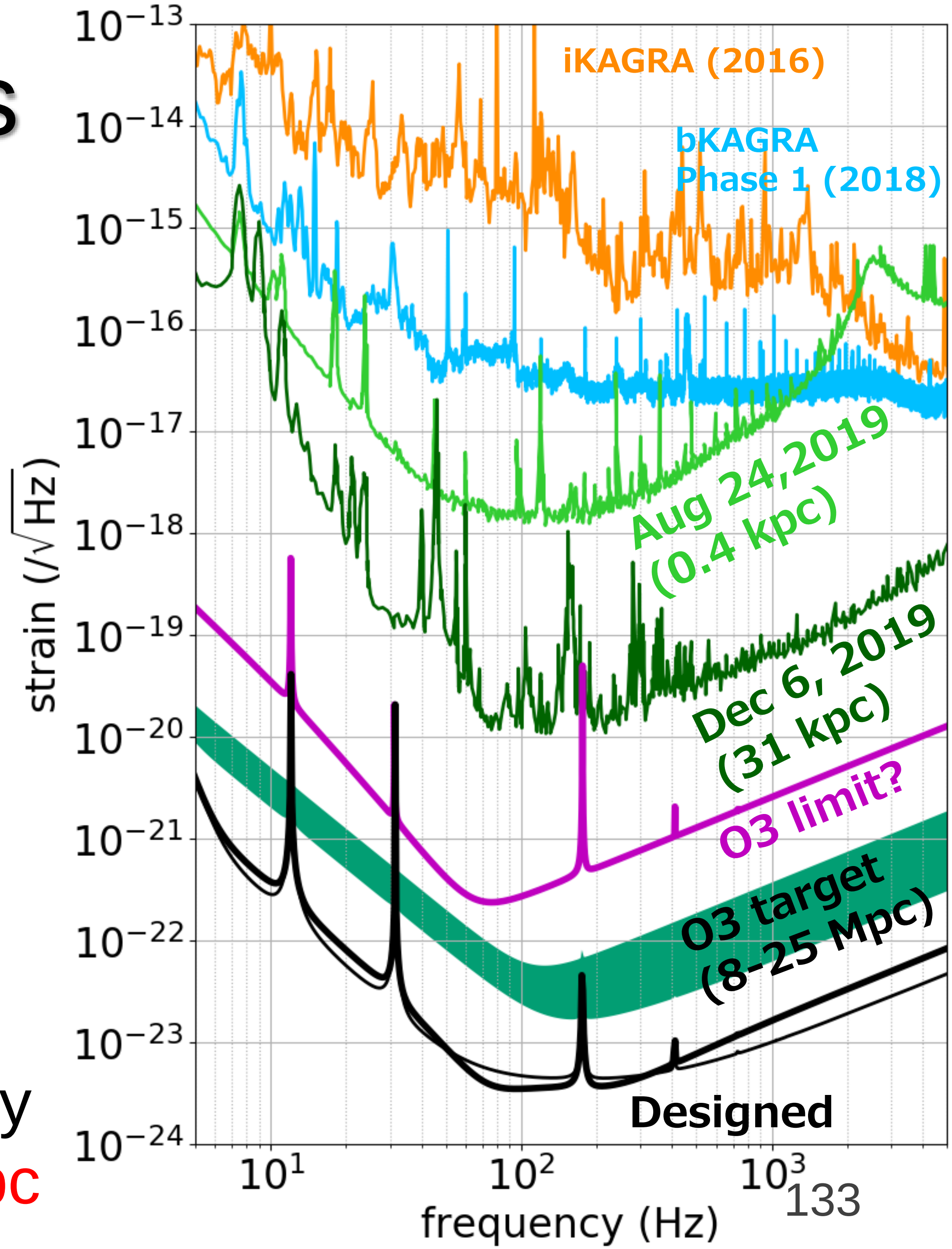

Effect of Frosting

- Finesse decreases at cryogenic temperatures (below ~30 K)
- Frosting from residual gas adsorption on mirrors
- Need to cool down the mirror at good vacuum

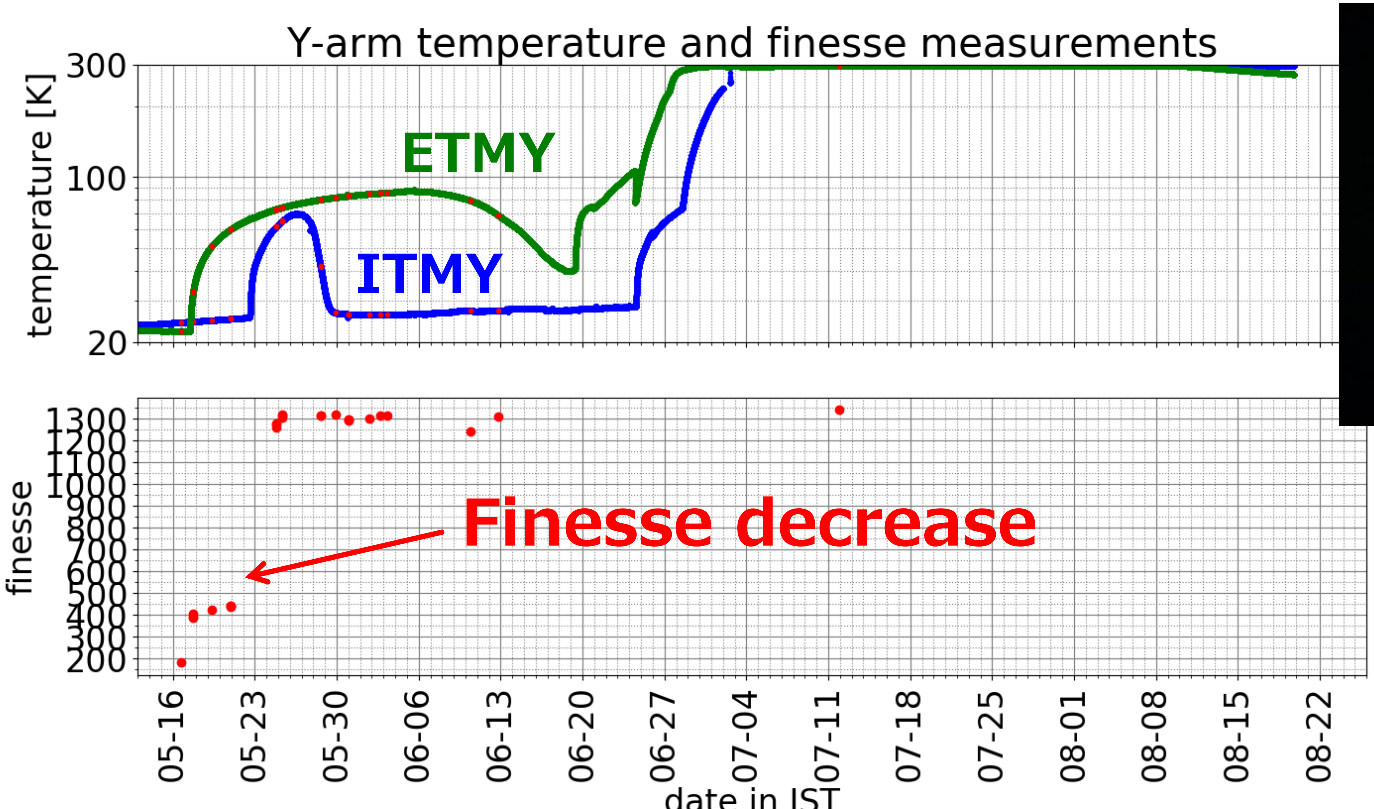

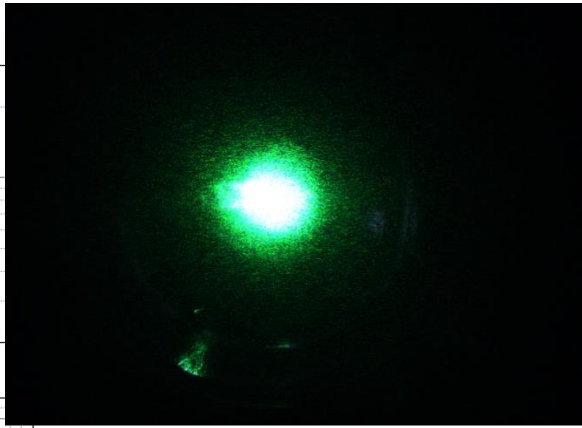

Frosted mirror seen with green laser

Y. Enomoto+, [klog #9861]

Effect of Birefringence

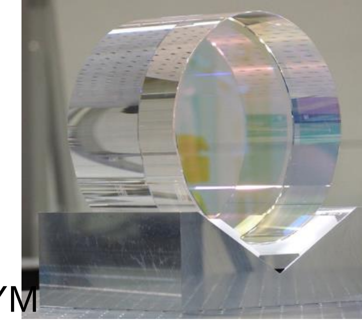

- Sapphire crystal axis and beam axis was not aligned well enough, and there's also inhomogeneity
- Hard to lock power and signal recycling cavities due to large losses and dirty effects

K. Somiya, E. Hirose, YM
PRD 100, 082005 (2019)

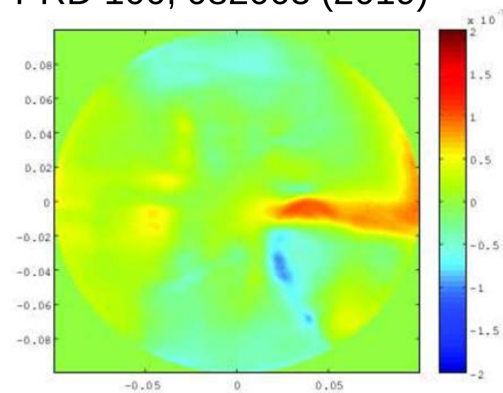

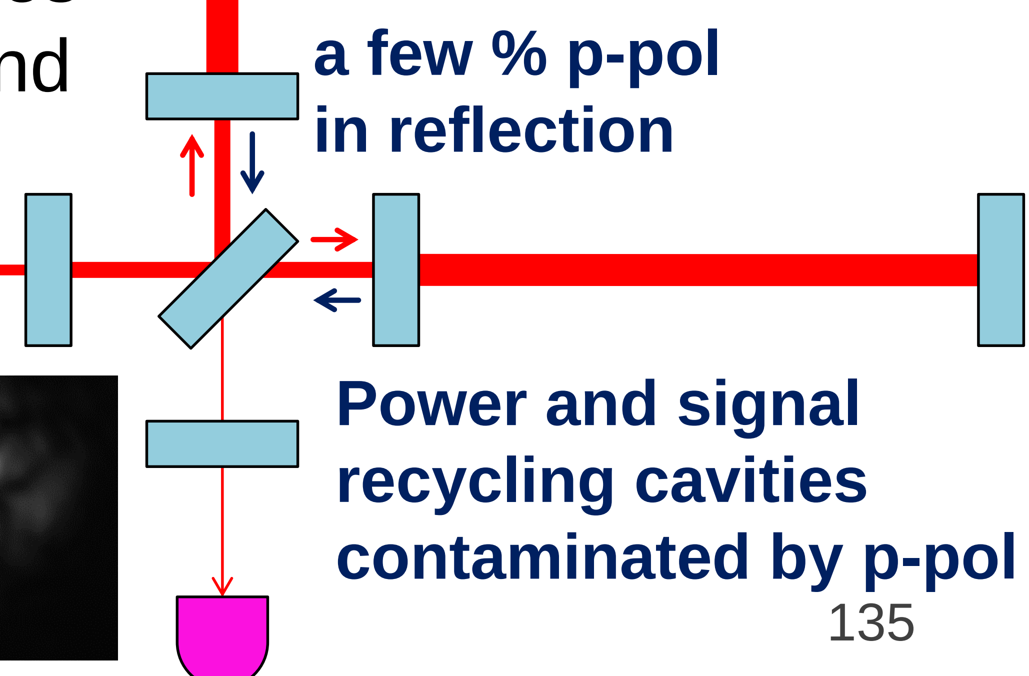

a few % p-pol in reflection

Power and signal recycling cavities contaminated by p-pol

p-pol beam shape from ITM reflection

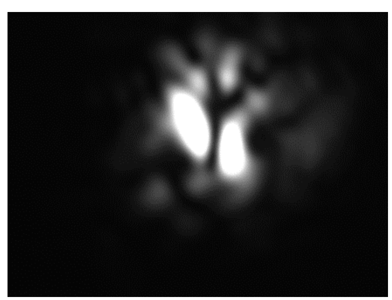

K. Kokeyama+, klog #9495

Latest KAGRA Noise Budget

- Limited by controls noise and frequency noise

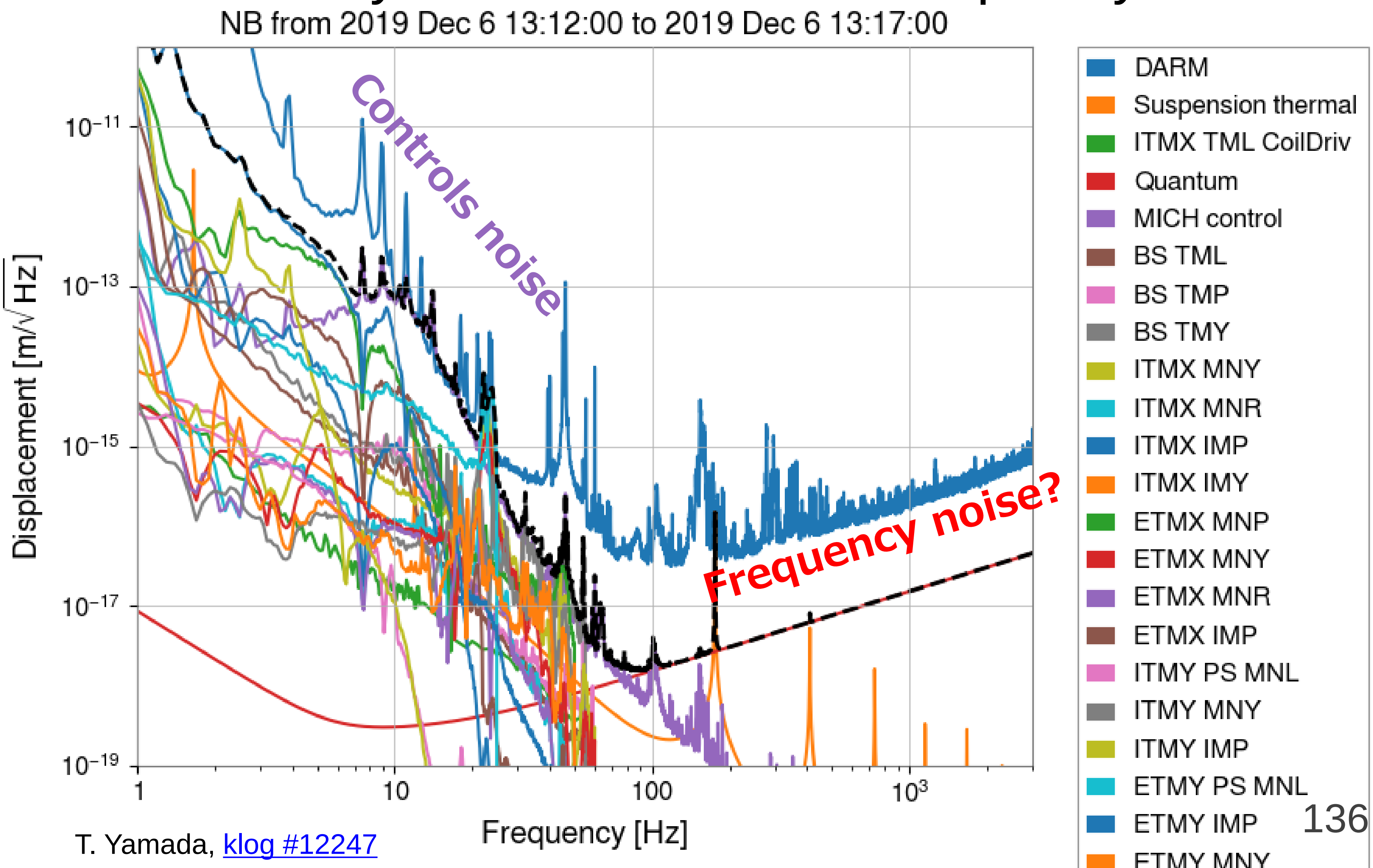

T. Yamada, klog #12247

Future Plans of KAGRA

- O3b (2020): ~2.3 Mpc at max
  (PR)FPMI at room temperature
- O4 (2021-2023): ~80 Mpc at max
  Install polarizers to remove unwanted polarizations
- O5 (2024-): ~180 Mpc
  Install new sapphire mirror
  Frequency dependent squeezing with 60 m filter cavity
- Ultimately 500 Mpc?
  Lower absorption 200 kg mirror
  300 m filter cavity

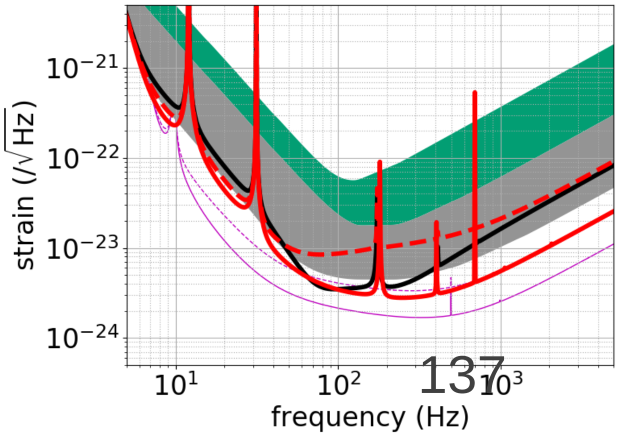

Summary of KAGRA

- More news to come in next decades

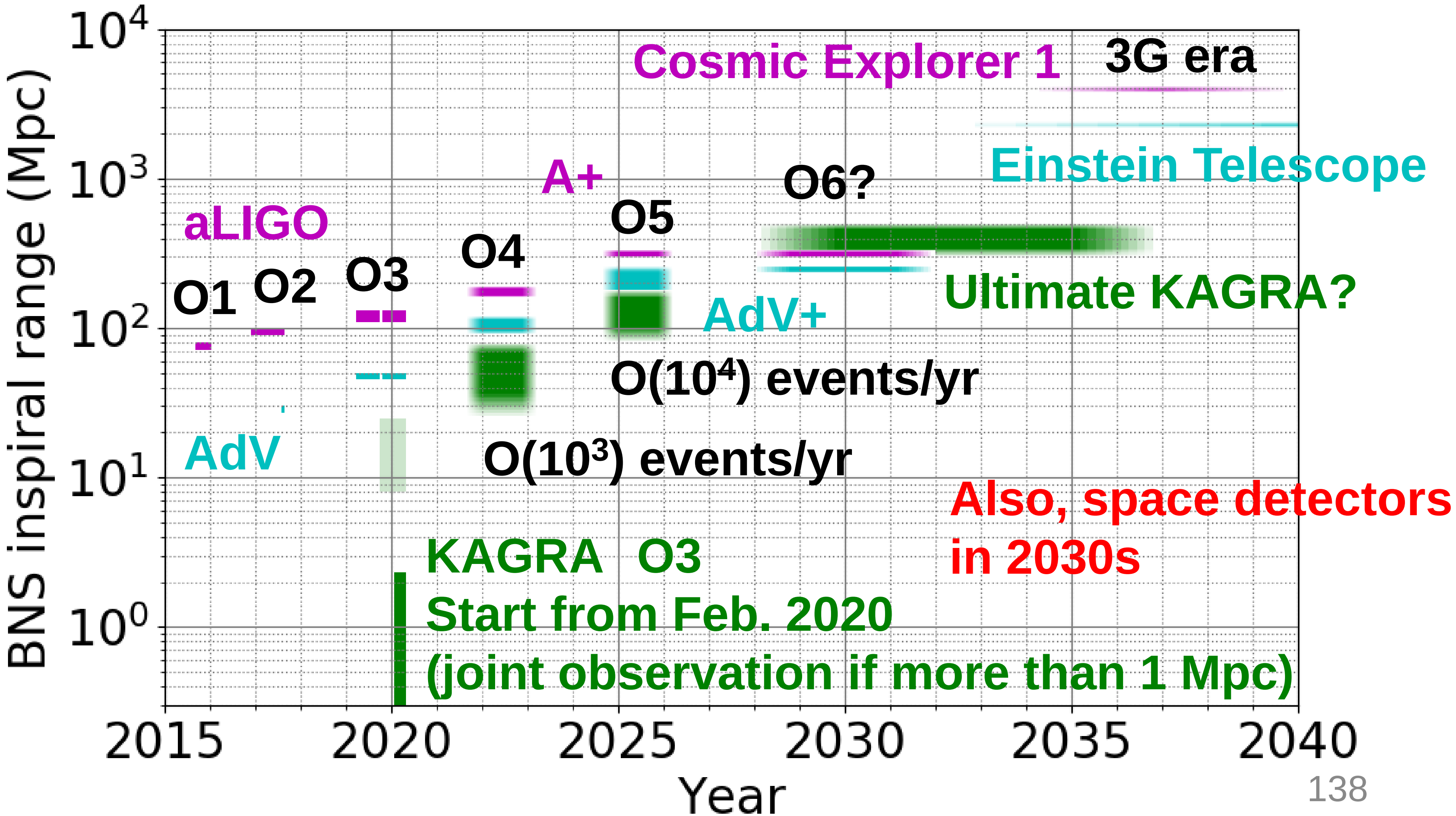

Our Group

Department of Physics, University of Tokyo

Ando Lab

Home About Research Members Directions

Group members

http://granite.phys.s.u-tokyo.ac.jp/en/

日本語 / English / RSS

- About
- Research
- Members
- Access
- Publications
- Annual Reports
- Theses
- News

Search this site

search

Acknowledgements

- **Test of Lorentz Invariance**
  Supported by JSPS

- **Search for Axion Dark Matter**
  Supported by Sumitomo Foundation

- **Macroscopic Quantum Mechanics**
  Supported by JSPS, JST CREST, MEXT Q-LEAP

Summary of Summary

- **Test of Lorentz Invariance**
  First experiment done, upgrade on-going
  YM+, PRL **110**, 200401 (2013) ; YM+, PRD **88**, 111101(R) (2013)
- **Search for Axion Dark Matter**
  Proposed, prototype experiment on-going
  Obata, Fujita, YM, PRL **121**, 161301 (2018)
  Nagano, Fujita, YM, Obata, PRL **123**, 111301 (2019)
  YM+, arXiv:1911.05196
- **Macroscopic Quantum Mechanics**
  Experiments on-going at milligram scale with different approaches (pendulum, torsion pendulum, optical levitation)
  Matsumoto+, PRL **122**, 071101 (2019) ; Komori+, arXiv:1907.13139
  YM+, Optics Express **25**, 13799 (2017)
- **KAGRA Gravitational Wave Telescope**
  Will start the run from Feb 2020